INFORMATION TO USERS

This manuscript has been reproduced from the microfilm master. UMI films the text directly from the original or copy submitted. Thus, some thesis and dissertation copies are in typewriter face, while others may be from any type of computer printer.

The quality of this reproduction is dependent upon the quality of the copy submitted. Broken or indistinct print, colored or poor quality illustrations and photographs, print bleedthrough, substandard margins, and improper alignment can adversely affect reproduction.

In the unlikely event that the author did not send UMI a complete manuscript and there are missing pages, these will be noted. Also, if unauthorized copyright material had to be removed, a note will indicate the deletion.

Oversize materials (e.g., maps, drawings, charts) are reproduced by sectioning the original, beginning at the upper left-hand corner and continuing from left to right in equal sections with small overlaps.

Photographs included in the original manuscript have been reproduced xerographically in this copy. Higher quality 6" x 9" black and white photographic prints are available for any photographs or illustrations appearing in this copy for an additional charge. Contact UMI directly to order.

ProQuest Information and Learning
300 North Zeeb Road, Ann Arbor, MI 48106-1346 USA
800-521-0600

Synthesis and Characterisation of Bisaminopnictines (pnict. = P, As and Sb)

by

Denise M. Walsh

Submitted in partial fulfilment of the requirements
for the degree of Doctor of Philosophy

at

Dalhousie University
Halifax, Nova Scotia
December 2001

DALHOUSIE UNIVERSITY

FACULTY OF GRADUATE STUDIES

The undersigned hereby certify that they have read and recommend to the Faculty of Graduate Studies for acceptance a thesis entitled "Synthesis and Characterisation of Bisaminopnictines (pnict = P, As and Sb)" by Denise M. Walsh, in partial fulfillment of the requirements for the degree of Doctor of Philosophy.

Dated: December 7, 2001

External Examiner:

Research Supervisor:

Examining Committee:

Dalhousie University

DATE: December 2001

AUTHOR: Denise M. Walsh

TITLE: Synthesis and Characterisation of Bisaminopnictines (pnict. = P, As and Sb).

DEPARTMENT OF SCHOOL: Chemistry

DEGREE: Ph. D. CONVOCATION: May YEAR: 2002

Permission is herewith granted to Dalhousie University to circulate and to have copied for non-commercial purposes, at its discretion, the above title upon the request of individuals or institutions.

Signature of Author

For Mom, Dad and Sinead

Table of Contents

List of Figures

List of Tables

Abstract

Reactions involving lithium amides and $PnCl_3$ (Pn = P, As and Sb) were performed under different reaction conditions and stoichiometry. The sterics associated with the substituents and the size of the pnictogen atom were some of the factors that governed the compounds prepared from these reactions. The types of products isolated included aminopnictines, iminopnictines, pnictetidines and pnictenium salts. Few low coordinate compounds are known for Pn = As or Sb (i.e. iminopnictines or pnictenium salts). The use of sterically demanding substituents can provide both thermodynamic and kinetic stability with respect to saturated alternatives (i.e. pnictetidines). The bulky substituent, Mes*, facilitated the isolation of the first acyclic bisaminoarsenium salt. Sterically demanding substituents have also been used to isolate iminophosphines. Similar reactions were performed using the heavier pnictogens (As or Sb) and resulted in the isolation of pnictetidines. However, pnictetidines (for Pn = P) were observed to dissociate under certain conditions. For example, the mode of crystallisation, effects of heating or the addition of $GaCl_3$ disrupted dimeric phosphetidines and allowed monomeric iminophosphines to be obtained. Evidence suggests that the arsetidine isolated may also be susceptible to a similar dissociation, to form the iminoarsine.

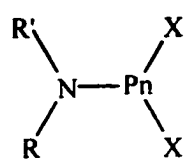

Aminopnictine

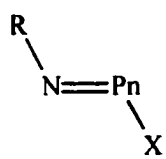

Iminopnictine

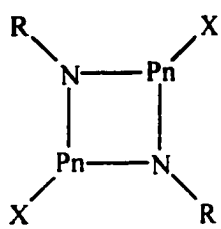

Pnictetidine

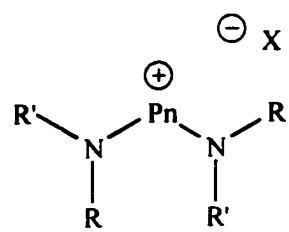

Pnictenium salt

List of Abbreviations and Symbols

Ar	Aryl
br.	Broad (vibrational spectroscopy)
δ	Chemical shift
CP	Cross polarisation
Cp*	Pentamethylcylcopentadienyl
Δ	Change in
Δ	Heat (reaction schemes)
d	Doublet
DBU	1,8-Diazabicyclo[5.4.0]undec-7-ene
D_{calc}	Density (calculated)
Dip	2,6-Diisopropylphenyl
dipyr	2,2'-Dipyridyl
DMesp	2,6-bis(2,4,6-trimethylphenyl)phenyl
DNA	Deoxyribonucleic acid
DTipp	2,6-Bis(2,4,6-triisopropylphenyl) phenyl
E	Element
EA	Elemental analysis
EI-MS	Electron impact ionisation mass spectrometry
Fmes	2,4,6-(trifluoromethyl)phenyl
FT	Fourier transform
H	Enthalpy
δ_{iso}	Isotropic chemical shift
IR	Infrared
MAS	Magic angle spinning
Me	Methyl
Mes	2,4,6-Trimethylphenyl
Mes*	2,4,6-Tri-tert-butylphenyl
m.p.	Melting point
mW	Milliwatts
NMR	Nuclear magnetic resonance
OD	Outside diameter
ORTEP	Oak Ridge thermal ellipsoid program
Ph	Phenyl
Pn	Pnictogen (group 15 element)
ppm	parts per million
R	Substituent (general)
R_1	Unweighted agreement factor

s	Singlet (NMR spectroscopy)
sept	Septet (NMR spectroscopy)
sh.	Shoulder (vibrational spectroscopy)
Tbt	2,4,6-Tris(bis(trimethylsilyl)methyl)phenyl
THF	Tetrahydrofuran
TMS	Tetramethylsilane
UV	Ultraviolet
X	Halogen (group 17 element)

Acknowledgements

I could not have accomplished all that I have without the constant support and guidance of many friends and colleagues and for that I am truly grateful.

I would especially like to thank my supervisor, Neil Burford for all your advice and encouragement over the years. Your enthusiasm and dedication to "doing the best science" was a constant source of inspiration. I would also like to thank Dr. Jason Clyburne for recommending and encouraging me to come to Dalhousie.

As a member of the Burford group I have had the ability to meet and work with a variety of people who have made the last few years a truly unique experience. I would like to thank the current members of my group (Paul Ragogna, Heather Spinney, Robyn Ovans and Melanie Eelman) for all their patience and support over the past few months. I have had the privilege of working with some great undergraduate students (Natasha Zwarun, Bobby Ellis and Korey Conroy) and their work has contributed directly to this thesis. I am also grateful for the experience and guidance of past members in particular, Dr. Roland Roesler, Dr. Edgar Ocando-Mavarez, Dr. Glen Briand and Dr. Andrew Phillips. I would especially like to thank Dr. Charles Macdonald - I could not have survived the last few years without your help, advice and friendship.

There have been many members outside my group that have contributed to this thesis. I would like to acknowledge the work carried out by the members of DALX and ARMRC. The help of Dr. Lumsden who ran all the solid state NMR experiments was gratefully appreciated. I would like to thank Dr. Cameron, Dr. Robertson and Dr. McDonald for solving crystal structures and providing assistance when needed. I would

also like to thank Dr. Cameron for allowing me to invade his lab while writing my thesis - your stories were a valued distraction. I am also extremely grateful to Dr. Robertson for all her help and understanding - I am in your debt.

I would like to thank Giselle, Deanna and Gail, who were always willing to help and J. Müller, R. Shortt and R. Conrad - I could not have carried out the work in this thesis without your support. I would also like to thank all my friends at Dalhousie, both past and present - you have all helped in so many ways.

I would also like to acknowledge all the great teachers and Professors who inspired my interest in Chemistry (Dr. S. Draper, Prof. McMurry, Mr. Bassette and Mr. O'Rielly). I am especially indebted to Dr. Cowley and Dr. Carmalt for their great advice. Finally, I thank my family for everything - I could not have done any of this without you!

Chapter 1 - Introduction

1.1 General Introduction

The elements of group 15 (N, P, As, Sb and Bi) can be collectively referred to as pnictogens. The term (pnictogen) is derived from the Greek *pniktos*[(i)] (to suffocate - the origin of the prefix 'pnicto')[1]. While the term, pnictogens is not officially accepted, it is commonly used amongst chemists who work with group 15 elements[2] and as such "pnictogens" or "Pn" is used throughout this thesis to refer to group 15 element(s). As with groups 14 and 16, the elements of group 15 are quite diverse in their nature, nitrogen and phosphorus are non-metals, arsenic and antimony are semi-metals and bismuth is a metal. Differences can also be found in the elemental forms of nitrogen and the heavier pnictogens (P, As, Sb and Bi). Nitrogen (in its elemental form) exists as a gaseous, diatomic molecule, N_2. However, elemental phosphorus only exists as a diatomic, P_2 molecule in the gas phase at high temperatures and pressures; its stable forms are known as white, red and black phosphorus. White phosphorus is a tetrahedral P_4 molecule, while red and black phosphorus have polymeric structures, containing three coordinate P atoms. The elemental forms of arsenic, antimony and bismuth are isostructural and are similar to black phosphorus.

Compounds containing pnictogens are also diverse in their interactions with humans; nitrogen is in the air we breathe and compounds containing nitrogen are essential to life

---

[(i)] According to Liddell and Scott's Greek-English Lexicon (Oxford University Press, 1979) the verb pnigo (πνιγω) means I stifle, choke, seize by the throat or throttle. Pniktos (or πνικτός) is the participle, passive adjective describing that which has been choked.

(for example, amino acids are the building blocks of proteins). Phosphates are found in the bones and teeth, and are a crucial part of the backbone of DNA. Arsenic compounds are generally considered poisonous but have, in the past, been used[3] medicinally to treat syphilis. Compounds containing antimony can be used[3] to treat Schistosomiasis, a disease caused by parasites (flukes). Bismuth compounds have long been used to treat gastric diseases and research into their medicinal properties is ongoing.

The reactivity of the elements of group 15 is governed (as with all elements of the periodic table) by fundamental properties, such as electronegativity, atomic size, oxidation potentials and Lewis acidity. The goal of this thesis was to examine how amines (or more accurately amides) interact with the pnictogen trichlorides (Pn = P, As, Sb and Bi) in order to determine the types of products that are formed and the differences that arise between the various pnictogen species (where Pn ≠ N). There has been extensive research carried out on the interactions between P and N, including both saturated (e.g. aminophosphines, $R_2N\text{-}PR'_2$) and unsaturated or low-coordinate compounds (such as the iminophosphines, R-N=P-R'). In contrast, few low-coordinate compounds containing both nitrogen and the heavier group 15 elements are known. The various possibilities and compounds which have been isolated are discussed over the next few sections. Unless otherwise stated, the compounds discussed throughout this thesis are restricted to examples that have been isolated as solids. It is also worth noting that the reaction schemes illustrated in this thesis are not necessarily balanced equations, but rather represent the products isolated from the relative stoichiometric addition of the reagents.

1.2 Amines and Pnictogen trihalides.

When considering reactions between pnictogen trihalides (PnX_3) and amines (NRR'R"), a variety of products are possible and there are a number of factors that influence the compound (or compounds) that are formed and isolated. Most obvious are the reaction conditions; stoichiometry, temperature and order of addition will naturally control the outcome. However the atomic size of the pnictogen, the bulk associated with the amine substituents and the type of amine (i.e. primary, secondary or tertiary) will also play a role.

The lone pair of electrons on nitrogen allows an amine to act[4] as both a base and a nucleophile. Under the appropriate stoichiometry and conditions it is possible to carry out reactions involving amines and PnX_3 (X = halogen) that display this nature. In addition, metathesis reactions between PnX_3 and lithium amides, $LiNR_2$, can result in the formation of compounds containing N and a heavier group 15 element (P, As, Sb or Bi). The types of products that can be envisaged are shown in Figure 1.1. Compound types **A** and **B** represent amines acting as Lewis bases, examples of which include Me_3NAsCl_3[5] and (dipyr)$SbCl_3$[6]. Monoaminopnictines (compound type **C**) result from the reaction between two equivalents of amine and one equivalent of a pnictogen trichloride (e.g. the reaction between 2,2,6,6-tetramethylpiperidine and PBr_3 which yields 2,2,6,6-tetramethylpiperidinophosphine dibromide[7]) and alternatively, **C** can be prepared by the reaction between a lithium amide, RR'NLi, and PnX_3 (for example, $(^tBu)_2NPCl_2$[8] is prepared by the reaction of $^tBu_2NLi$ and PCl_3). Addition of a base to **C** can yield the

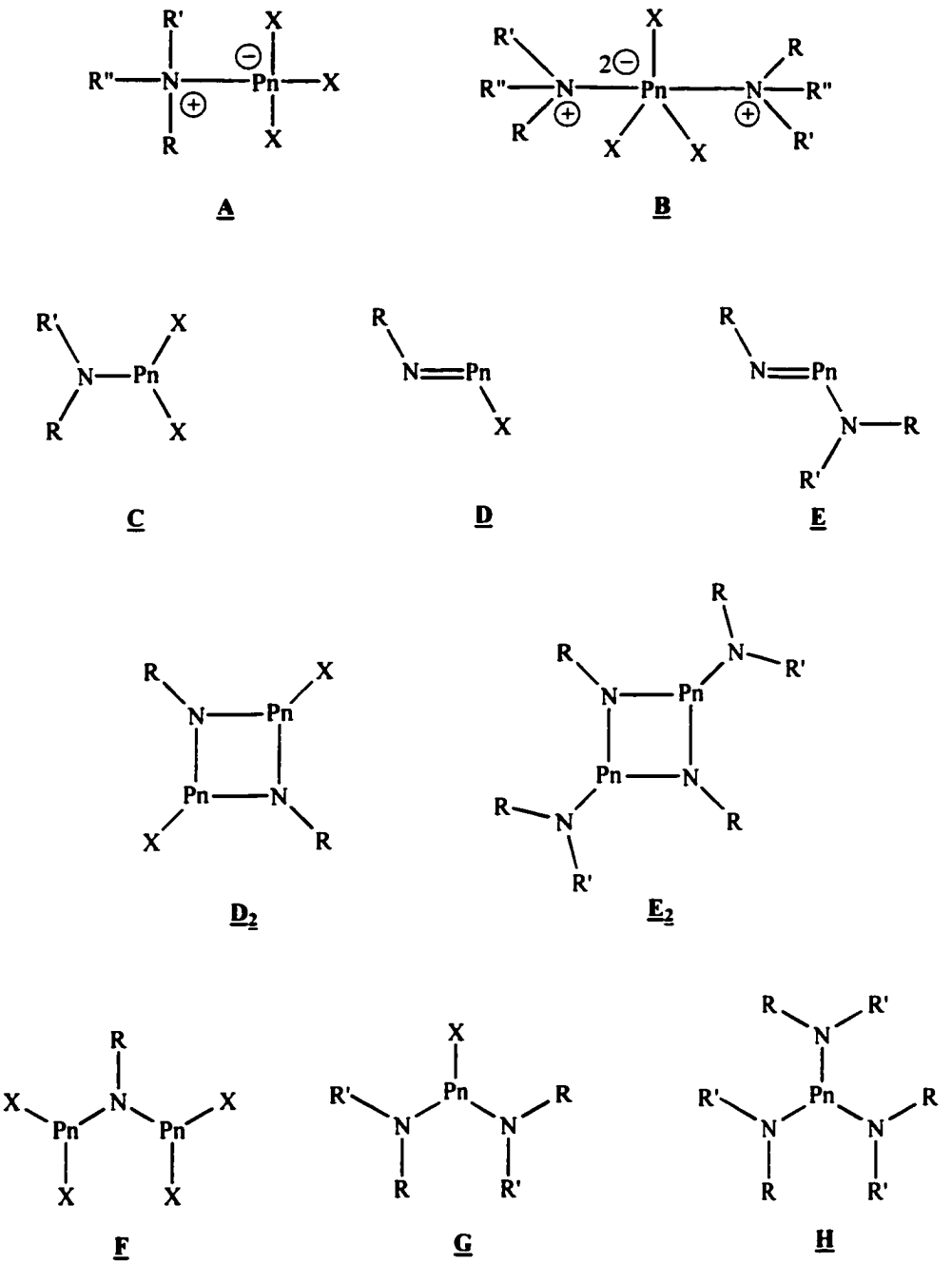

Figure 1.1 Possible products from reactions involving pnictogen trihalides (PnX_3) and amines, NRR'R".

iminopnictine, **D** (as in the preparation of Mes*NPCl[9], which is isolated from the reaction of NEt_3, Mes*NH_2 and PCl_3). However, **D** is susceptible to dimerisation to form the pnictetidine, $\mathbf{D_2}$ (i.e. $[DipNPCl]_2$[10] verses Mes*NPCl), depending on the atomic size of the pnictogen and the bulk of the substituent (R). Metathesis reactions of lithium amides, RHNLi, and PnX_3 (in a 3:1 ratio) form compounds of the general type $\mathbf{E_2}$, **E** and **H**. A number of factors govern the products isolated from these 3:1 reactions. Most notably, the atomic size of the pnictogen and the bulk of the amine substituent (R) will govern product formation. For example, when R = Dip and Pn = P, As, Sb or Bi, the four-membered NPnNPn pnictetidine ring ($\mathbf{E_2}$) is isolated[11]. However when R = Mes* and Pn = P or As, the increased size of the substituent allows the iminopnictine, **E**, to be isolated[12]. The same reaction for the heavier pnictogens antimony and bismuth (i.e. when three equivalents of Mes*NHLi is added to $PnCl_3$ where Pn = Sb or Bi) yields[13] the trisaminopnictine, **H** (these reactions are discussed in more detail in Chapter 5). There are few derivatives of compound **F**, one example is $RN(AsCl_2)_2$ (where R = 2-(6-Me)pyridyl)[14]. Equally halo-bisaminopnictines (**G**) are also rare. Some cyclic compounds[15-20] do exist but the only acyclic halo-bisaminopnictines that have been isolated as solids are $\{RN(SiMe_3)\}_2PnCl$, where R = 2-(6-Me)pyridyl and Pn = Sb or Bi (see **22Pn**[21], see Figure 1.13).

1.3 Aminopnictines

There are several examples of trisaminopnictines (H) for P[22-24], As[23,25,26], Sb[13,14,27] and Bi[13,14,28,29], some of which are shown in Figure 1.3. Reaction of an excess of the appropriate amine (or at least three equivalents of lithium amide) with PnX_3 allows derivatives of compound type H to be isolated. The isolation of H is favoured (over other alternatives such as, C, F or G) by adding the pnictogen trihalide to the amine (or lithium amide), thereby allowing the amine to be always in excess and thus providing stoichiometric control of the reaction. In a similar way, formation of the monoaminopnictines (C) can be promoted by ensuring that the PnX_3 is always in excess.

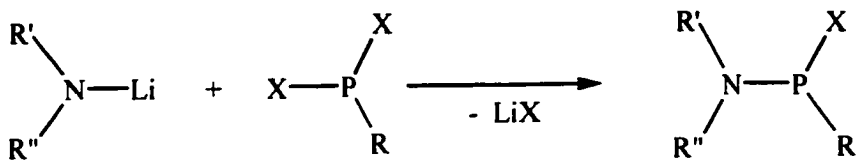

For example,
R = X, Me, ^{t}Bu, ^{i}Pr, Ph
R' = $SiMe_3$, Mes*
R" = $SiMe_3$, Mes*
X = F, Cl or Br

Figure 1.2 Reaction scheme, preparation of aminophosphines.

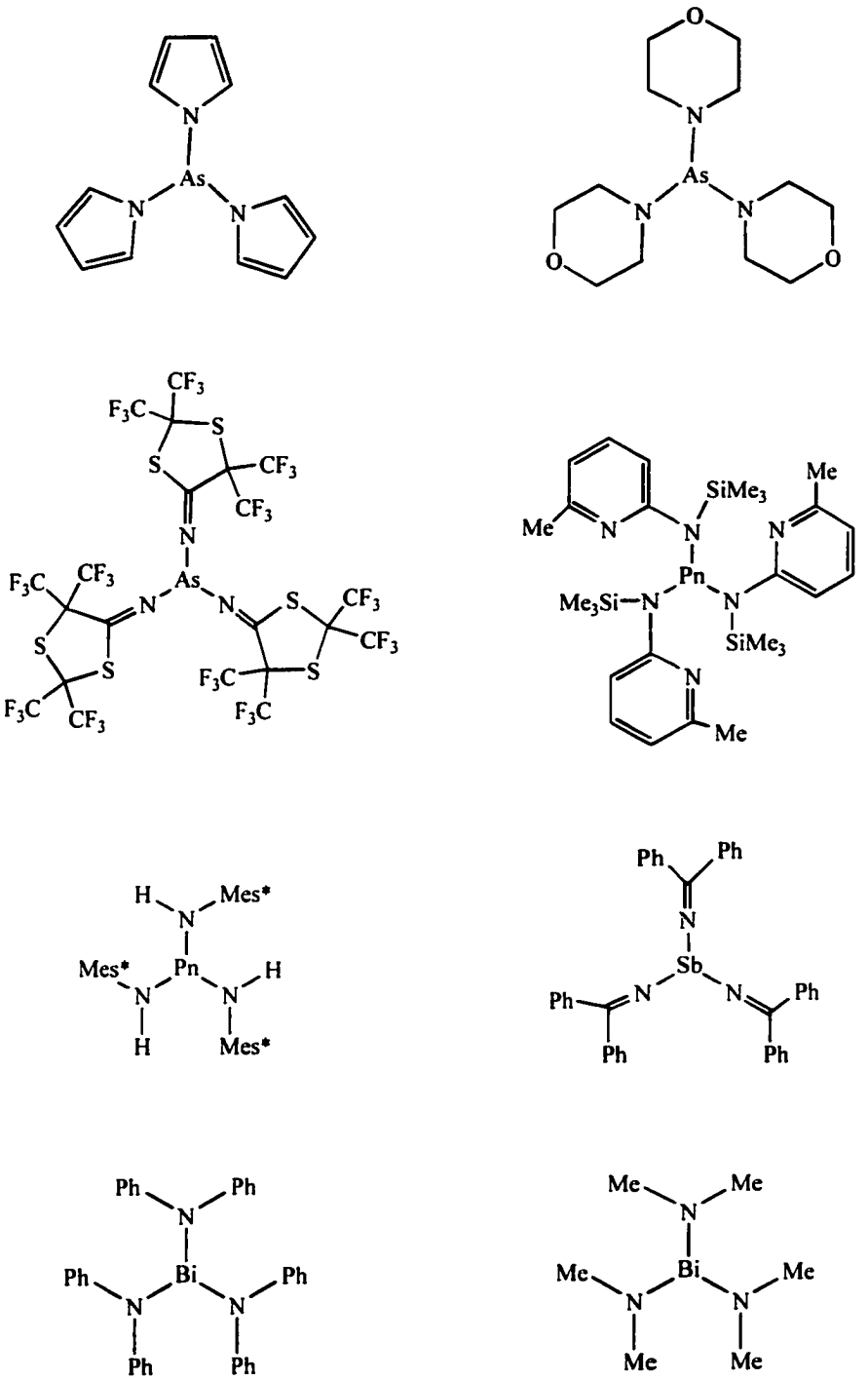

Figure 1.3 Examples of trisaminopnictines.

1.3.1 Monoaminopnictines

Monoaminophosphines[8,30-34] are (in general) synthesised by the addition of lithium amide, R'R"NLi, to either PX_3 or PX_2R (see Figure 1.2). A number of derivatives have been prepared and some examples of monoaminophosphines that have been isolated[7,35,36] are shown in Figure 1.4. Examples of monoaminopnictines (for As and Sb) that have been structurally characterised are shown in Figure 1.5. To date, there are no reports of the synthesis or isolation of any monoaminobismuthines.

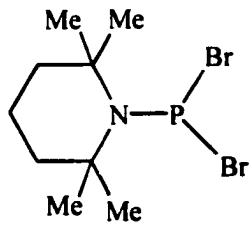

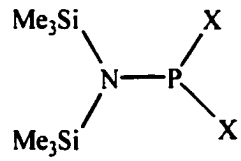

X = F, Cl

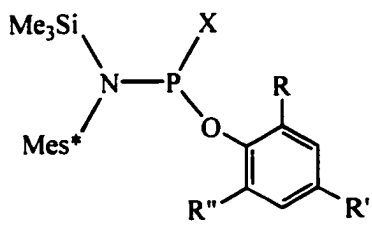

R = R' = R" = Me or H
R = R" = ^{t}Bu, R' = Me
R = R' = H, R" = Me

X = Cl or Br

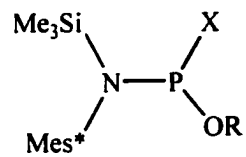

R = ^{t}Bu, ^{i}Pr, Me

X = Cl or Br

Figure 1.4 Examples of monoaminophosphines.

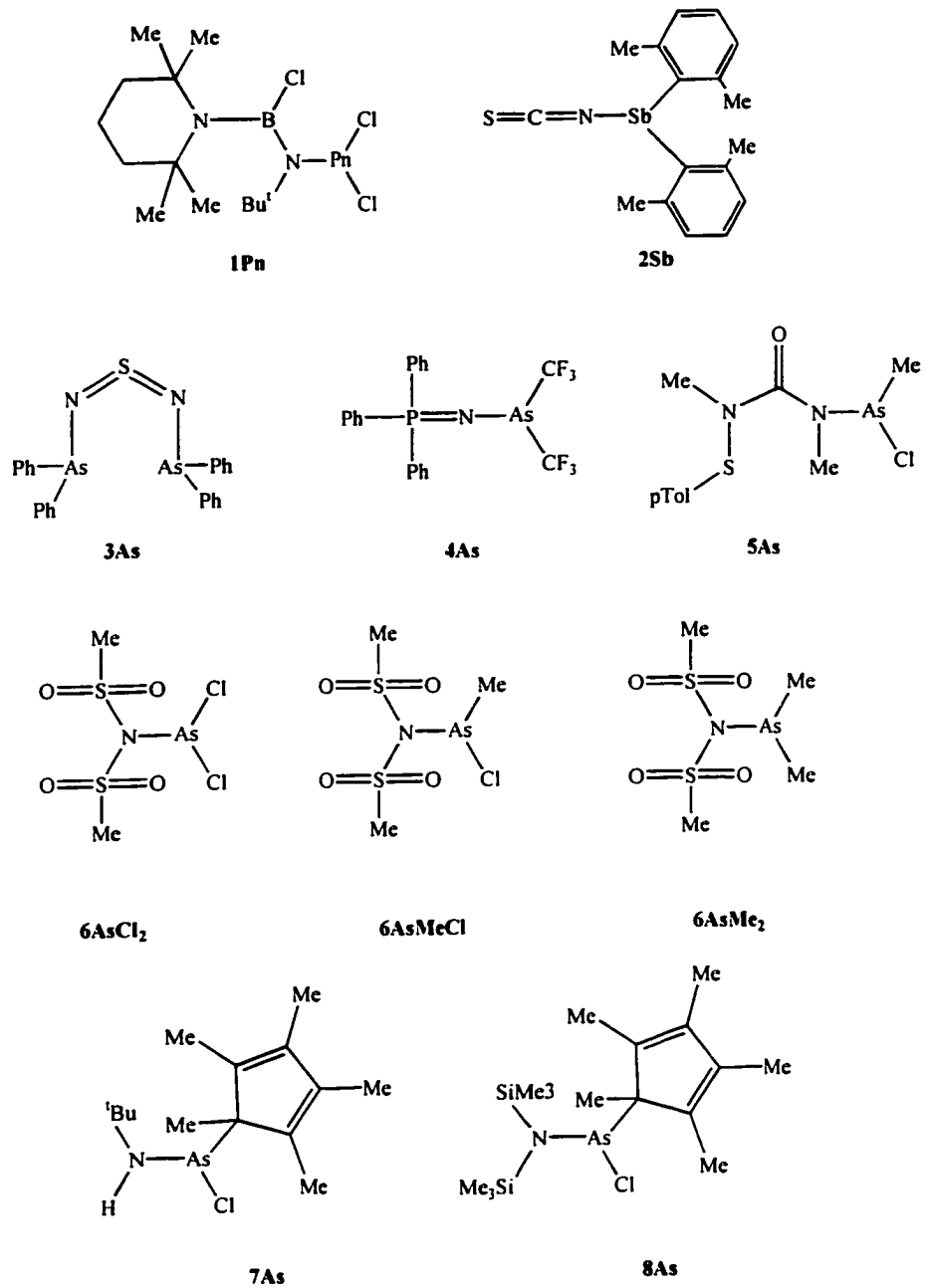

Figure 1.5 Examples of monoaminoarsines and monoaminostibines (Pn = As and Sb).

The monoaminopnictines, **1As** and **1Sb,** are formed[37] as shown in Figure 1.6. This reaction is carried out at 0 °C in hexane. Both compounds were isolated as solids and characterised by m.p., EA, NMR (^{11}B, ^{13}C and ^{1}H) spectroscopy and X-ray analysis. The N-As and N-Sb bond lengths are 1.869(4) and 2.071(3) Å, respectively. There are also close contacts between the N atom of the 2,2,6,6-tetramethylpiperidino substituent and the pnictogen atoms (As, 2.619 Å and Sb, 2.592 Å).

Preparations of compounds **5As**[38], **7As**[39] and **8As**[39] are illustrated in Figure 1.7 and require the preparation of $RAsCl_2$ (R = Me, **5As** and R = Cp*, **7As** and **8As**) before the addition of the corresponding amine. All three compounds were characterised by m.p., EA, NMR spectroscopy (^{1}H and ^{13}C) and X-ray analysis. In addition EI-MS was performed on **7As** and **8As**. The N-As bond length of **8As** (1.874(3) Å) is within the range of a typical N-As single bond (1.84 - 1.87 Å[12]). The monoaminoarsine **7As** has a

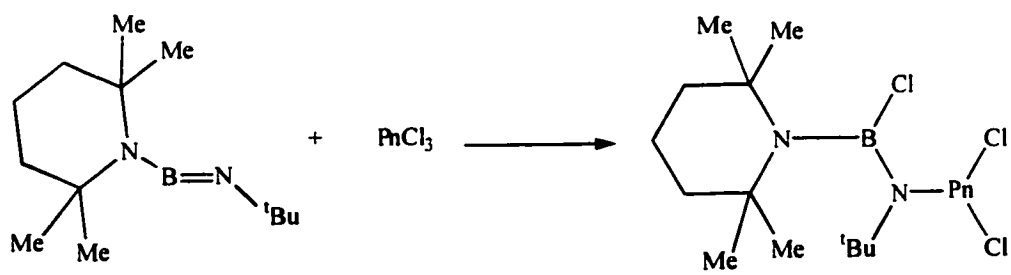

1Pn

Figure 1.6 Reaction scheme, preparation of the monoaminopnictines, **1Pn** (Pn = As, Sb).

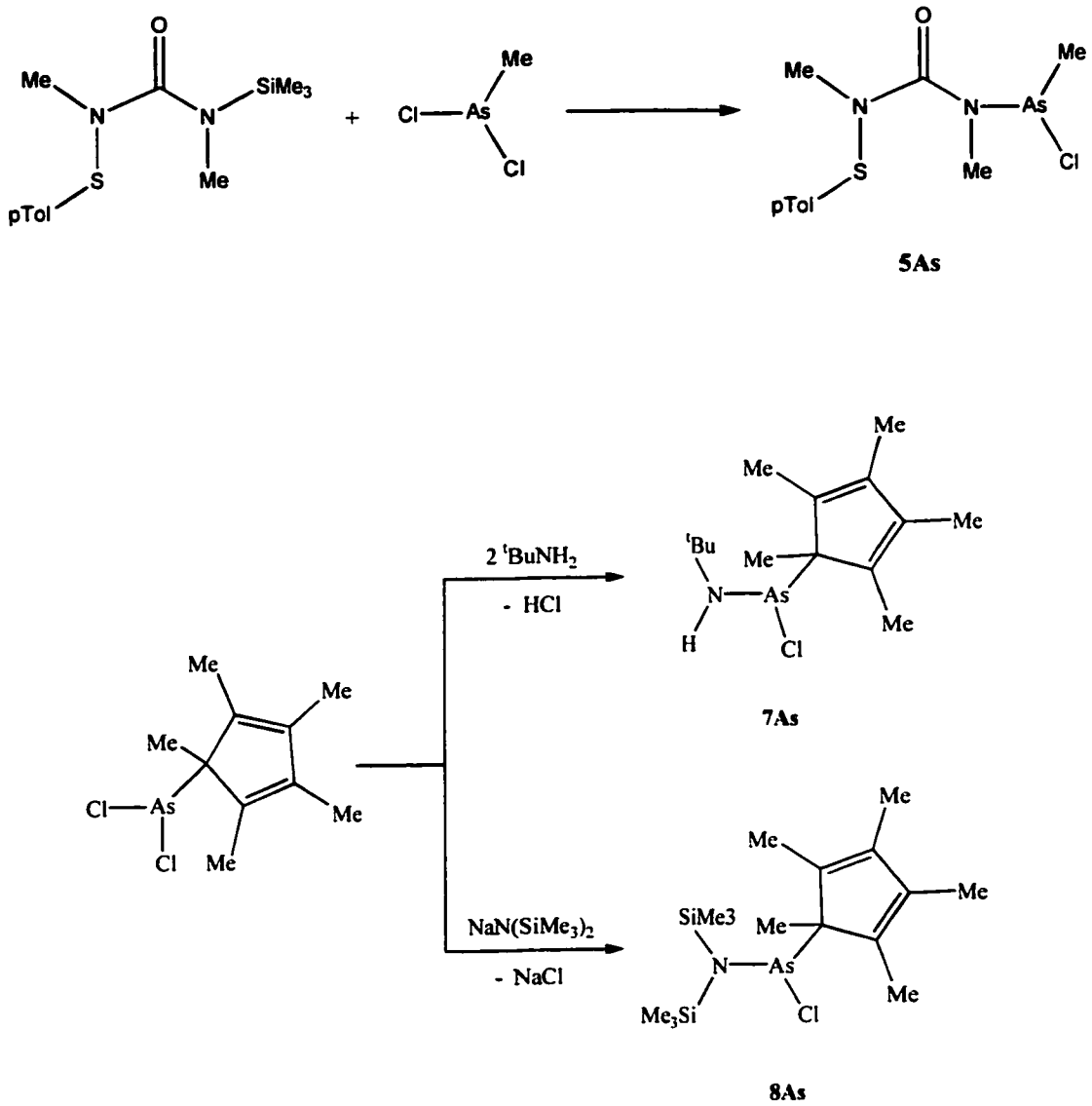

Figure 1.7 Reaction scheme, preparation of the monoaminoarsines, **5As**, **7As** and **8As** from $RAsCl_2$ where R = Me, Cp* or Cp*, respectively.

N-As bond length of 1.802(3) Å that is considerably shorter than **8As** and reflects the effects of using different substituents on the N atom. Compound **5As** crystallises with two independent molecules in the unit cell and has N-As bond lengths of 1.888(3) Å and 1.881(3) Å.

Reaction of the monohalopnictine, R_2SbBr (where R = 2,6-dimethylphenyl), with KSCN forms the aminostibine, **2Sb**[40]. In a similar manner, K_2SN_2 is added to Ph_2AsCl to yield **3As**[41] (Figure 1.8). The monoaminopnictines, **2Sb** and **3As**, were isolated as solids and characterised by m.p., EA and X-ray analysis. In addition EI-MS, NMR (^1H, ^{13}C, ^{14}N) and IR spectra were recorded for **2Sb**. The N-Pn bond lengths in **2Sb** and **3As** are 2.304(5) Å and 1.888(4) Å, respectively.

Addition of $AsCl_3$, $AsCl(Me)_2$ or $AsCl_2(Me)$, to a suspension of $AgN(SO_2Me)_2$ in CH_2Cl_2 resulted in the isolation of **6AsCl$_2$**[42], **6AsMe$_2$**[43] and **6AsClMe**[42], respectively. The N-As bond lengths are 1.938 Å (**6AsCl$_2$**), 1.913 Å (**6AsMeCl**) and 1.979 Å (**6AsMe$_2$**) which are considerably longer than those in any other reported monoaminoarsines.

Distillation of $(CF_3)_2AsN_3$ into a solution of triphenylphosphine in CH_2Cl_2 (Figure 1.9) at liquid nitrogen temperatures allows **4As**[44] to be isolated as a solid. Similar to the previously discussed monoaminopnictines, **4As** was characterised by m.p., EA, X-ray analysis, EI-MS, NMR (^1H, ^{13}C, ^{31}P and ^{19}F) and IR spectroscopy. The N-As

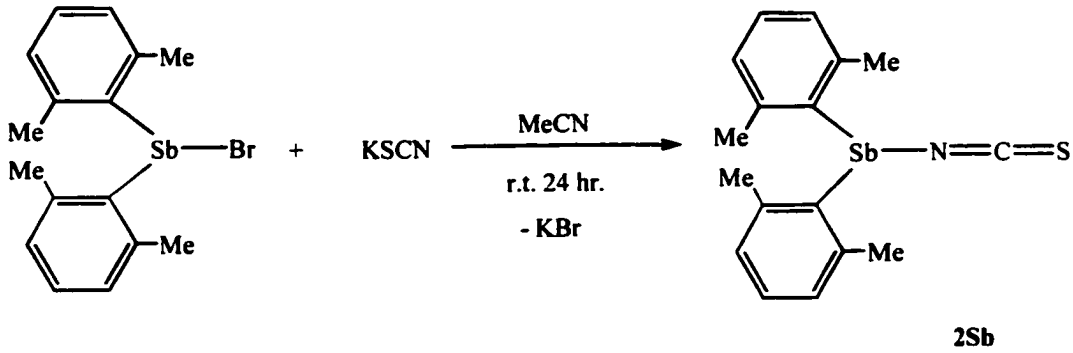

2Sb

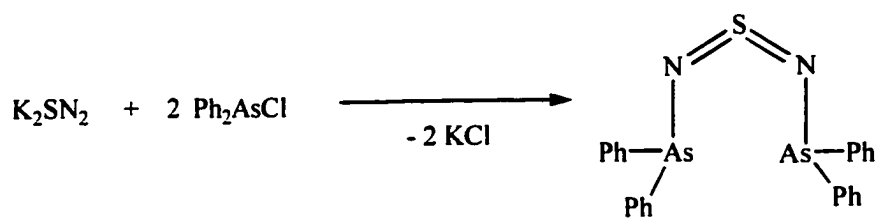

3As

Figure 1.8 Reaction scheme, preparation of the monoaminopnictines, **2Sb** and **3As** from R_2PnCl precursors, where R = 2,6-dimethylphenyl or Ph, respectively.

bond length is 1.783(10) Å, the shortest bond length yet reported for a monoaminoarsine. The N-As and C-As stretches in the IR spectrum (ν(N-As) 443 cm^{-1} and ν(C-As) 537 cm^{-1}) were also identified for **4As**.

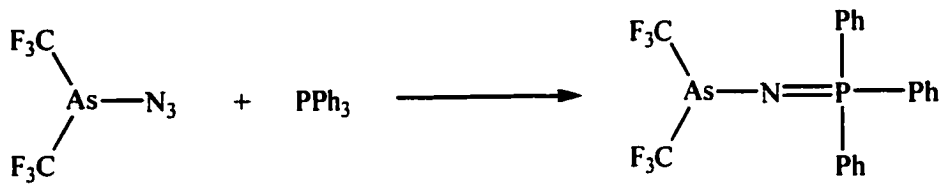

4As

Figure 1.9 Reaction scheme, preparation of **4As**.

The monoaminoarsines (**3As-8As** and **1As**) and the monoaminostibines (**1Sb** and **2Sb**) have N-Pn bond lengths which range from 1.78 - 1.98 Å for Pn = As and 2.30 - 2.59 Å for Pn = Sb. The monoaminopnictines can be characterised by a number of techniques that include IR and NMR spectroscopy, EA, X-ray analysis and EI-MS. In general monoaminopnictines can be prepared using $PnCl_3$, $PnCl_2R$ and $PnClR_2$ as starting materials.

1.3.2 Bisaminopnictines

Both cyclic and acyclic bisaminopnictines have been prepared for P[15,45-55], As[15,17,52,56,57], Sb[19,21,56] and Bi[21,56] and some cyclic examples are shown in Figure 1.11. Cyclic bisaminopnictines are generally prepared[15,49,56] by the reaction of PnX_3 and a lithium diamide, RLiN(R")NRLi (see Figure 1.10). Alternatively, the diamine can be added directly to PnX_3 followed by the addition of base[17,49] (or excess diamine[17]).

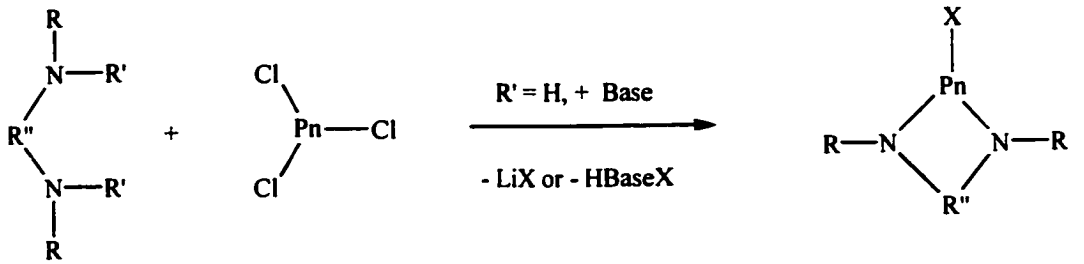

9Pn R = ^{t}Bu, R" = $(CH_2)_2$, R' = Li, Pn = P, As

10As R = Me, R" = $(CH_2)_2$, R' = H, Base = diamine, H(Me)N$(CH_2)_2$ N(Me)H

11P R = ^{t}Bu, R" = $(CH)_2$, R' = Li

12P R = Mes, R" = $(CH)_2$, R' = Li

13P R = ^{t}Bu or Mes, R" = $(CH)_2$, R' = H, Base = NEt_3

14P R = ^{t}Bu, R" = $SiMe_2$, Pn = As, Sb, Bi

15As R = Me, R" = $(CH_2)_3$, R' = H, Base = NEt_3

Figure 1.10 General reaction scheme, preparation of cyclo-bisaminopnictines.

A wide variety of acyclic bisaminophosphines are known and have been isolated as solids[7,30,45-48,51,52,54,58] (such as the derivatives shown in Figure 1.12). The bisaminophosphines, **16P**[59] and **18P**[60], were prepared from the reaction of two equivalents of lithium amide, R'(H)NLi (R' = Mes* or Fmes, respectively), and the corresponding dichlorophosphine, $RPCl_2$ (R = R'). Alternatively, the addition of four equivalents of amine ($R'NH_2$ where R' = Ph or ^{i}Pr) and $PhPX_2$ (X = Cl or Br) will yield **17P**[61] and **19P**[61], respectively.

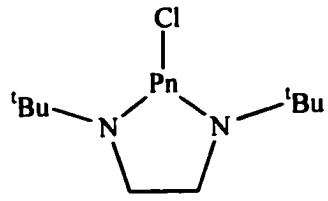

Pn = P, As

9Pn

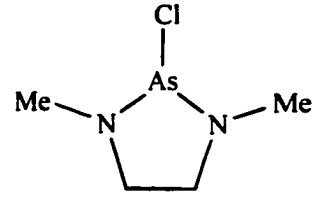

10As

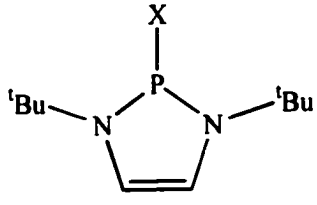

X = F, Cl

11P

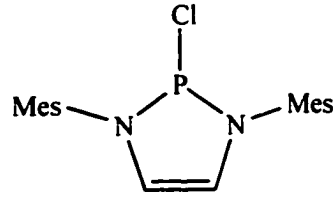

12P

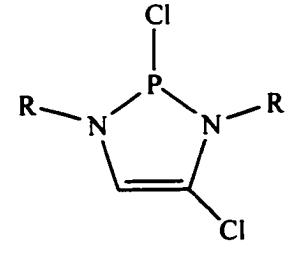

R = tBu, Mes

13P

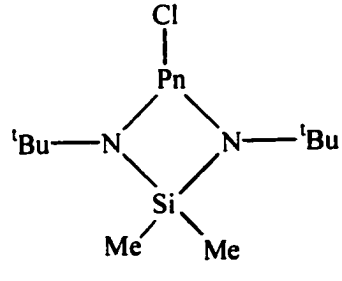

Pn = As, Sb, Bi

14Pn

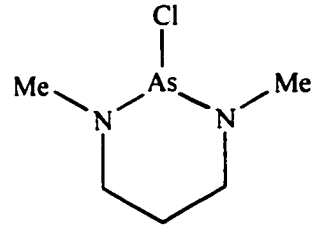

15As

Figure 1.11 Examples of cyclo-bisaminopnictines.

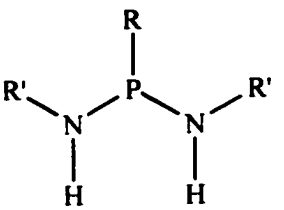

16P R' = R = Mes*

17P R' = R = Ph

18P R' = R = Fmes

19P R' = ^{i}Pr and R = Ph

Figure 1.12 Derivatives of acyclic bisaminophosphines prepared from primary amines (or the corresponding amides).

In comparison to the acyclic bisaminophosphine derivatives, there is only a limited number of examples (isolated in the solid state) for the heavier elements As, Sb and Bi (Figure 1.13). The acyclic bisaminopnictines, **22Sb**[21] and **22Bi**[21], were prepared by the addition of two equivalents of lithium amide to $PnCl_3$ (Pn = Sb or Bi). Characterisation of **22Pn** included m.p., EA, X-ray analysis and NMR (^{1}H, ^{13}C and ^{15}N) spectroscopy. The bismuth analogue (**22Bi**) forms a dimeric unit in the solid state with two adjacent molecules being bridged by chlorine atoms. In contrast, **22Sb** does not have any significant close contacts with any neighbouring molecules. The bisaminostibine, **22Sb**, has two closely related molecules in the unit cell and thus two sets of bond lengths and angles are reported. Both species (**22Sb** and **22Bi**) have intramolecular donation to

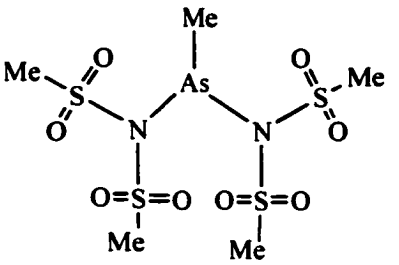

20As

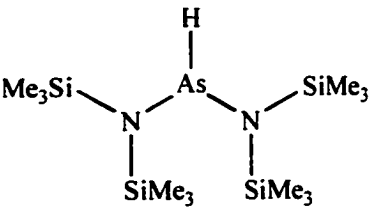

21As

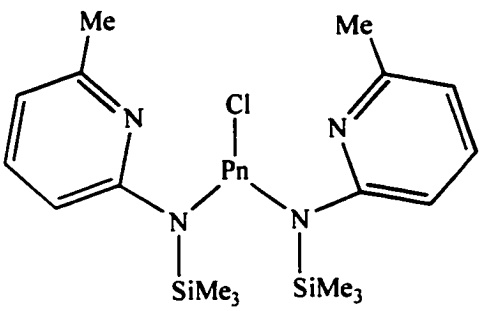

Pn = Sb or Bi

22Pn

Figure 1.13 Examples of acyclic bisaminopnictines.

the pnictogen centre from the N atoms of the aromatic ring (2.401(8), 2.397(8), 2.607(9) and 2.63(1) Å for **22Sb** and 2.49(1) and 2.60(1) Å for **22Bi**). The Pn-N(1) (2.074(3) and 2.095(7) Å for Pn = Sb and 2.15(1) for Pn = Bi) and Pn-N(2) (2.108(9) and 2.127(8) Å for Pn = Sb and 2.271(8) Å for Pn = Bi) bond lengths are not crystallographically equivalent.

The bisaminoarsine, **20As**[43], was prepared by the addition of $MeAsCl_2$ to two equivalents of $AgN(SO_2Me)_2$. The N-As bond lengths are 1.942 and 1.954 Å, which are considerable longer than a typical N-As single bond (1.84 - 1.87 Å[12]). Similarly, long N-As bond lengths were observed for the monoaminoarsines, **6AsCl$_2$** (1.938 Å), **6AsMeCl** (1.913 Å) and **6AsMe$_2$** (1.979 Å). Compound **21As**[52] was isolated from the reaction of $(N(SiMe_3)_2)_2AsCl$ and $LiAlH_4$ and was characterised by X-ray analysis, ^1H NMR and IR spectroscopy. The N-As bond lengths (1.879(3) and 1.874(4) Å) are crystallographically equivalent in this case.

Few acyclic bisaminopnictines for Pn = As, Sb or Bi have been prepared and isolated as solids. The N-As bond lengths are similar to those observed for the monoaminoarsines. The N-Sb bond lengths for **22Sb**[21] (2.40 - 2.63 Å) are comparable to the monoaminostibines, **1Sb** and **2Sb** (N-Sb bond lengths range from 2.30 - 2.59 Å). In general bisaminopnictines are prepared by the reaction of $PnCl_3$ or $PnRCl_2$ and two equivalents of RR'NM (M = Ag or Li). Characterisation techniques include EA, X-ray analysis, NMR and IR spectroscopy.

1.4 Pnictetidines

Four-membered rings consisting of a combination of any four group 15 elements (i.e. R_4Pn_4) are collectively known as pnictetidines. A diazadipnictetidine is the general name for a 4-membered ring consisting of two nitrogen atoms and two heavier pnictogens (P, As, Sb or Bi). However, within this thesis phosphetidine, arsetidine,

stibetidine and bismetidine are used to refer to the series of diazadipnictetidines, $[RNPnR']_2$ (where Pn = P, As, Sb or Bi).

1.4.1 Phosphetidines

There are a number of phosphetidines that have been prepared and isolated[61-77]. Some examples are shown in Figure 1.15. One of the most common synthetic routes involves the reaction of excess amine (or amide) with PX_3. In some cases the dihalophosphetidine, $[RNPX]_2$, can be isolated and used to form additional phosphetidines derivatives. For example, the synthesis of **24P**[78] (Figure 1.14)

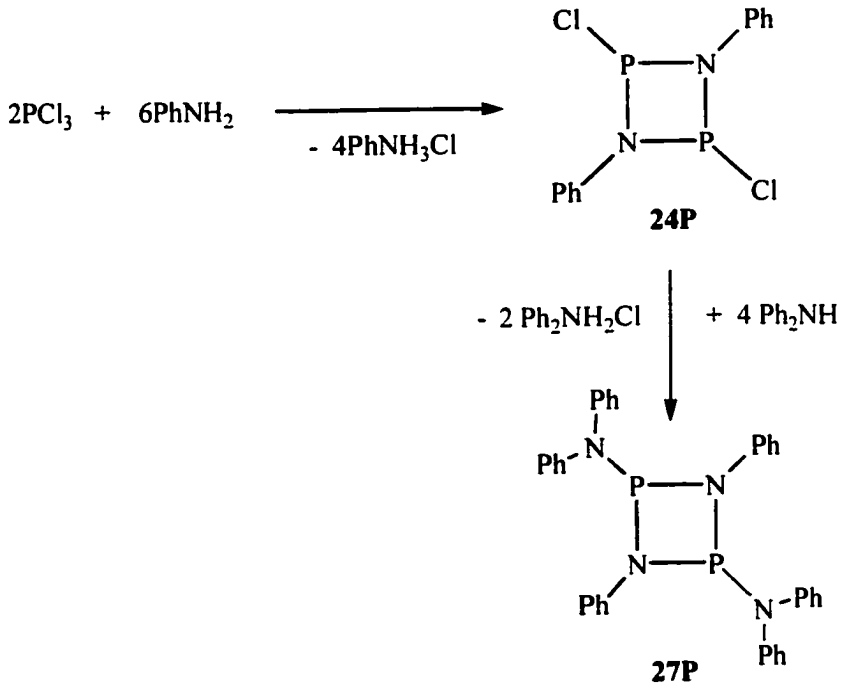

Figure 1.14 Reaction scheme, preparation of **24P** and **27P**.

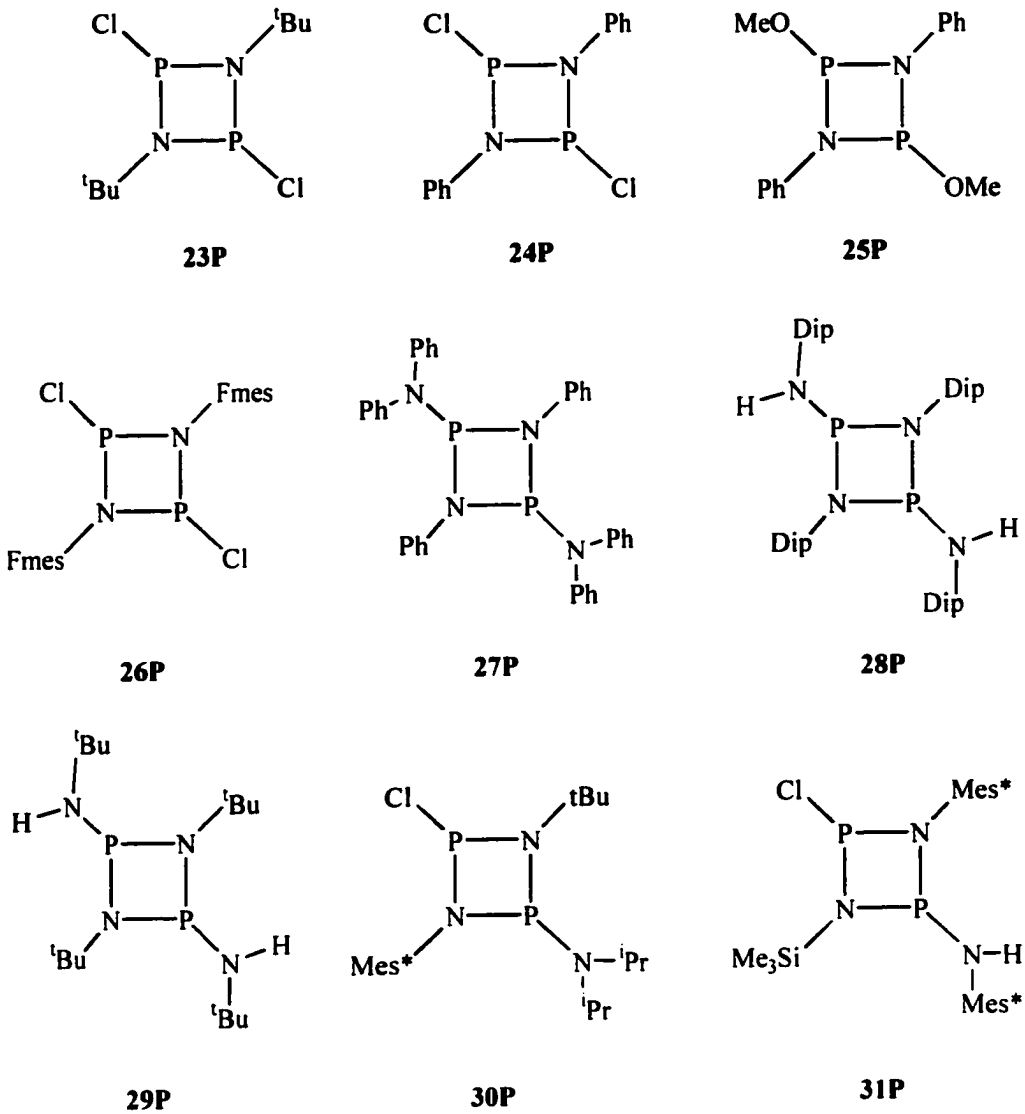

Figure 1.15 Examples of phosphetidines.

is achieved by the reaction of aniline and PCl_3. When two equivalents of Ph_2NH are added to **24P**, the phosphetidine, **27P**[78], is formed. Phosphetidines can also be prepared from the reaction between metal amides and PnX_3. For example, the addition of DipNHLi or FmesNHK to PCl_3 yields **28P**[11] or **26P**[60], respectively (Figure 1.18). It is

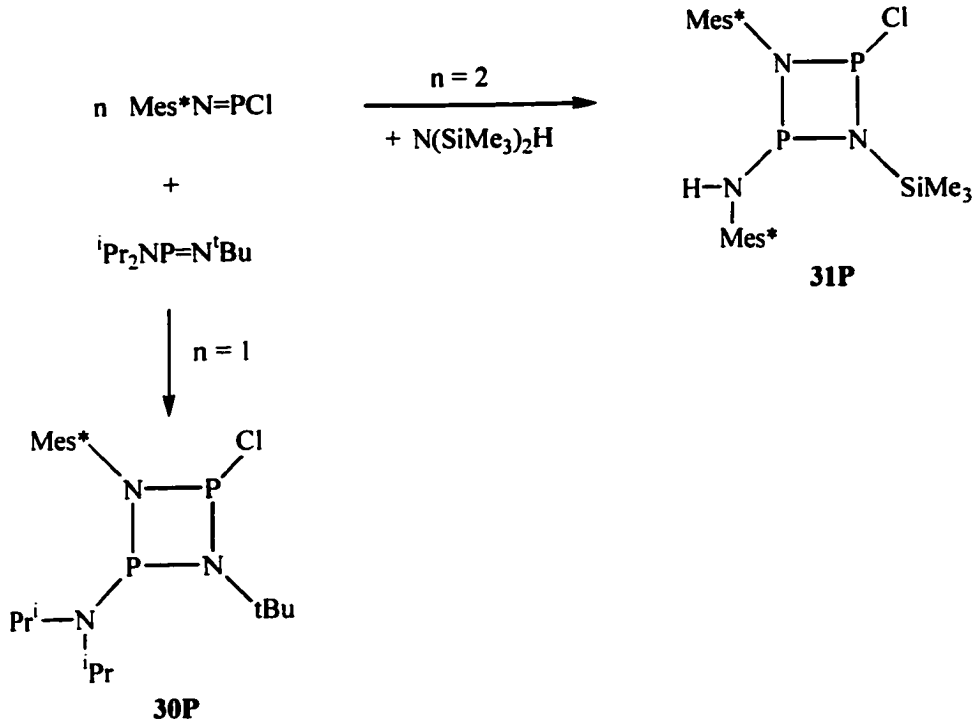

Figure 1.16 Reaction scheme, preparation of asymmetric phosphetidines, **30P** and **31P**.

also possible to isolate asymmetric phosphetidines, such as **30P**[79] and **31P**[80], which are formed by the addition of either $^{t}BuNPN(^{i}Pr)_2$ or $N(SiMe_3)_2H$ to Mes*NPCl (Figure 1.16).

1.4.2 Arsetidines

There are seven compounds containing four-membered AsNAsN rings that have been characterised by X-ray analysis (Figure 1.17). The arsetidines, **23As**[81], **28As**[11] and **34As**[14], were prepared by the reaction of $AsCl_3$ and the corresponding lithium amide (see

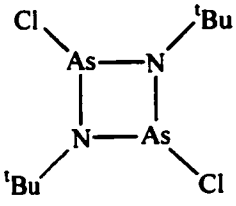

23As

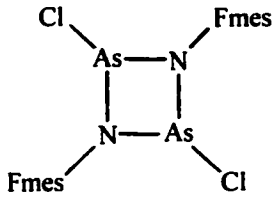

26As

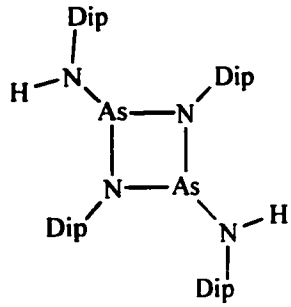

28As

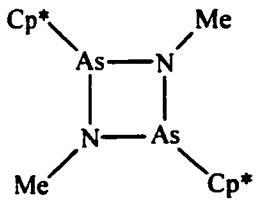

32As

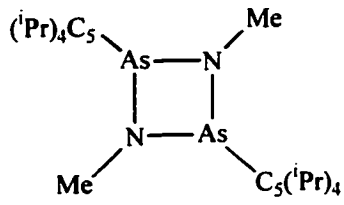

33As

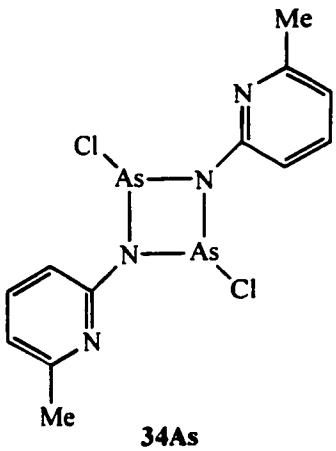

34As

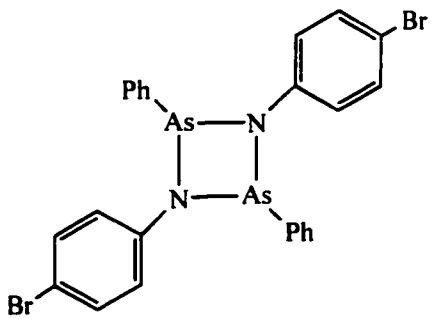

35As

Figure 1.17 Examples of arsetidines.

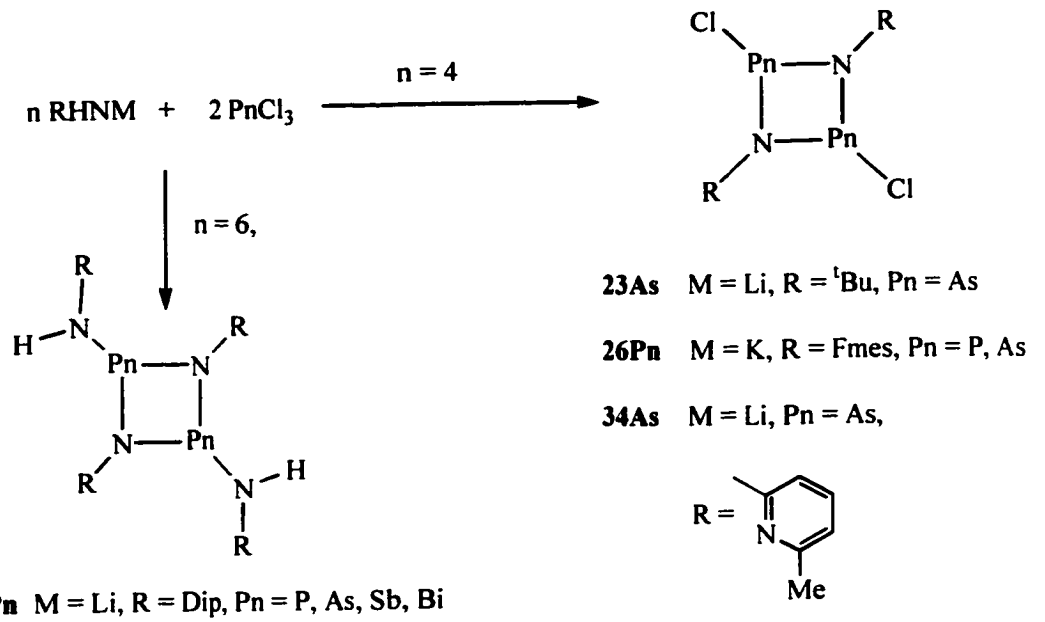

Figure 1.18 Reaction scheme, preparation of pnictetidines from metal amides.

Figure 1.18). In a similar process **26As**[60] was isolated from the addition of FmesNHK to $AsCl_3$. However, **32As**[39] and **33As**[39] were prepared by condensing gaseous $MeNH_2$ into solutions of $Cp'AsX_2$ in diethyl ether (Cp' = Cp* and X = Cl for **32As** and Cp' = $C_5(^iPr)_4$ and X = I for **33As**).

1.4.3 Stibetidines and Bismetidines

There are a total of ten stibetidines (Figure 1.19) that have been characterised by X-ray analysis. The most common[82-84] synthetic method involves the reaction between equimolar amounts of $Sb(NMe_2)_3$ and RNH_2 (see Figure 1.20). Alternatively, the stibetidine, $[^tBuNSbCl]_2$, can be prepared and reacted *in situ* with two equivalents of

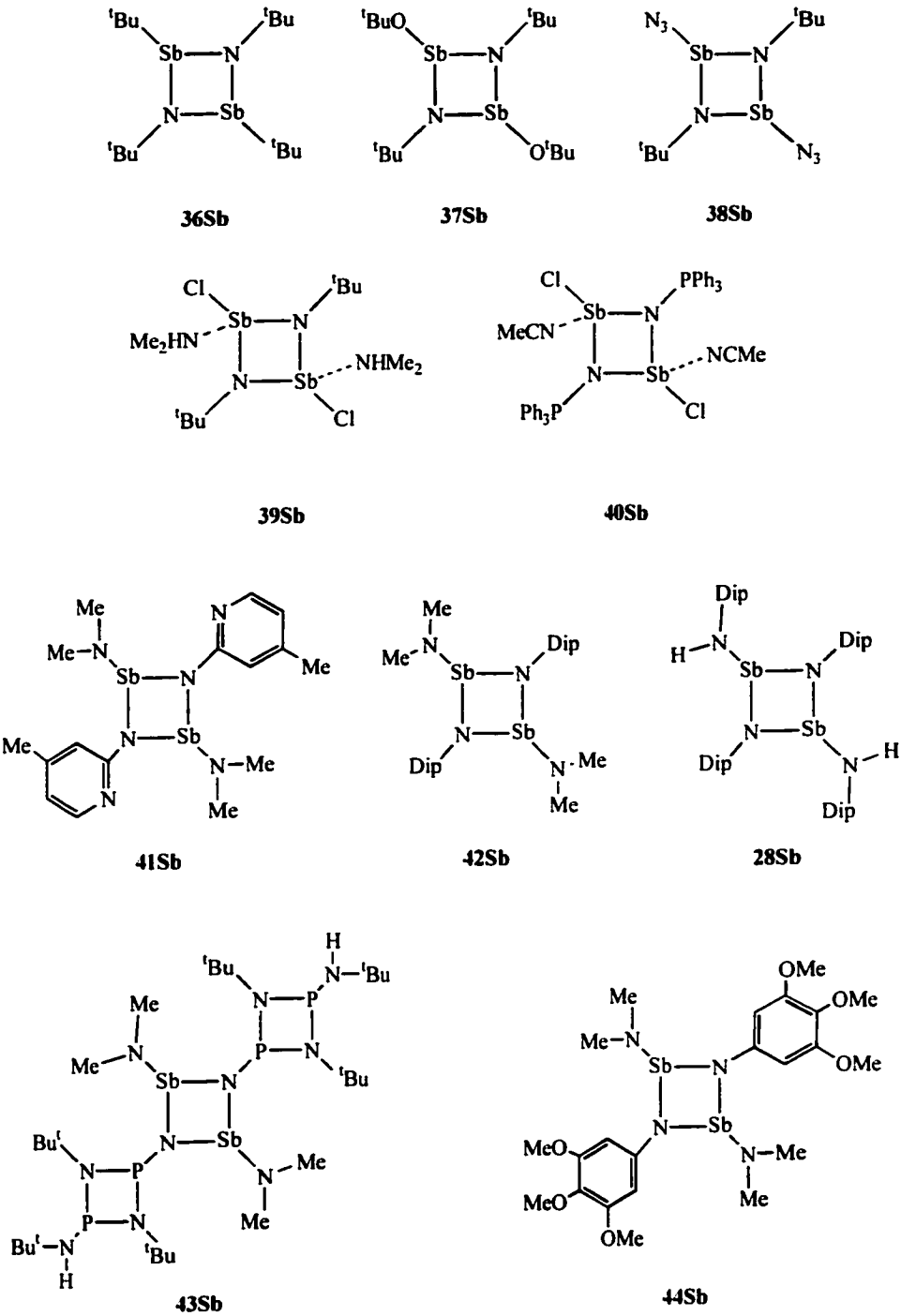

Figure 1.19 Examples of stibetidines structurally characterised.

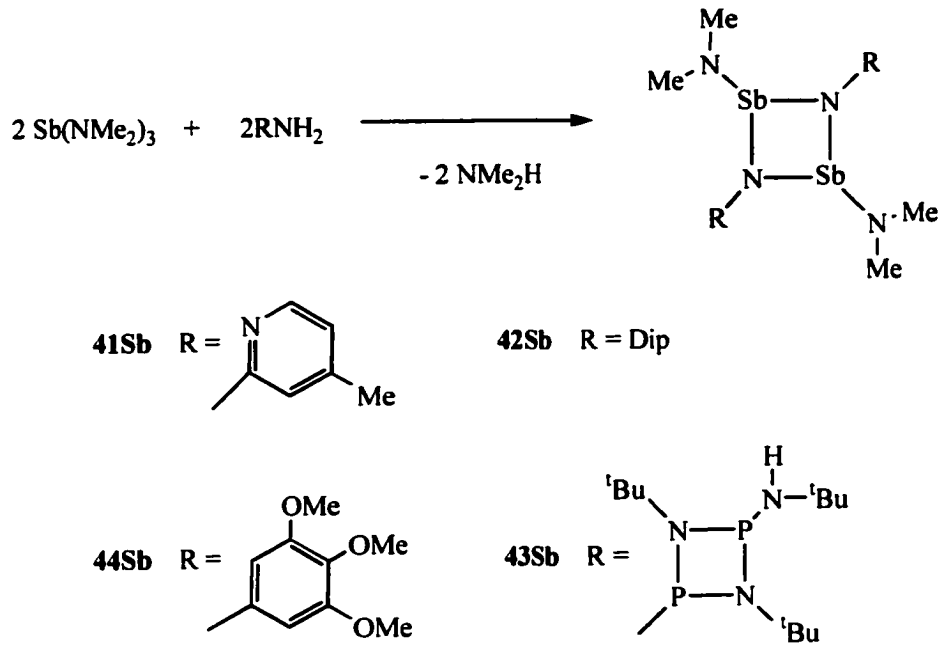

Figure 1.20 Reaction scheme, preparation of stibetidines from $Sb(NMe_2)_3$.

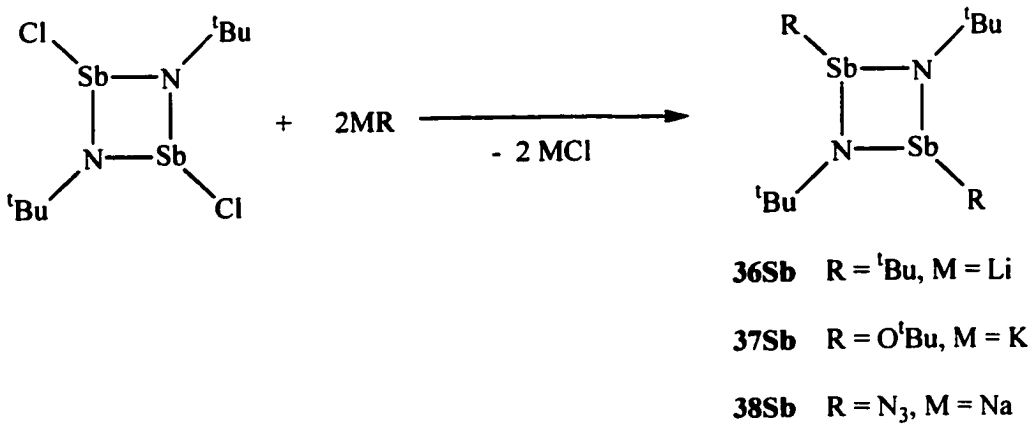

Figure 1.21 Reaction scheme, preparation of stibetidines from $[^tBuNSbCl]_2$.

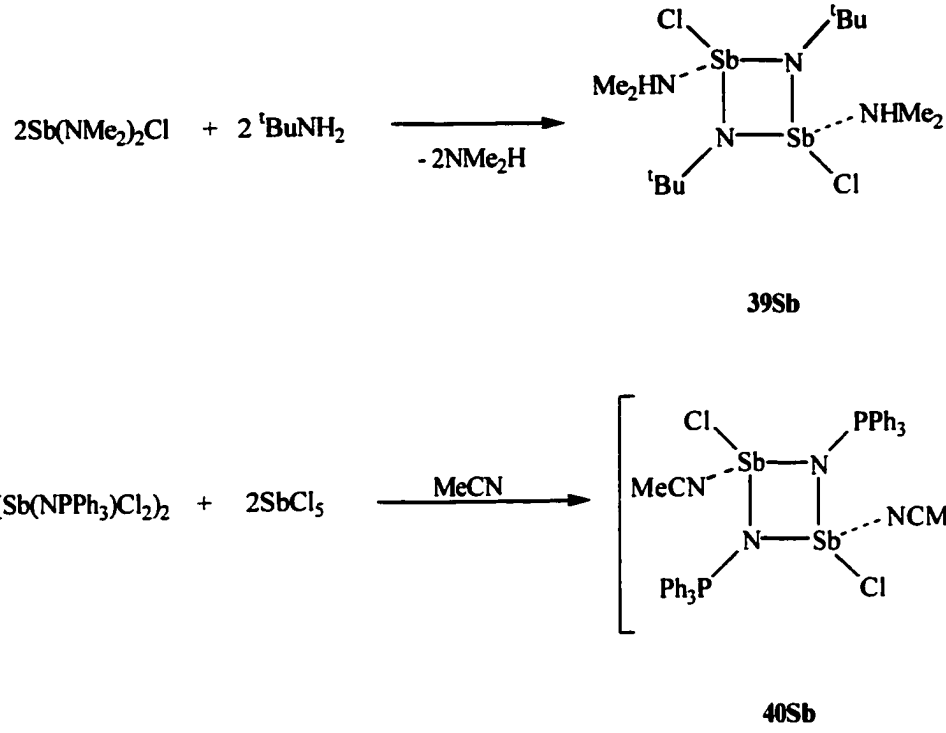

Figure 1.22 Reaction scheme, preparation of **39Sb** and **40Sb**.

NaN_3, KO^{t}Bu or Li^{t}Bu, to yield **38Sb**[85], **37Sb**[85] and **36Sb**[86], respectively (Figure 1.21). Compounds **39Sb**[87] and **40Sb**[88] have been prepared from the reaction between $Sb(NMe_2)_2Cl$ and ^{t}BuNH (**39Sb**) and from the addition of $SbCl_5$ to $(Sb(NPPh_3)Cl_2)_2$ in MeCN (**40Sb**), respectively (Figure 1.22). There is only one bismetidine (**28Bi**[89]) that has been structurally characterised and it was prepared in a manner similar to **28P**, **28As** and **28Sb** (see Figure 1.18).

The pnictetidines (**23P - 44Sb**) were characterised (with few exceptions) by m.p., EA, ^{1}H NMR spectroscopy and X-ray analysis. ^{31}P NMR spectra were also measured for the phosphetidines **24P**, **26P - 28P**, **30P** and **31P**. Other techniques used include ^{13}C (**30P**, **31P**, **34As**, **36Sb**, **37Sb**, **38Sb**) and ^{19}F(**26Pn**) NMR, IR (**23As**, **26Pn**, **27P**, **28Pn**, **31P**, **38Sb**, **39Sb**, **42Sb**), Raman (**28Pn**) and UV-visible (**28Pn**) spectroscopy. In addition, EI-MS was performed on **26Pn**, **27P**, **30P**, **31P**, **32As** and **33As**. The N-Pn (Pn = P, As, Sb or Bi) bond lengths for the pnictetidines (**23P - 44Sb**) are listed in Table 1.1. The Pn-N bond lengths range from 1.68 - 1.78 Å, 1.80 - 1.89 Å and 2.01 - 2.13 Å for Pn = P, As and Sb, respectively. The N atoms, for the planar

Table 1.1 N-Pn bond lengths (reported in Å) of pnictetidines, RNPnR (Pn = P, As, Sb, Bi).

	N-Pn		N-Pn		N-Pn
30P	1.680(3), 1.700(4), 1.744(4), 1.783(3)	**23As**	1.799(5), 1.819(4), 1.826(5), 1.827(4)	**40Sb**	2.018(3), 2.028(3)
23P	1.681(9), 1.687(9), 1.691(9), 1.695(8)	**34As**	1.821(7), 1.809(3), 1.854(3), 1.857(3)	**28Sb**	2.032(6), 2.064(6)
31P	1.687(2), 1.712(2), 1.747(2), 1.757(2)	**33As**	1.851(2), 1.865(2)	**36Sb**	2.043(5), 2.051(4)
24P	1.691(10), 1.698(10)	**26As**	1.852(3), 1.858(3), 1.858(3), 1.865(3)	**42Sb**	2.048(7), 2.052(8), 2.056(8), 2.062(8)
29P	1.702(6),1.725(5), 1.743(5), 1.763(6)	**28As**	1.872(7), 1.878(6), 1.885(7), 1.888(6)	**43Sb**	2.048(9), 2.071(9)
27P	1.703(9), 1.722(9)	**32As**	1.883(2), 1.885(2), 1.885(2), 1.889(2)	**44Sb**	2.048(4), 2.060(4)
25P	1.721(4), 1.734(4)	**37Sb**	2.014(3), 2.027(3)	**41Sb**	2.052(5), 2.068(5)
26P	1.725(3), 1.727(3), 1.730(3), 1.730(3)	**38Sb**	2.015(3), 2.027(3)	**39Sb**	2.071(3), 2.131(3)
28P	1.727(3), 1.739(3)			**28Bi**	2.158(4), 2.174(5)

pnictetidines, are in a trigonal planar environment (sum of the angles around the N atom *ca.* 360°). Phosphetidines and arsetidines can adopt either a *cis* or *trans* arrangement (with respect to the substituents on the pnictogen atoms). However, with the exception of **42Sb**, all other stibetidines have a *trans* configuration (see Table 1.2). Most pnictetidines are planar or have only small deviations from planarity. The only exceptions are **28P**, **28As**, **32As** and **42Sb**, which are folded (butterfly shape) and have dihedral angles (N-Pn-N-Pn) of 154.5 °, 150.4 °, 145 ° and 153.4 °, respectively. The N-Pn-N bond angles for the various pnictetidines are shown in Table 1.2 and range from 84.3 ° to 73.6 °. This reflects the strain associated with the four-membered NPnNPn rings.

1.5 Iminophosphines

A variety of synthetic approaches have been developed for the preparation[90] of iminophosphines, which in turn enables access to numerous derivatives. The most general and versatile reactions are those involving a 1,2-elimination from a coordinatively saturated P-N single bond. For example, the monoaminophosphines shown in Figure 1.4 undergo such reactions. Elimination of SiR_3X or HX can be achieved either thermally or through the addition of a suitable reagent. Other reaction pathways include dissociation[91,92] or substitution reactions[93,94] at the central P atom.

Table 1.2 Structural features of the pnictetidines, RNPnR' where Pn = P, As, Sb, Bi (bond angles are reported in °).

	Pn-N-Pn	N-Pn-N	[PnNPnN]
23P	97.54(14)	80.01(15)	*cis*, folded, 154.5[a]
32As	95.92(8), 96.10(9)	79.38(8), 79.32(8)	*cis*, folded, 145[a]
28As	97.6(3), 97.9(3)	79.0(3), 78.9(3)	*cis*, folded, 150.4[a]
42Sb	101.2(4), 101.6(3)	76.5(3), 76.1(3)	*cis*, folded, 153.4[a]
31P	96.75(11), 97.36(11)	84.31(11), 81.24(11)	*cis*, almost planar, 0.033 Å[b]
30P	96.8(2), 99.1(2)	83.3(2), 79.1(2)	*cis*[c]
23P	96.9(5), 97.6(5)	82.6(4), 82.3(4)	*cis*, almost planar, 0.045 Å[b]
29P	97.2(3), 98.8(3)	81.8(2), 79.6(2)	*cis*[c]
24P	99.7(4)	80.5(4), 80.1(3)	*cis*, planar
25P	99.9(2)	80.1(2)	*trans*
26P	100.0(2)	80.1(2), 80.0(2)	*trans*
27P	101.1(5)	78.9(5)	*trans*
23As	98.6(2), 99.9(2)	80.6(2), 80.1(2)	*cis*, almost planar, 0.09 Å[b]
26As	101.1(1), 101.5(2)	78.9(1), 78.5(2)	*trans*
33As	101.87(10)	78.13(9)	*trans*
34As	103.2(2), 103.5(2)	76.8(3), 76.5(3)	*cis*, planar
40Sb	101.6(1)	78.4(1)	*trans*
37Sb	101.65(12)	78.35(12)	*trans*
36Sb	101.7(2)	78.3(2)	*trans*
28Sb	102.3(3)	77.7(3)	*trans*
38Sb	102.52(11)	77.48(11)	*trans*
43Sb	102.7(4)	77.3(4)	*trans*
39Sb	103.5(1)	76.5(1)	*trans*
44Sb	104.2(2)	75.8(2)	*trans*
41Sb	106.4(2)	73.6(2)	*trans*
28Bi	101.5(2)	78.5(2)	*trans*

(a) dihedral angle N-Pn-N-Pn, *(b)* max deviation of atoms from the plane defined by N_2Pn_2, *(c)* deviation not reported.

1.5.1 Thermal elimination reactions

Thermal elimination reactions of organohalogenosilanes[33,91] (SiR_3X) from aminophosphines, (see Figure 1.23) is one of the most common synthetic methods for the preparation of iminophosphines, R'N=PR". However, depending on the substituents, R' and R", the high temperatures required to remove SiR_3X can result in the formation of a phosphetidine. For example, the bisaminophosphine, ^{t}BuN($SiMe_3$)P(F)NR_2 (**45P**[95], see Figure 1.24), can thermally lose a molecule of $FSiMe_3$, when R is a sterically demanding ligand (such as $SiMe_3$, ^{t}Bu, or ^{i}Pr), to form the iminophosphine, **46P**. However, when R = Et or Me, the formation of [^{t}BuNPF]$_2$, **47P**, is thermodynamically preferred. Formation of **47P** can be avoided by distilling **46P** from the reaction mixture as it is formed. However, this is only suitable for the preparation of volatile compounds.

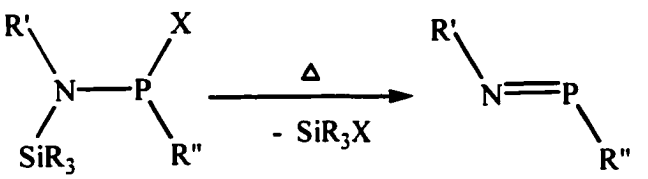

Figure 1.23 General reaction scheme, preparation of iminophosphines by thermal elimination of SiR_3X.

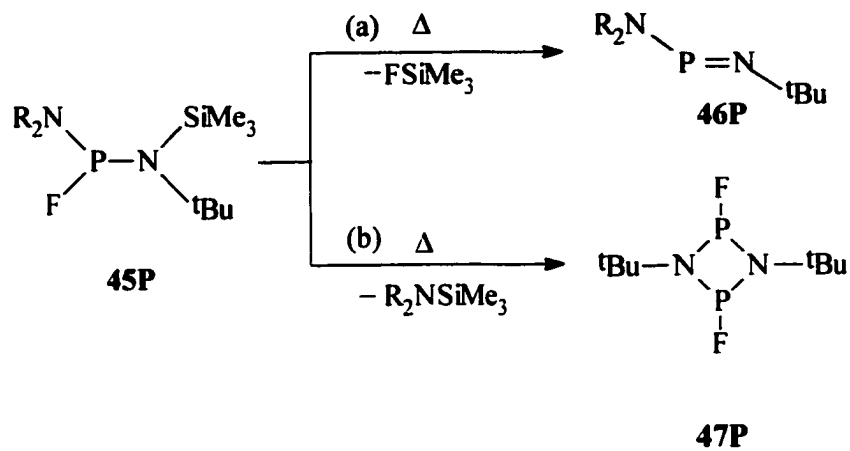

Figure 1.24 Thermal elimination from bisaminophosphine, **45P** governed by the sterics of the substituent, R

(a) R = $SiMe_3$, ^tBu and ^iPr

(b) R = Et and Me

1.5.2 Reagent-induced elimination reactions

Elimination of $SiMe_3Cl$ from the aminophosphines (or amidochlorophosphites), Mes*N($SiMe_3$)PCl(OR) (**48P**, where R = 2,6-^{t}Bu-4-methylphenyl, Me, 1-adamantyl, Ph, 2-MeC_6H_4 or 4-FC_6H_4), is catalysed by the addition (0.05 - 0.2 molecular equivalent) of trimethylsilyltriflate, $SiMe_3OSO_2CF_3$[96], to yield the iminophosphines, **49P** (Figure 1.25).

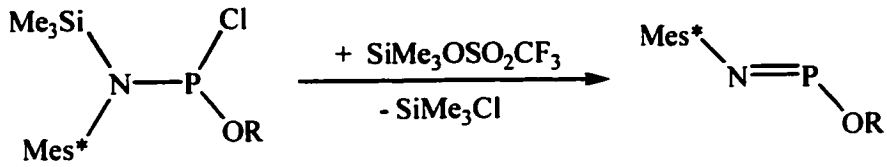

48P **49P**

Figure 1.25 Reaction scheme, preparation of **49P** by the catalytic addition of $SiMe_3OSO_2CF_3$ to **48P**.

Base-induced elimination of HX (more accurately defined as deprotonation), where X = halogen, can result in the formation of phosphetidines[97,98] (e.g. **D2** or **E2**) or higher P, N oligomer[99]. In a few cases, the monomer has been isolated. One example is Mes*N=PCl, **50P**, which is formed from the reaction of the chloroaminophosphine, Mes*N(H)-PCl_2 (**51P**) and triethylamine[9] (Figure 1.26).

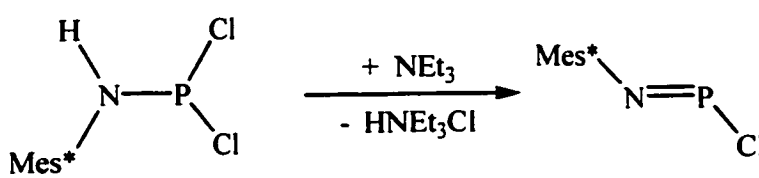

51P **50P**

Figure 1.26 Reaction scheme, preparation of **50P**.

1.6 Iminoarsines

Three iminoarsines have been prepared and characterised by X-ray analysis. The first reported was Mes*N(H)-As=N-Mes*[12] (**52As**), which was produced in the reaction of three equivalents of LiN(H)Mes* with $AsCl_3$. When the monoaminoarsine, $R(Me_3Si)NAsCl_2$ (where $R = N(SiMe_3)_2$), is reacted with Mes*NHLi, followed by the addition of DBU, compound **53As**[100] is isolated. The iminoarsine, **54As**[101], was synthesised by reacting two equivalents of FmesNHK with $FmesAsCl_2$ (see Figure 1.27 for all three reaction schemes). The iminoarsines (**52As** - **54As**) were characterised by X-ray analysis, NMR, mass spectroscopy (for **54As** only), IR and EA. The reported N-As bond lengths are 1.714(7), 1.708(3) and 1.707(2) Å for **52As**, **53As** and **54As**, respectively, all of which are considerably shorter than a typical N-As single bond which ranges from 1.84 - 1.87 Å[12].

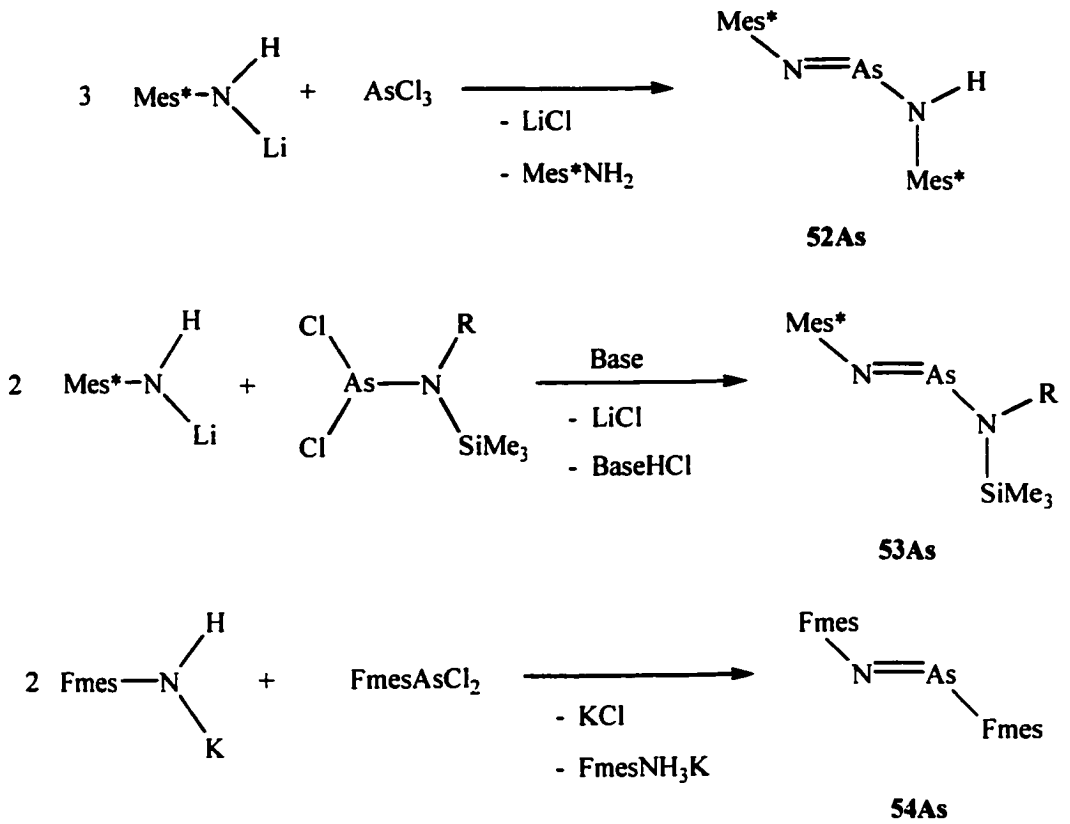

Figure 1.27 Reaction scheme, synthesis of **52As**, **53As** and **54As**.

1.7 Summary

Reactions between amines (or amides) have produced a wide variety of N-Pn compounds (where Pn ≠ N). Aminopnictines (mono, bis and tris) and pnictetidines have been prepared and isolated in the solid state for all the heavier pnictogens (with the exception of monoaminobismuthines). However, low-coordinate compounds containing N and the heavier pnictogens (As, Sb or Bi) are much less common than the

corresponding P derivatives. For example, a number of iminophosphines have been synthesised and characterised. In contrast, there are few examples of low-coordinate compounds containing N and the heavier group 15 elements, As, Sb and Bi (examples of pnictenium cations, $(R_2N)_2Pn^+$, are discussed in Chapter 4). In fact, only three iminoarsines have been isolated and fully characterised and examples of iminostibines or iminobismuthines have not been reported. Synthesis of low-coordinate compounds containing N and As, Sb or Bi would represent a significant contribution to the understanding of the interaction between N and the heavier pnictogens in low-coordinate environments. In this thesis I report the (attempted) synthesis of low-coordinate bisaminopnictines (such as iminopnictines and bisaminopnictenium salts for the heavier group 15 elements As, Sb and Bi) and examine the effects that substituents have on the "R-N-P" framework.

Chapter 2 – Monoaminopnictines, $RR'NPnX_2$ (for Pn = As, Sb)

2.1 Introduction

As discussed in Chapter 1 (Section 1.3.1) monoaminoarsines, such as $^tBuN(H)As(Cl)Cp^*$, **7As**, and $(SiMe_3)_2NAs(Cl)Cp^*$, **8As**, have been isolated[39]. However, in general, there are few examples of structurally characterised monoaminopnictines involving the heavier pnictogen atoms (As, Sb). In comparison, a number of monoaminophosphines have been prepared and are commonly used in the preparation of iminophosphines, RN=PR' (as discussed in section 1.5). With the exceptions of **7As** and **8As**, the previously reported aminoarsines[37,38,41-44] and aminostibines[37,40] do not contain suitable substituents on the N and Pn (Pn = As or Sb) atoms to allow elimination reactions (as observed for the monoaminophosphines) to be carried out. Monoaminopnictines of the general type $Mes^*N(R)PnX_2$ (where R = H or $SiMe_3$, X = halogen and Pn = As or Sb) are ideal substrates from which to begin examination of the desilylation and deprotonation reactions of the heavier pnictogens.

2.2. $Mes^*N(SiMe)PnCl_2$ derivatives

The dichloromonoaminopnictines, $Mes^*N(SiMe_3)AsCl_2$ (**55As**) and $Mes^*N(SiMe_3)SbCl_2$ (**55Sb**) were prepared by the reaction of $Mes^*N(SiMe_3)Li$ (generated *in situ*) with the corresponding $PnCl_3$, as shown in Figure 2.1. Both reactions were carried out by the slow addition of lithium amide (Mes^*NSiMe_3Li) to an excess of

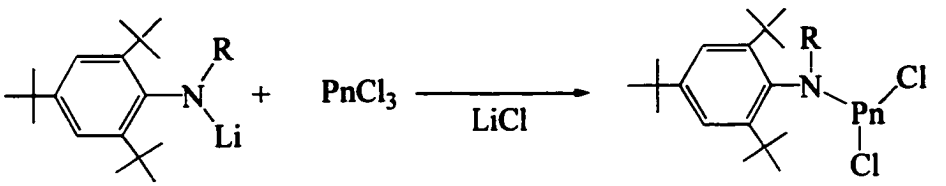

55Pn R = $SiMe_3$ and Pn = As, Sb

56As R = H and Pn = As

Figure 2.1 Reaction scheme for the synthesis of **55Pn** (where R = $SiMe_3$ and Pn = As or Sb) and **56As** (where R = H).

the $PnCl_3$/solvent mixture. The solution was filtered and the solvent removed to yield a yellow oil (for Pn = As) or a yellow solid (for Pn = Sb). The arsenic derivative, **55As**, was isolated by sequential crystallisations (upon standing) of viscous oils. In one such instance, a total of four crystalline batches of **55As** were collected. Preparation of the antimony derivative was performed at both room temperature and 0 °C, however, better yields of **55Sb** were achieved when the reaction was carried out at the lower temperature. Unlike **55As**, the reaction producing the antimony derivative produced a crude solid from which a crystalline material could be obtained by recrystallisation from diethyl ether. During one attempt to prepare **55Sb**, the crude solid material was spectroscopically characterised and showed the presence of two different Mes* environments and both $SiMe_3$ and H substituents (^{1}H NMR and IR spectroscopy). After further work up and recrystallisation, yellow crystals were obtained and characterised as Mes*NH_2·$SbCl_3$ by X-ray analysis. Additional characterisation data (IR, m.p. and EA) for the isolated

crystals showed no evidence of **55Sb**. Even though the crystalline material obtained was not the intended product, it must have been present in the crude reaction mixture. This indicates that additional products are formed in the reaction of Mes*N(SiMe$_3$)Li and SbCl$_3$ but that isolation of **55Sb** is preferred in most cases. Attempts to prepare the bismuth analogue were unsuccessful; the reaction produced more than one product, which complicated the isolation. The most likely products formed, based on the IR and ^{1}H NMR data collected, are a combination of Mes*NH$_2$·BiCl$_3$, Mes*N(SiMe$_3$)BiCl$_2$ and others(such as free amine). The spectroscopic (IR and ^{1}H NMR) features observed were similar to those found in the spectra of the analogous antimony compounds.

The phosphorus analogue, Mes*N(SiMe$_3$)PCl$_2$ (**55P**), has been prepared previously[10] and is spectroscopically similar to the arsenic and antimony derivatives. All three derivatives (**55P**, **55As** and **55Sb**) were characterised by X-ray analysis (see Figures 2.2 and 2.3 for **55As** and **55Sb**, respectively), ^{1}H NMR, IR, and Raman spectroscopy. The purity of the bulk samples was confirmed by m.p. and EA. Selected Raman, IR and NMR data are summarised in Table 2.1. The ^{1}H NMR spectra of the compounds are similar and indicate the presence of both Mes* and SiMe$_3$ substituents, as expected. The Raman and IR spectra are also comparable for all three compounds, **55P**, **55As** and **55Sb**. Intense stretches arising from the SiMe$_3$ substituent are found *ca.* 850 cm^{-1} in the IR spectra. In the fingerprint region, two relatively intense bands are found in each sample (**55P**, **55As** and **55Sb**), ranging between 378 and 312 cm^{-1}. These peaks are tentatively assigned to the Pn-Cl symmetric and asymmetric stretches. Similar

Table 2.1 Comparison of selected spectroscopic data and assignments for compounds **55P**, **55As**, **55Sb** and **56As** (IR and Raman stretches reported in cm^{-1} and NMR signals in ppm).

	55P	**55As**	**55Sb**	**56As**
$PnCl_2$ (IR)	378, 320	364, 321	338, 312	362
$PnCl_2$ (Raman)	376, 325	362, 322	338, 313	370
p-tert-Bu (^{1}H NMR)	1.30	1.31	1.29	1.30
o-tert-Bu (^{1}H NMR)	1.54	1.56	1.57	1.51
Ar-H (^{1}H NMR)	7.46	7.53	7.47	7.38
$SiMe_3$ (IR)	849	855, 841	865	
$SiMe_3$ (^{1}H NMR)	0.27	0.34	0.31	
N-H (IR)				3386
N-H (^{1}H NMR)				5.85

peaks are found in the Raman spectra (**55P**, 376 and 325 cm^{-1}; **55As**, 362 and 322 cm^{-1}; **55Sb**, 338 and 313 cm^{-1}). This suggests that the spectroscopic characteristics of the Mes* and $SiMe_3$ substituents are not significantly perturbed by the pnictogen atom.

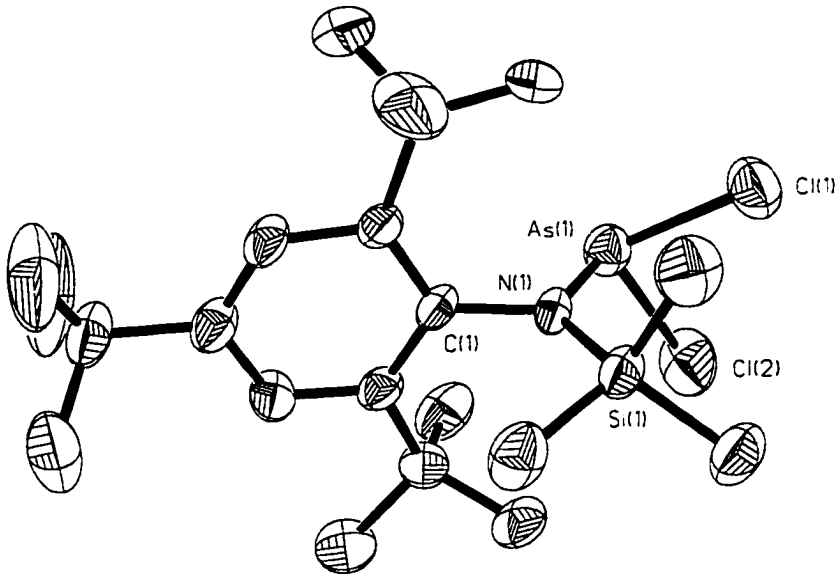

Figure 2.2 Diagram (ORTEP) of the molecular structure of **55As**.

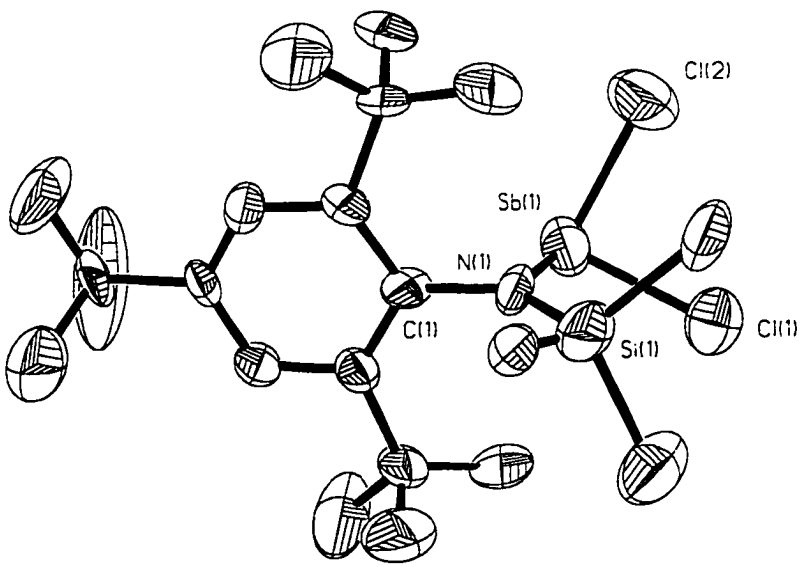

Figure 2.3 Diagram (ORTEP) of the molecular structure of **55Sb**.

2.3 Mes*N(H)PnCl$_2$ derivatives

The addition of Mes*N(H)Li (prepared *in situ*) to $AsCl_3$ (excess) in diethyl ether at room temperature initially produces a cloudy dark purple solution which fades over time (8 hours to 3 days) to yield a pale peach coloured solution and a white precipitate. Upon work up of the solution, a crystalline material was isolated and characterised as Mes*N(H)AsCl$_2$ (**56As**) by ^{1}H NMR, IR, Raman and X-ray spectroscopy (see Figure 2.1 for reaction scheme). The ^{1}H NMR spectrum of the dark purple reaction mixture, showed a number of different Mes* environments. The compounds present, based on the chemical shifts observed in the reaction mixture include, **56As**, **52As** (Mes*N=AsN(H)Mes*, which is a dark purple colour in solution), and other possibilities (such as free amine).

Attempts to isolate the antimony derivative from the reaction of equimolar amounts of Mes*NHLi and $SbCl_3$, led to rapid decomposition of the mixture. However during one procedure a few yellow crystals were isolated from the reaction of two equivalents of Mes*NHLi (prepared *in situ*) added dropwise to a $SbCl_3$/toluene solution at -90 °C (liquid nitrogen/ethanol bath). The isolated crystals were shown to be Mes*N(H)SbCl$_2$·Mes*NH$_2$, **56Sb·Mes*NH$_2$** (see Figure 2.4), by X-ray analysis. The second equivalent of Mes*NH$_2$ apparently facilitates crystallisation and is π-coordinated to the Sb centre (Sb(1)-phenyl centroid distance is 3.395 Å) as shown in Figure 2.5. While the product from this reaction could not be isolated quantitatively, due to the rapid

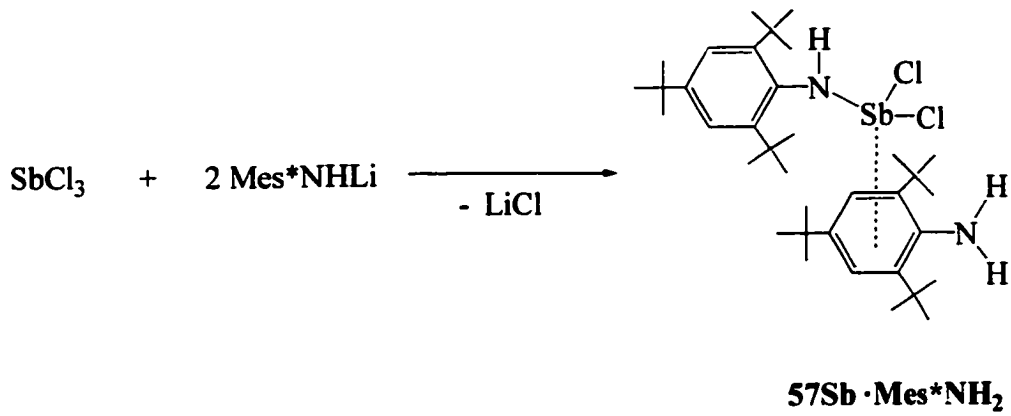

57Sb·Mes*NH$_2$

Figure 2.4 Reaction scheme for the synthesis of **56Sb·Mes*NH$_2$**.

decomposition of the mixture, it confirms that "Mes*N(H)SbCl$_2$" must be present in solution. Spectroscopic characterisation of **56As** by IR and ^{1}H NMR revealed similar results to those observed for the SiMe$_3$ derivatives (see Table 2.1). Since only a few crystals of **56Sb·Mes*NH$_2$** were isolated, a full spectroscopic characterisation could not be carried out. Selected bond lengths and angles are presented in Table 2.2 for **55As**, **55Sb**, **56As** and **56Sb·Mes*NH$_2$**. An ORTEP diagram of the molecular structure of **56As** is shown in Figure 2.6.

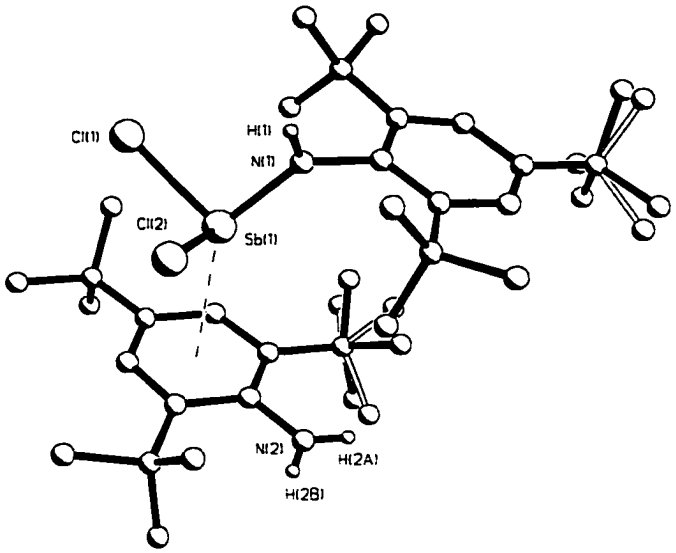

Figure 2.5 Diagram of the molecular structure of **56Sb·Mes*NH$_2$**.

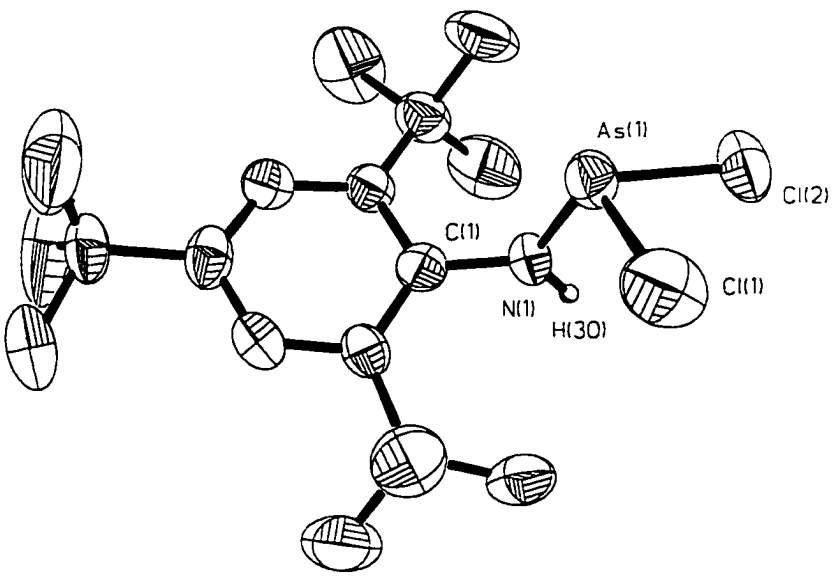

Figure 2.6 Diagram (ORTEP) of the molecular structure of **56As**.

Table 2.2 Selected bond lengths (Å) and angles (°) for $Mes^*N(X)PnCl_2$ (**55As**, **55Sb**, **56As** and **56Sb·Mes*NH$_2$**).

	55As X = $SiMe_3$	**55Sb** X = $SiMe_3$	**56As** X=H	**56Sb·Mes*NH$_2$** X=H
Pn-Cl(1)	2.208(1)	2.342(5)	2.231(3)	2.366(5)
Pn-Cl(2)	2.239(2)	2.367(5)	2.171(3)	2.364(5)
Pn-N	1.809(4)	2.04(1)	1.789(6)	1.955(11)
N-C(1)	1.491(6)	1.47(2)	1.423(9)	1.46(2)
N-X	1.797(4)	1.82(1)	0.95	0.86
Cl(1)-Pn-Cl(2)	91.09(7)	90.1(2)	94.0(1)	87.9(2)
Cl(1)-Pn-N	101.2(1)	99.7(4)	108.0(2)	96.3(4)
Cl(2)-Pn-N	107.2(1)	105.4(4)	96.1(2)	94.7(4)
Pn-N-C(1)	113.6(3)	107.3(9)	119.8(5)	128.0(9)
Pn-N-X	127.7(2)	129.0(6)	120.1	116.0
X-N-C(1)	118.6(3)	124(1)	120.1	116.0
$\Sigma_{N\ angles}$	359.9	360.3	360	360

The Pn-Cl bond lengths in all four dichloromonoaminopnictines (**55As**, **55Sb**, **56As** and **56Sb·Mes*NH$_2$**) are comparable to those found in the corresponding trichlorides, $PnCl_3$[102] (As-Cl, 2.162 Å; Sb-Cl, 2.333 Å) and in the monoaminoarsines (**1As**[37], **5As**[38], **7As**[39] and **8As**[39]), which range from 2.22 - 2.26 Å. The Sb-Cl bond lengths in **1Sb** (2.389(2) and 2.438(2) Å) are consistent with those in **55Sb** and **56Sb·Mes*NH$_2$**. The Pn-N bond lengths in **55As**, **55Sb**, **56As** and **56Sb·Mes*NH$_2$** are within the range established for the previously reported monoaminopnictines (1.78 - 1.89 Å for As-N and 2.07 - 2.30 Å for Sb-N). The N-Si bond lengths are slightly longer than those typically found for R_2N-SiR_3 bonds (1.74 - 1.76 Å)[103] and suggest some steric interaction between the $SiMe_3$ and Mes* substituents. The geometry around the nitrogen atom in all four compounds is planar (see Table 2.2, $\Sigma_{N\ angles}$) suggesting sp^2 hybridisation of the N. Therefore, the structural parameters of **55As**, **55Sb**, **56As** and **56Sb·Mes*NH$_2$** (bond lengths and angles) are as expected for molecules of this type.

2.4 Summary

The synthesis and full characterisation of dichloromonoaminopnictines of the type Mes*N(R)$PnCl_2$ has been achieved for one antimony and two arsenic derivatives (**55As**, **55Sb** and **56As**). The isolation of **56Sb·Mes*NH$_2$** suggests that Mes*N(H)$SbCl_2$ can be prepared *in situ*. The synthesis of compounds such as **55As**, **55Sb**, **56As**, and **56Sb·Mes*NH$_2$** will allow for the future examination of their deprotonation and desilylation reactions with the goal of producing the chloroiminopnictines, Mes*N=Pn-Cl for Pn = As and Sb.

Chapter 3 – Elimination reactions involving the monoaminopnictines, Mes*N(R)PnCl$_2$.

3.1 Introduction

A number of iminophosphines have been prepared[90] from precursors of the general type RR'NPXR through the loss of R'X, where R' = SiR_3 or H and X = halogen. One of the most common elimination reactions[7,8,32,33,35,53-55] is the thermally induced loss of an organosilyl halide group, such as $SiMe_3Cl$. Alternatively, when R' = H the loss of HX can be prompted[9,90] by the addition of a base (as discussed in section 1.5). Similar attempts were made using the monoaminoarsines, **7As** and **8As** (Figure 3.1). However, removal of $SiMe_3Cl$ from **8As** did not occur and the addition of base to **7As** resulted in similar to the arsetidine, **32As**.

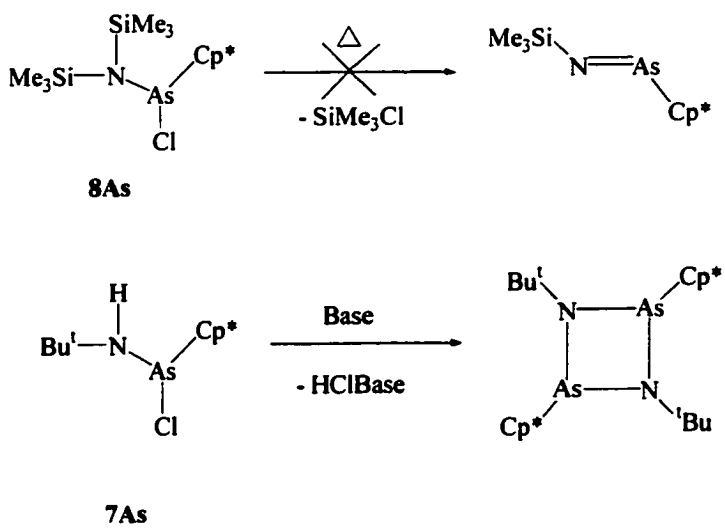

Figure 3.1 Reaction scheme, desilylation (attempted) and deprotonation of monoaminoarsines (**7As** and **8As**).similar to the arsetidine, **32As**.

3.2 Deprotonation reactions involving Mes*N(H)PnCl$_2$.

Reaction of Mes*N(H)AsCl$_2$, **56As**, with an excess of triethylamine in diethyl ether resulted in the immediate formation of a white precipitate and a dark purple solution. Attempts to isolate the product of this reaction by slow evaporation of solvent at room temperature resulted in the formation of a yellow crystalline material. This compound was characterised (in collaboration with C.L.B. Macdonald[10]) as the bicyclic arsine, **57As** (shown in Figure 3.2). However, if small aliquots (about 3-5 ml) of solvent were removed periodically throughout the crystallisation process and the reaction mixture was kept cold (approximately 10 °C), a dark yellow crystalline material was obtained. This compound was characterised as the arsetidine dimer, **58As** (Figure 3.2).

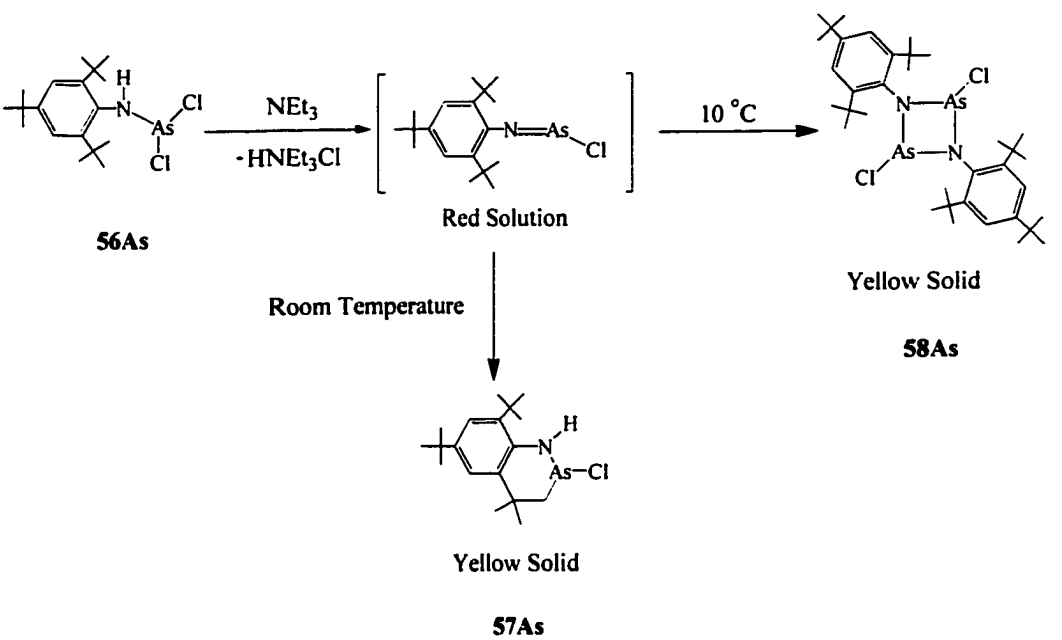

Figure 3.2 Reaction scheme for the preparation of **57As** and **58As**.

Despite the isolation of a crystalline sample of **58As**, it proved difficult to obtain a pure bulk sample. One impurity identified (^{1}H NMR spectroscopy and X-ray analysis) was $HNEt_3Cl$, a by-product of the reaction. In general, reactions producing $HNEt_3Cl$ as by-product are carried out in a non-polar solvent (such as hexane), allowing it to be removed by filtration. However it is necessary to perform the reaction and isolation of **58As** in a donor solvent, such as Et_2O. Separation of $HNEt_3Cl$ from the crude mixture was not possible by sublimation because **58As** and $HNEt_3Cl$ cosublime. Purification of a bulk sample was only achieved by dissolving the crude solid mixture in hexane, followed by rapid filtration (while keeping the solution below room temperature) and removal of solvent to produce a yellow powder. This powder was then dissolved in a minimal amount of Et_2O producing a dark red solution. The yellow, cube-shaped crystals, which grew from the solution over a period of 1-2 weeks (at 10°C), were shown to be **58As** by X-ray analysis, ^{1}H NMR and IR spectroscopy. The purity of the bulk sample (of **58As**) was verified by m.p. and EA. Interestingly, before **58As** melts it undergoes a colour change from yellow to red. There is also a change in colour from solution (reaction mixture, dark purple and redissolved solid, red) to solid state (dark yellow). It is proposed, based on these colour changes, that **58As** exists as a monomer in solution and a dimer in the solid state based on these colour changes.

Reaction of **56Sb·Mes*NH$_2$** (prepared *in situ*, as described in section 2.3) and one equivalent of $AgOSO_2CF_3$ in toluene (see Figure 3.3), yields orange crystals which were characterised (NMR, IR and X-ray spectroscopy) as the stibetidine, $[Mes^*NSbOSO_2CF_3]_2$ (**59Sb**).

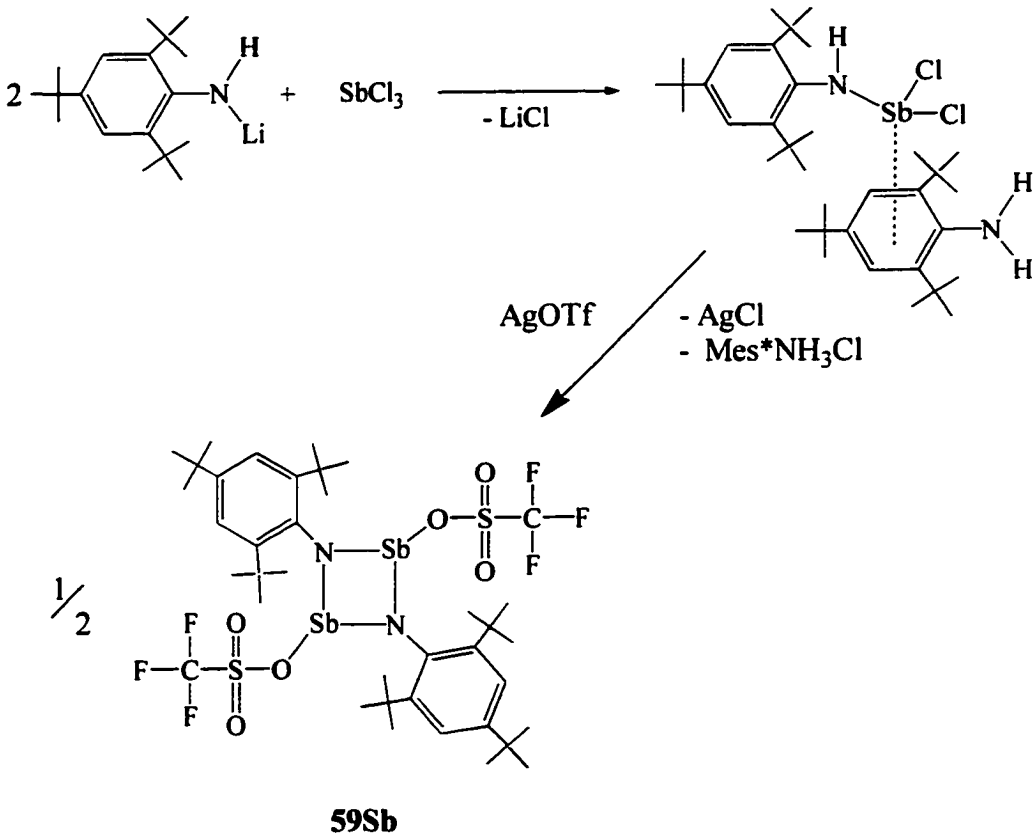

59Sb

Figure 3.3 Reaction scheme for the preparation of **59Sb**.

The pnictetidines, **58As** and **59Sb**, were characterised by NMR, IR and Raman (**58As** only) spectroscopy, X-ray analysis, m.p. and EA. The ^{1}H and ^{19}F (**59Sb** only) NMR chemical shifts for **58As** and **59Sb** are listed in Table 3.1. The corresponding spectroscopic data for the monomeric phosphorus compounds, Mes*NPCl (**50P**) and Mes*NPOSO$_2$CF$_3$ (**60P**), are included in Table 3.1 for comparison. As observed in the

Table 3.1 Selected NMR data (^1H and ^{19}F in ppm) for **58As**, **50P**, **59Sb** and **60P**.

	58As	**50P**	**59Sb**	**60P**
p-tert-Bu (^{1}HNMR)	1.31	1.35	1.29	1.32
o-tert-Bu (^{1}HNMR)	1.62	1.49	1.64	1.49
Ar-H (^{1}H NMR)	7.37	7.40	7.41	7.42
OSO_2CF_3 (^{19}F NMR)			- 78.1	- 78.3

starting materials, **55P**, **55As**, **55Sb** and **56As** (Table 2.1 Chapter 2), the proton chemical shifts of the Mes* group for **58As**, **59Sb**, **50P** and **60P** are similar. This is not unexpected considering the similarity of the proton environments of the Mes* substituent.

The dimeric structure of **58As** is shown in Figure 3.4 and selected bond lengths and angles are listed in Table 3.2. The NAsNAs four-membered ring is planar with the substituents on As out of the plane of the ring in a trans configuration. The N atoms are in a trigonal planar environment (the sum of the angles is 358 °). The N-As bond lengths (1.84(1) and 1.87(1) Å) are crystallographically equivalent and are within the range of typical N-As single bonds (1.79 - 1.88 Å[12]). Interestingly the monoaminoarsine precursor **55As** has a slightly shorter N-As bond length (1.789(6) Å) than in **58As**. There are seven related NAsNAs four-membered rings that have been crystallographically

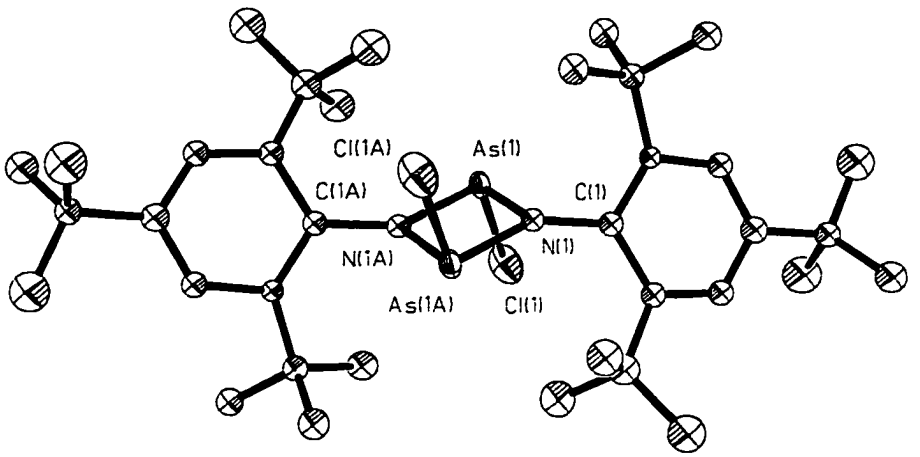

Figure 3.4 Diagram (ORTEP) of the molecular structure of **58As**.

characterised (see also Section 1.4, Chapter 1). Four have a *cis* configuration (**23As**, **28As**, **32As** and **34As**) while the others (**26As**, **34As** and **35As**) are planar and have a *trans* configuration. In most cases, the N-As bond lengths within the ring are not crystallographically equivalent. The bond lengths range from 1.78 - 1.89 Å and are comparable to those in **58As**. The Mes* substituent of **58As** is not planar (C(*ipso*) deviates from the plane defined by the aromatic ring) and is twisted 117.3 ° from the NAsNAs plane, indicating a degree of steric strain. The As-Cl bond length (2.233(5) Å) is within the range typical of As-Cl bonds and is also similar to those found in **34As** (2.228(2) and 2.233(2) Å), **26As** (2.2216(1) Å) and **23As** (2.249(3) and 2.252(2) Å).

Table 3.2 Selected bond lengths (Å) and angles (°) for **58As** and **59Sb**.

	58As	**59Sb**
Pn(1)-N(1)	1.84(1)	2.019(5)
Pn(1)-N(1)'	1.87(1)	2.031(5)
N(1)-C(ipso)	1.43(2)	1.464(8)
Pn(1)-O(1)		2.139(4)
S(1)-O(1)		1.499(5)
S(1)-O(2)		1.402(6)
S(1)-O(3)		1.429(6)
Pn(1)-Cl(1)	2.233(5)	
N(1)-Pn-N(1)'	80.7(5)	79.3(2)
Pn(1)'-N(1)-Pn(1)	99.3(5)	100.7(2)
Pn(1)-N(1)-C(ipso)	140.4(9)	142.1(4)
Pn(1)'-N(1)-C(ipso)	118.1(8)	113.5(4)
N(1)-Pn(1)-O(1)		96.82(19)
N(1)'-Pn(1)-O(1)		90.90(18)
Cl(1)-Pn(1)-N(1)	104.7(3)	
Cl(1)'-Pn(1)-N(1)	99.3(5)	

The solid state structure of $[Mes^*NSbOSO_2CF_3]_2$, **59Sb**, is shown in Figure 3.5 and selected bond lengths and angles are found in Table 3.2. There are ten structural reports for NSbNSb dimers (as discussed in section 1.4), nine of which are centrosymmetric and one that adopts a *cis* conformation, **28Sb**[11]. The N-Sb bond lengths in **59Sb** (2.019(5) and 2.031(5) Å) are comparable to those in previously isolated stibetidines (range from 2.02 - 2.07 Å). The N atoms are in a trigonal planar environment (the sum of the bond angles is 356.3°). The Mes* substituent of **59Sb** is twisted 112.6 ° from the NSbNSb plane, suggesting a degree of steric strain.

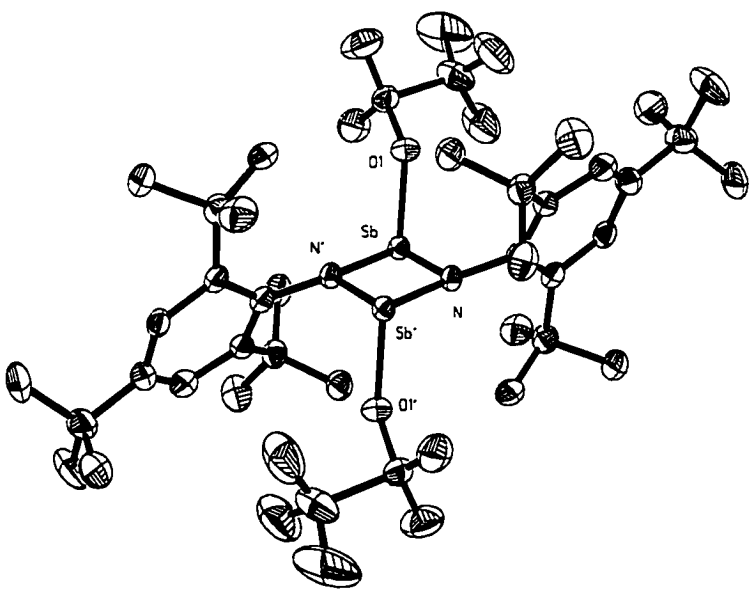

Figure 3.5 Diagram (ORTEP) of the molecular structure of **59Sb**.

3.3 Desilylation reactions involving Mes*N(SiMe$_3$)PnCl$_2$

Thermal desilylation of Mes*N(SiMe$_3$)AsCl$_2$, **55As**, was carried out in tetrahydrofuran (THF-d$_8$) over a range of 20-128 °C, for a period of 4 days. The use of a deuterated solvent allowed the reaction to be monitored by ^{1}H NMR spectroscopy. Initially a red solution was formed. Peaks observed in the ^{1}H NMR spectrum were assigned to the starting material (**55As**), to SiMe$_3$Cl and to a unique Mes* environment. As the sample was heated for longer periods of time, the second set of Mes* peaks and those attributed to SiMe$_3$Cl, increased in intensity. However, refluxing a bulk sample of **55As** in a high boiling solvent (THF or mesitylene) did not result in the elimination of SiMe$_3$Cl and no colour change was observed during this reaction. On only one occasion the bicyclic arsine, **57As**, was obtained[10] from this reaction. Reaction of the ortho-^{t}Bu groups of the Mes* substituent to form cyclic species has been reported previously for a compound containing both As and the Mes* substituent[104]. This result shows that desilylation has in fact occurred. However, the high temperatures utilised in the reaction allowed the formation of an alternative isomer instead of the targeted iminoarsine, Mes*N=AsCl.

3.4 Summary

The pnictetidines, $[Mes^*NAsCl]_2$ (**58As**) and $[Mes^*NSbOSO_2CF_3]_2$ (**59Sb**), were prepared from the corresponding monoaminopnictine precursors, **56As** and **56Sb·Mes*NH$_2$**, respectively. The arsetidine, **58As**, and the stibetidine, **59Sb**, were characterised as dimers in the solid state. However, the colour changes observed for **58As** suggest that it may exist as a monomer in solution. The temperatures required for the thermal desilylation of **55As** resulted in the formation of the cyclodecomposition product, **57As**. This compound was also observed in the preparation of the arsetidine, **58As**, when the reaction mixture was allowed to remain at room temperature for more than 10-15 minutes.

Chapter 4 – Acyclic Pnictenium Cations

4.1 Introduction

Few examples of bisaminopnictenium cations, $(R_2N)_2Pn^+$ (where Pn = P, As, Sb or Bi), have been isolated as solids and most of the cited examples are cyclic[15,17,18,105] in nature (see Figure 4.2). They are generally prepared by the abstraction of a halide ion from the corresponding cyclic bisaminopnictine (such as those shown in Figure 1.11) using for example ECl_3, where E = Al or Ga. However, these salts can have significant anion/cation interactions[18] (**64PnAlCl$_4$**) and in some cases the cations form dimeric units in the solid state[17] (**61AsX**). Three derivatives of acyclic bisaminophosphenium salts, **66PGaCl$_4$**[106], **67PX**[107,108] and **68POSO$_2$CF$_3$**[109] (Figure 4.1), have been characterised in the solid state, but synthetic or structural information for acyclic bisaminopnictenium salts containing the heavier pnictogens (As, Sb and Bi) have not yet been reported.

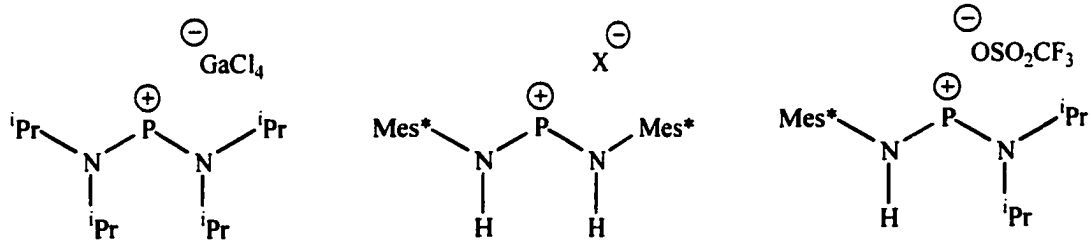

66PGaCl$_4$ **67PX** **68POSO$_2$CF$_3$**

Figure 4.1 Examples of bisaminophosphenium salts.

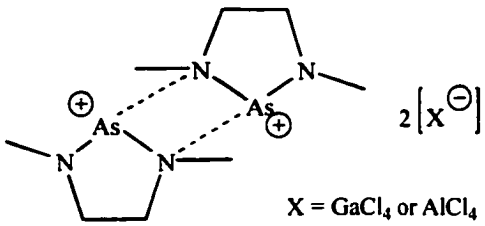

$X = GaCl_4$ or $AlCl_4$

61AsX

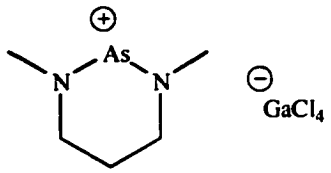

62AsGaCl$_4$

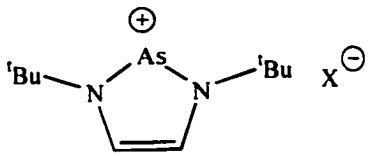

$X = Cl$ or $GeCl_5$

63AsX

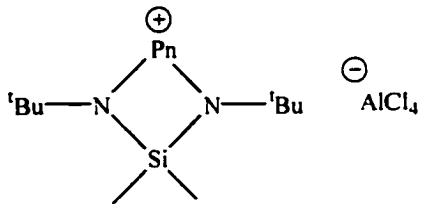

Pn = P, Sb or Bi

64PnAlCl$_4$

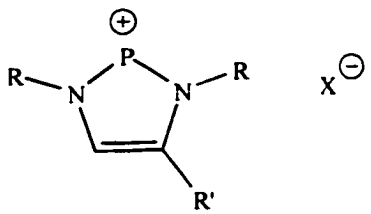

R = ^{t}Bu, R' = H and X = PF_6, Cl, $GeCl_5$, and BF_4

R = ^{t}Bu, R' = Cl and X = OSO_2CF_3

R = Fmes, R' = Cl and X = OSO_2CF_3

R = cyclohexane R' = Cl and X = $SbCl_6$

65PX

Figure 4.2 Examples of cyclic pnictenium salts (for Pn = P, As, Sb or Bi) that have been structurally characterised.

The bisaminopnictenium salt, **66PGaCl$_4$**, was successfully obtained from the reaction of $GaCl_3$ and $PCl(NPr^i_2)_2$, carried out in a manner similar to that described for the cyclic derivatives (see Figure 4.3). It was the first acyclic bisaminophosphenium salt to be characterised in the solid state. Previously, phosphenium cations had only been identified[109] primarily by NMR (^{31}P, ^{13}C and ^{1}H) spectroscopy. The P-N bond lengths (1.611(4) and 1.615(4) Å) in **66PGaCl$_4$** are crystallographically equivalent and are significantly shorter then the standard value for a P-N single bond[110] (1.800(4) Å). The N atoms are in planar environments and the N-P-N bond angle is 114.8(2)°. The structural features of **66PGaCl$_4$** suggest there is conjugation between the lone pair of electrons on N and the P centre (vacant 3p-orbital).

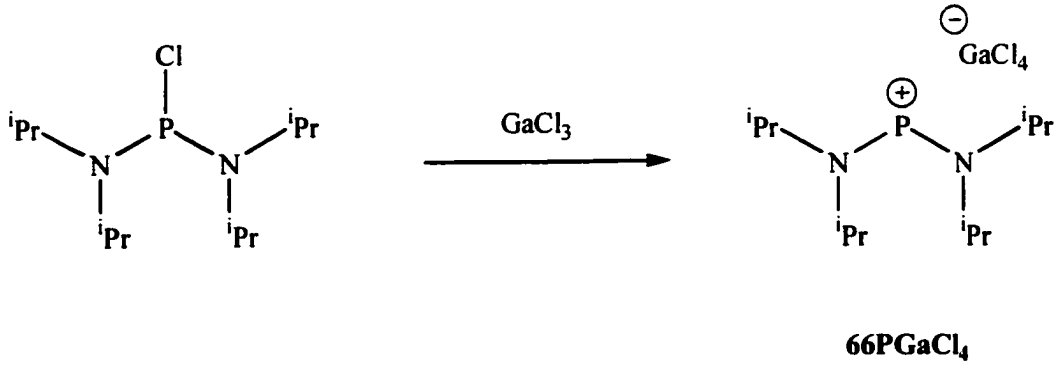

66PGaCl$_4$

Figure 4.3 Reaction scheme for the preparation of **66PGaCl$_4$**.

The reaction between $HOSO_2CF_3$ (triflic acid) and $Mes^*N{=}PN(^iPr)_2$ results in the formation of **68POSO$_2$CF$_3$** (see Figure 4.4). The phosphenium salt has been characterised by NMR and X-ray spectroscopy and has features similar to those observed for **66PGaCl$_4$**. The P-N bond length in **68POSO$_2$CF$_3$** is 1.602(1) Å and the N-P-N bond

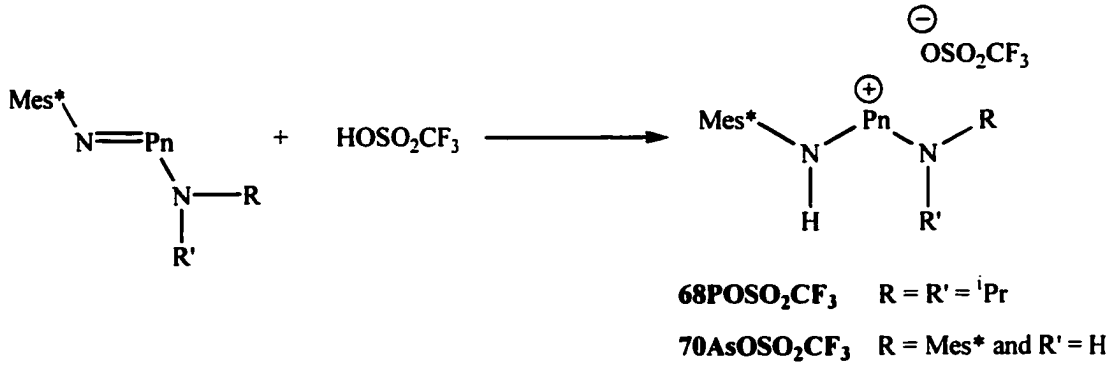

Figure 4.4 Reaction scheme for the synthesis of pnictenium salts (**68POSO$_2$CF$_3$** and **70AsOSO$_2$CF$_3$**).

angle is 107.89(7)°. The nitrogen atoms are in planar environments, suggesting donation of the lone pair of electrons to the P centre (as observed for **66PGaCl$_4$**). The ^{31}P NMR chemical shift measured for **68POSO$_2$CF$_3$** is 274.8 ppm. This compound has also been characterised by m.p., EA and NMR (^{1}H and ^{13}C) spectroscopy.

The addition of Mes*NH$_2$ to [Mes*NP][GaCl$_4$] (Figure 4.5) resulted in the formation of **67PGaCl$_4$**. The structural features of **67PGaCl$_4$** are similar to those found for **66PGaCl$_4$** and **68POSO$_2$CF$_3$**, with short P-N bond lengths (1.617(3) Å) and planar N environments. The N-P-N bond angle is 103.9(2) °. In addition to X-ray analysis,

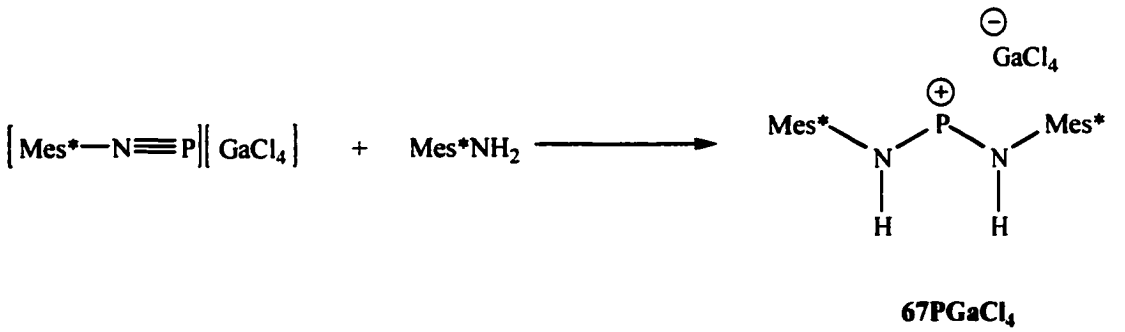

67PGaCl$_4$

Figure 4.5 Reaction scheme for the preparation of the **67PGaCl$_4$**.

67PGaCl$_4$, has been extensively characterised in the solid state (m.p., EA, ^{31}P MAS NMR and IR spectroscopy) and in solution (^{31}P, ^{1}H and ^{13}C NMR spectroscopy). The ^{31}P NMR chemical shift (272 ppm) and the isotropic ^{31}P NMR chemical shift (281 ppm) confirm that the salt is present both in solution and in the solid state. The synthesis of the corresponding aluminate salt, **67PAlCl$_4$**, has not been adequately described in the literature.

4.2 [Mes*N(H)PnN(H)Mes*][X], where X = OSO_2CF_3 or $GaCl_4$

The reaction between Mes*NHLi and $PnCl_3$ (Pn = P or As) had previously resulted in the isolation of the iminopnictines, **52P** and **52As** (Mes*N=PnN(H)Mes*). However, the P reaction was not examined by ^{31}P NMR spectroscopy in order to determine the possibility of other products being formed. The reaction between two equivalents of lithium amide, Mes*NHLi, and PCl_3 (Figure 4.6) was examined by ^{31}P NMR spectroscopy, which revealed the presence of three distinct P chemical shifts. The

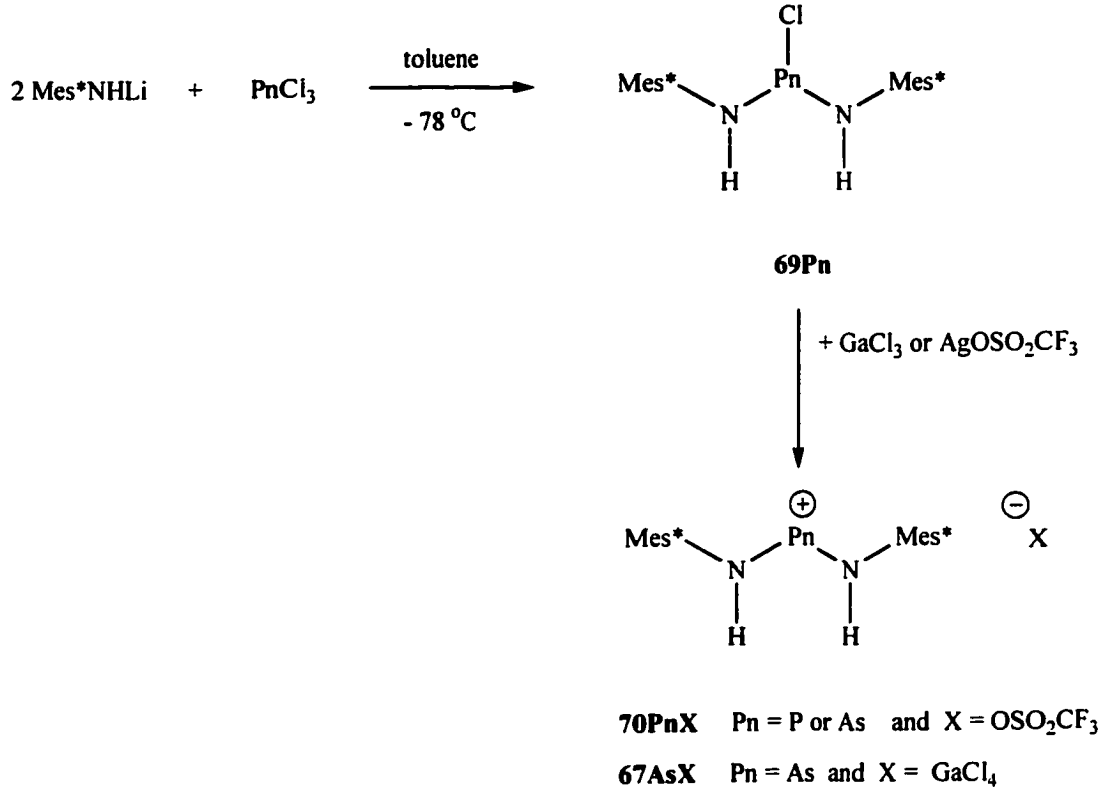

Figure 4.6 Reaction scheme for the formation of **70PnOSO$_2$CF$_3$** and **67AsGaCl$_4$**.

major peak at 152 ppm has been tentatively assigned to the chlorobisaminophosphine, **69P**. The additional minor peaks at 270 and 131 ppm have been assigned to the previously reported compounds, Mes*N=PN(H)Mes* (**52P**) and Mes*NPCl (**50P**), respectively. The crude reaction mixture (containing **69P**, **50P** and **52P**) was added to a solution of $AgOSO_2CF_3$ in toluene. The solvent was removed and the solid was dissolved in hexane, resulting in the precipitation of a new white solid, which was identified as, **70POSO$_2$CF$_3$**, [Mes*N(H)PN(H)Mes*][OSO_2CF_3]. The supernatant (or extract) was shown to contain **60P** and **52P** using ^{31}P NMR spectroscopy (see also Figure 4.7).

When the same reaction was performed using $AsCl_3$ instead of PCl_3, addition of either $AgOSO_3CF_3$ or $GaCl_4$ to **69As** produced [Mes*N(H)AsN(H)Mes*][OSO_2CF_3] (**70AsOSO$_2$CF$_3$**) or [Mes*N(H)AsN(H)Mes*][$GaCl_4$] (**67AsGaCl$_4$**), respectively (Figure 4.6). However, when two equivalents of Mes*NHLi was added to one equivalent of both $SbCl_3$ and $AgOSO_2CF_3$, the stibetidine, **59Sb**, was isolated (as discussed in Chapter 3) instead of the expected stibenium salt, [Mes*N(H)SbN(H)Mes*][OSO_2CF_3].

Differences in the reactivity of PCl_3, $AsCl_3$ and $SbCl_3$ when added to two equivalents of Mes*NHLi, can be understood by considering the first step of the reaction process (see also Figures 4.7 and 4.8). The observation of **50P** and **52P** in the ^{31}P NMR spectrum is not unexpected. The iminophosphine, **52P**, is formed by the reaction of three equivalents of Mes*NHLi with PCl_3. Reaction of equimolar amounts of Mes*NHLi and PCl_3, under the basic reaction conditions used would form **50P**. The

arsenic derivative, Mes*N=AsN(H)Mes*, **52As**, is also produced in the reaction of three equivalents of Mes*NHLi and $AsCl_3$ and it would seem reasonable to expect that $[Mes^*NAsCl]_2$ (**58As**) might also be formed (similar to **50P**). However, **52Pn**, **50P** and **58As** should all be minor components in the reaction, assuming that the reactions of PCl_3 and $AsCl_3$ proceed in a similar way. The major product observed in the ^{31}P NMR spectrum of the P reaction mixture is the bisaminopnictine, **69P**, from which addition of $AgOSO_2CF_3$ produces **70POSO$_2$CF$_3$**.

However, the addition of three equivalents of Mes*NHLi to $SbCl_3$ produces the trisaminopnictine, $(Mes^*NH)_3Sb$ (**71Sb**). The reaction of equimolar amounts of Mes*NHLi with $SbCl_3$ leads to rapid decomposition of the mixture (as discussed in Chapter 2). Some attempts were made to isolate the product from the reaction of two equivalents of Mes*NHLi and $SbCl_3$ and on one occasion a few crystals were isolated and characterised as $Mes^*NHSbCl_2 \cdot Mes^*NH_2$, **56Sb·Mes*NH$_2$** (see section 2.3), and not the bisaminostibine, **69Sb**. It would appear that the antimony reaction does not proceed in a manner similar to that of phosphorus.

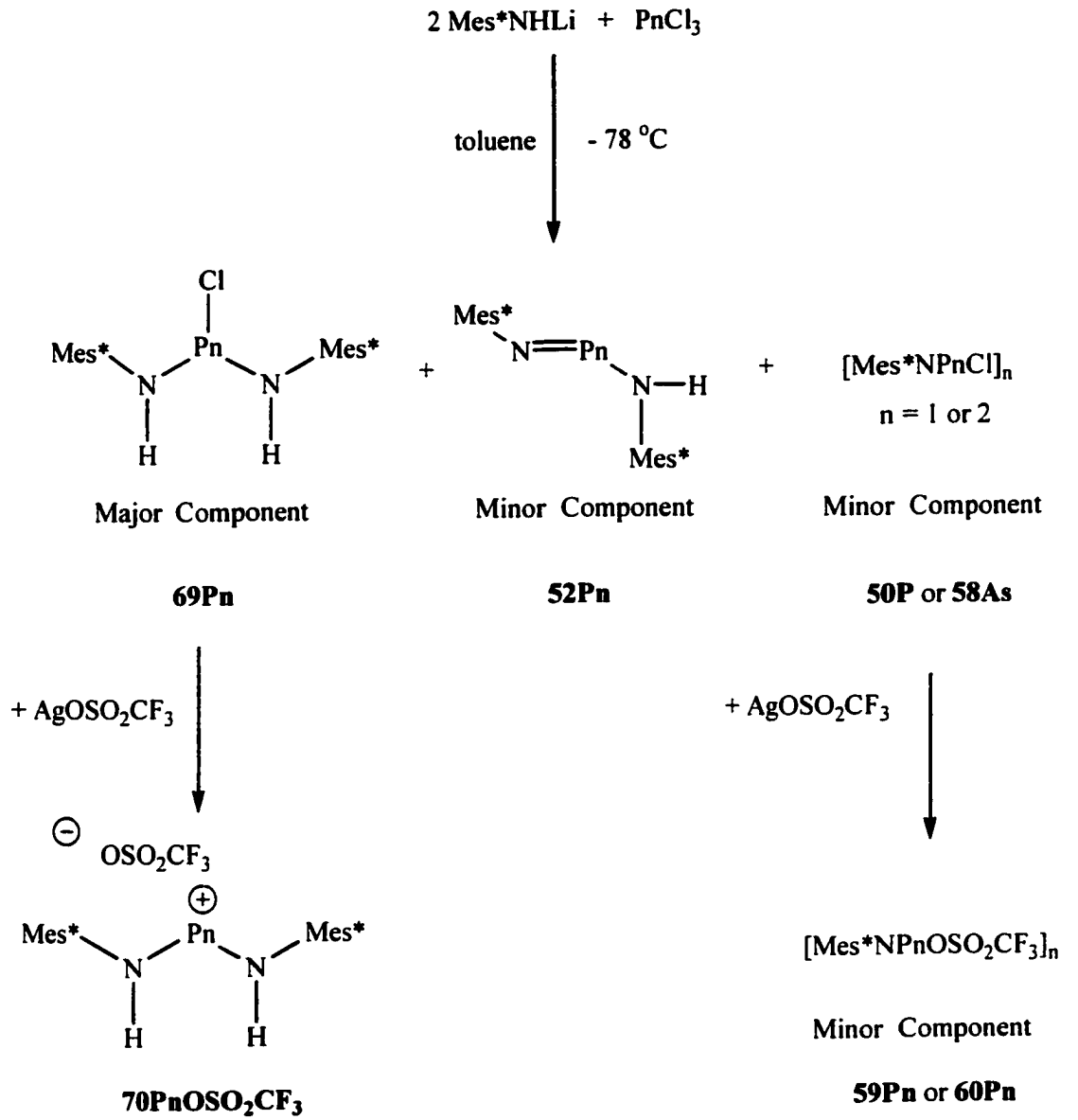

Figure 4.7 Proposed reaction scheme for the formation of **70PnOSO$_2$CF$_3$** and minor products, **51Pn**, **59Pn** and **60Pn** (where Pn = P or As).

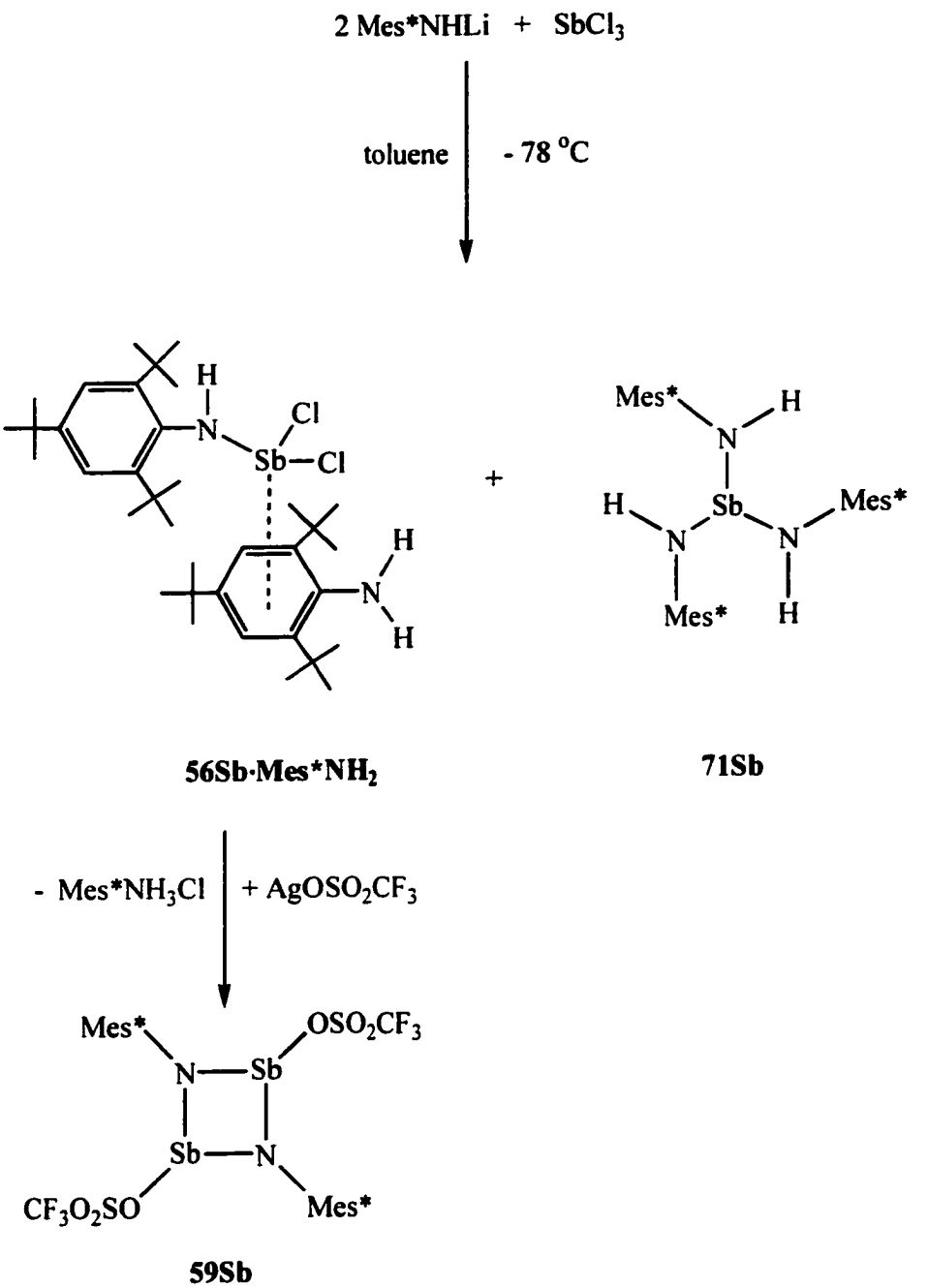

Figure 4.8 Possible reaction scheme for the formation of **59Sb**.

All three bisaminopnictenium salts (**67AsGaCl$_4$**, **70AsOSO$_2$CF$_3$** and **70POSO$_2$CF$_3$**) have been characterised by NMR (^{1}H and ^{19}F where appropriate, see Table 4.1) and IR spectroscopy, m.p., and X-ray analysis (see Figures 4.9, 4.10 and 4.11, respectively). In addition, the ^{31}P NMR chemical shift is 279.7 ppm for **70POSO$_2$CF$_3$** and is similar to the solid state isotropic chemical shift (as measured by ^{31}P MAS NMR spectroscopy) of 282.7 ppm. This indicates that the compound (**70POSO$_2$CF$_3$**) adopts a similar structure in solution and in the solid state. The ^{31}P NMR chemical shifts observed for **70POSO$_2$CF$_3$** are similar to those reported for the bisaminophosphenium salts, **68POSO$_2$CF$_3$** and **67PGaCl$_4$**.

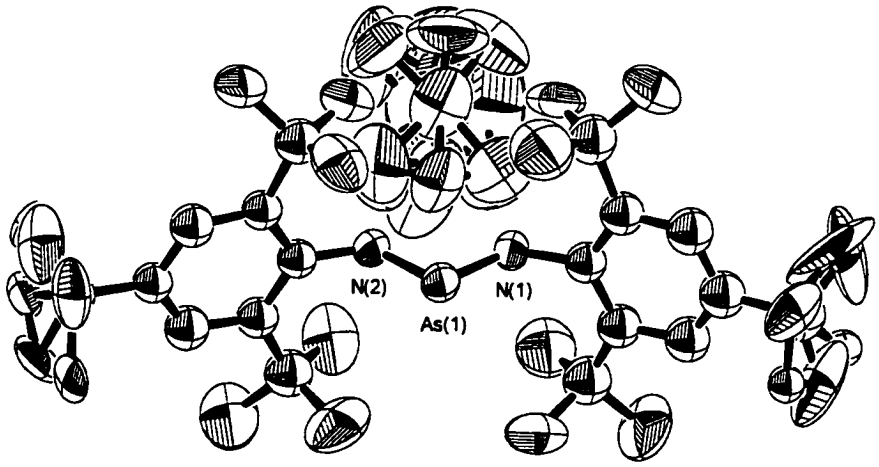

Figure 4.9 Diagram (ORTEP) of the molecular structure of **70AsOSO$_2$CF$_3$**.

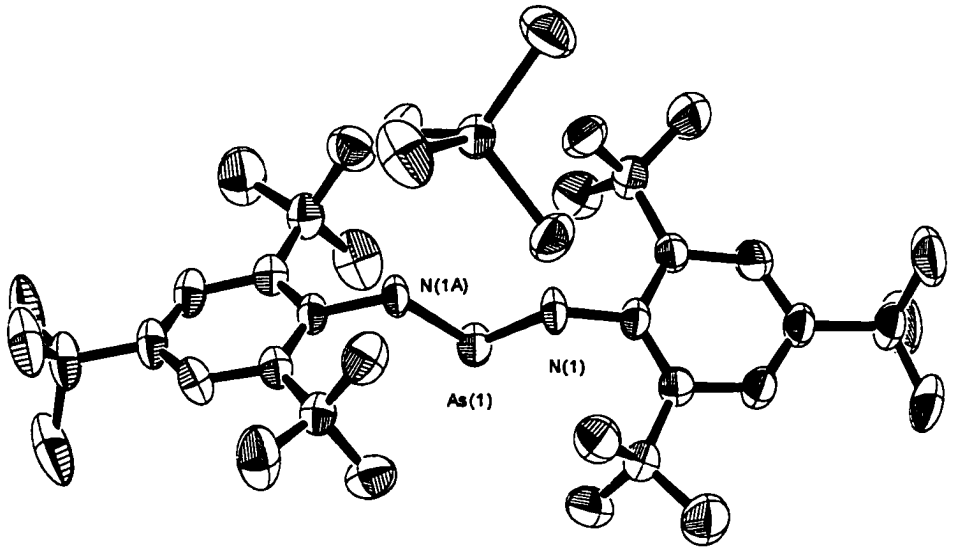

Figure 4.10 Diagram (ORTEP) of the molecular structure of **67AsGaCl$_4$**.

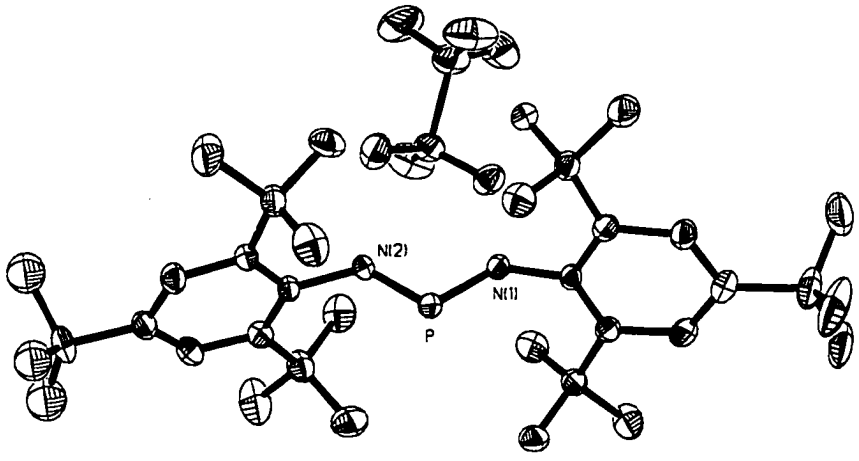

Figure 4.11 Diagram (ORTEP) of the molecular structure of **70POSO$_2$CF$_3$**.

Table 4.1 Selected NMR data for the pnictenium salts **67AsGaCl$_4$** and **70PnOSO$_2$CF$_3$** where Pn = P or As (NMR signals reported in ppm).

	67AsGaCl$_4$	**70POSO$_2$CF$_3$**	**70AsOSO$_2$CF$_3$**
p-tert-Bu (^{1}HNMR)	1.31	1.32	1.33
o-tert-Bu (^{1}HNMR)	1.55	1.59	1.56
Ar-H (^{1}H NMR)	7.51	7.50	7.52
OSO$_2$CF$_3$ (^{19}F NMR)		- 79.7	- 78.7

Selected bond lengths and angles for **67AsGaCl$_4$** and **70PnOSO$_2$CF$_3$** (where Pn = P and As, respectively) are listed in Table 4.2. The As-N bond lengths (1.75(4) and 1.73(5) Å in **70AsOSO$_2$CF$_3$** and 1.764(5) Å in **67AsGaCl$_4$**) are short compared to typical N-As single bonds, which range from 1.79 - 1.88 Å[12]. The N-P bond lengths for **70POSO$_2$CF$_3$** (1.612(2) and 1.6156(19) Å) are also shorter than a standard P-N bond (1.800(4) Å[110]) but are comparable to those observed for the previously reported acyclic phosphenium salts, **66PGaCl$_4$**, **67PGaCl$_4$** and **68POSO$_2$CF$_3$**. The N-Pn-N bond angles are 100.0(3)°, 99.2(3)° and 104.11(1)° for **67AsGaCl$_4$**, **70AsOSO$_2$CF$_3$** and **70POSO$_2$CF$_3$**, respectively.

The triflate anion of **70AsOSO$_2$CF$_3$** is disordered (as shown in Figure 4.9) and was modelled in the crystal structure determination by two separate triflate anions occupying different positions (see Figure 4.12). The S-C bond axes of the two anions lie at right angles to one another. As a result there are a total of nine possible S-O and C-F bond lengths. As shown in Table 4.2, the S-O bond lengths in both **70POSO$_2$CF$_3$** and **70AsOSO$_2$CF$_3$** are not equivalent. This generally indicates that at least one of the oxygen atoms of the triflate anion is interacting with the cation. The gallate anion in **67AsGaCl$_4$** has a distorted tetrahedral environment, which could indicate some form of similar interaction occurring between the Cl atoms of the anion and the phosphenium cation. The closest non-bonded contacts are between the N atoms of the cation and the Cl atoms of the anion (the shortest being Cl(1)-N(1), 3.457(6) Å).

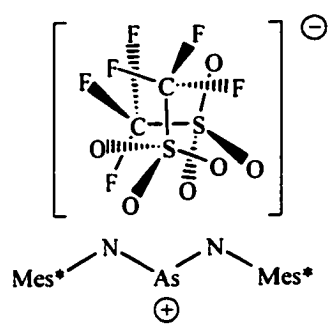

Figure 4.12 Schematic representation of the disordered triflate anion in **70AsOSO$_2$CF$_3$** (The H atoms are omitted from [Mes*N(H)AsN(H)Mes*]$^+$ for clarity).

Table 4.2 Selected bond lengths (Å) and angles (°) for **67AsGaCl$_4$** and **70PnOSO$_2$CF$_3$** (Pn = P or As).

	67AsGaCl$_4$	**70AsOSO$_2$CF$_3$**	**70POSO$_2$CF$_3$**
N-Pn	1.764(5)	1.765(7), 1.768(7)	1.612(2), 1.6156(19)
C_{ipso}-N	1.453(7)	1.47(1), 1.46(1)	1.471(3), 1.470(3)
S(1)-O		1.42(1), 1.47(2), 1.45(2) 1.51(3), 1.54(3)	1.426(2), 1.443(2) 1.447(2)
S(2)-O		1.31(3), 1.66(3), 1.64(3) 1.52(2)	
Ga-Cl	2.177(2), 2.152(2)		
N-Pn-N	100.0(3)	99.2(3)	104.11(10)
N-Pn-C_{ipso}	125.2(4)	121.6(6), 122.7(6)	126.51(16), 124.36(16)

The arsenium salt, **70AsOSO$_2$CF$_3$**, could also be isolated from the reaction of $HOSO_2CF_3$ (triflic acid) and Mes*N=AsN(H)Mes*, **52As** (see Figure 4.4). Interestingly, the reaction of $AgOSO_2CF_3$ and Mes*N(SiMe$_3$)AsCl$_2$, **55As** (Figure 4.13), also produced the arsenium salt, **70AsOSO$_2$CF$_3$**, instead of the desired product, [Mes*NAsOSO$_2$CF$_3$]$_2$, **59As**. Additional attempts were made to prepare **59As** utilising the reaction of Mes*N(H)AsCl$_2$, **56As**, with NEt_3 and $AgOSO_2CF_3$. The combination of **56As** with

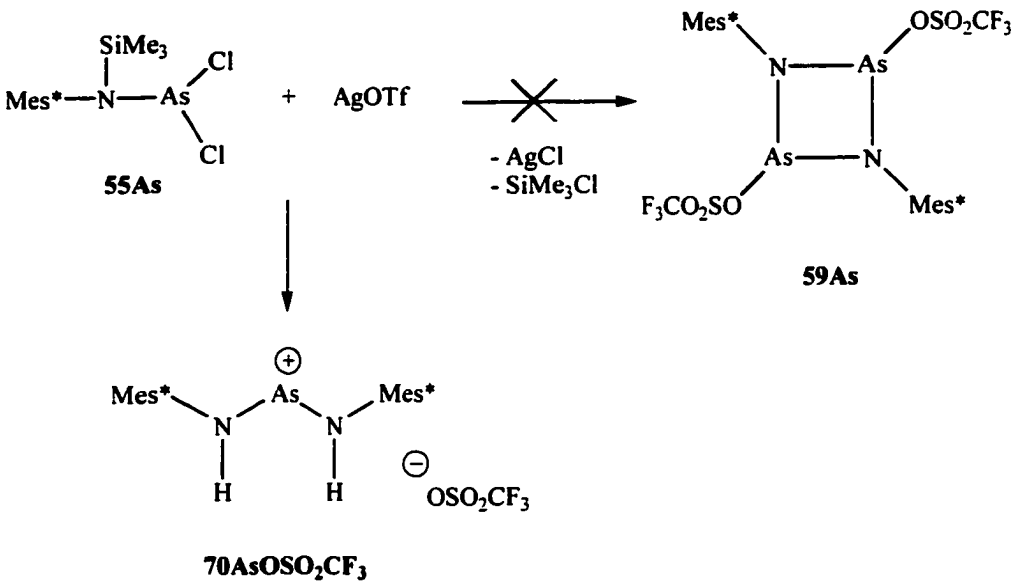

Figure 4.13 Reaction of Mes*N(SiMe$_3$)AsCl$_2$, **55As** with AgOSO$_2$CF$_3$.

NEt$_3$ forms the arsetidine, **58As** (as discussed in Chapter 3). When **58As** is reacted *in situ* with AgOSO$_2$CF$_3$, **70AsOSO$_2$CF$_3$**, is isolated instead of the expected **59As**. Interestingly, when AgOSO$_2$CF$_3$ is added to **56As** before the addition of base, the iminoarsine, **52As**, is isolated (see Figure 4.14).

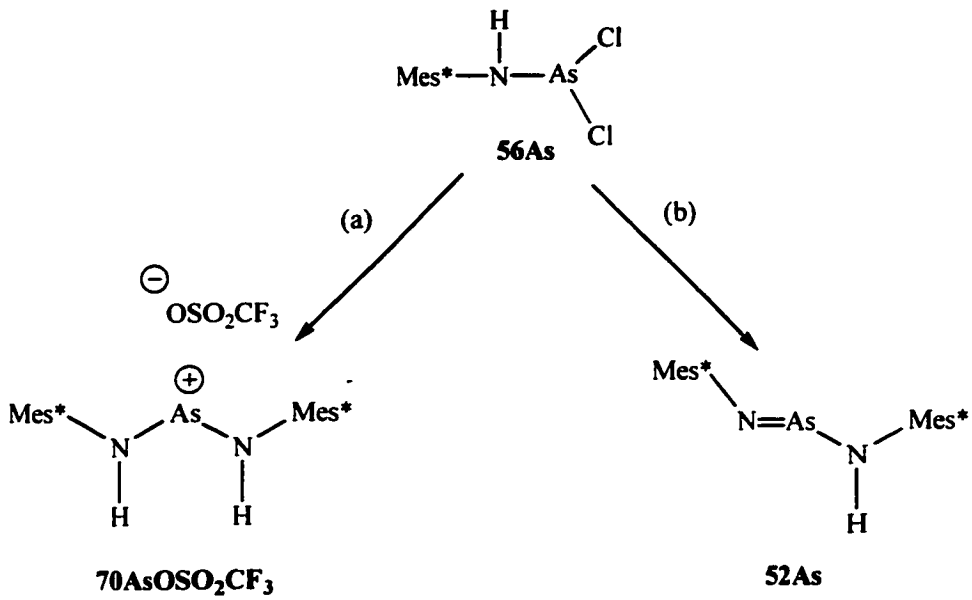

Figure 4.14 Reactions of Mes*N(H)$AsCl_2$, **56As** with

(a) NEt_3 followed by $AgOSO_3CF_3$ and

(b) $AgOSO_3CF_3$ followed by NEt_3.

The stibenium salt, [Mes*N(H)SbN(H)Mes*][OSO_2CF_3] (**70SbOSO$_2$CF$_3$**), could not be prepared by the above methods. An alternative synthesis was carried out using the trisaminostibine, (Mes*NH)$_3$Sb (**71Sb**), and triflic acid, $HOSO_2CF_3$ (see Figure 4.15), which produced a microcrystalline sample that was unsuitable for X-ray analysis, but was characterised by IR spectroscopy, m.p. and EA. The IR spectrum of **70SbOSO$_2$CF$_3$** was identical to that of the arsenium salt, **70AsOSO$_2$CF$_3$**, and EA was consistent with it being **70SbOSO$_2$CF$_3$**. Attempts to reproduce this reaction for a complete characterisation

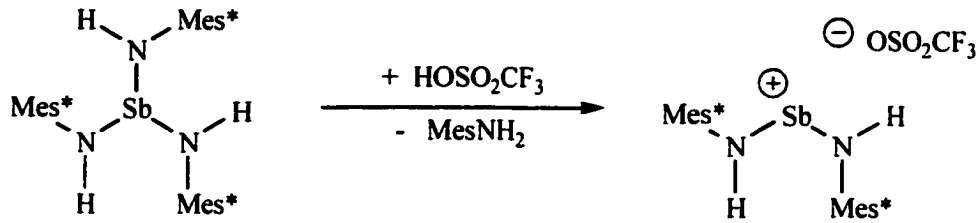

71Sb **70SbOSO$_2$CF$_3$**

Figure 4.15 Reaction scheme for preparation of **70SbOSO$_2$CF$_3$**.

of **70SbOSO$_2$CF$_3$** was complicated by the difficulty associated with the control of a stoichiometric addition of triflic acid. An excess of acid did not produce the desired salt, but rather a white solid was formed.

4.3 Summary

The acyclic pnictenium salts, [Mes*N(H)PnN(H)Mes*][OSO$_2$CF$_3$] (**70PnOSO$_2$CF$_3$**), were synthesised for Pn = P, As and Sb as well as the gallate salt, **67AsGaCl$_4$**. The use of the sterically demanding substituent, Mes*, facilitated the isolation of the first examples of acyclic pnictenium cations for the heavier pnictogen atoms (i.e. As and Sb).

Chapter 5 – Effects of different substituents, (R = Dip and Mes*) for reactions involving $[RNPCl]_n$

5.1 Introduction

A compound is kinetically stabilised when a high activation barrier separates it from other possible species. A compound is thermodynamically stabilised when it is in a deep minimum at the lowest energy structure on the energy surface of the reaction. In some cases the kinetically and thermodynamically stabilised products are the same, in others they differ. It is sometimes possible to have an effect on the outcome of a reaction by changing the experimental conditions. For example, if a suitable a catalyst is added to a reaction, the activation barrier will be reduced and the reactants will be able to proceed on to form the desired thermodynamically stabilised products. If the temperature of a reaction is increased (or decreased) this may also effect its thermodynamics and kinetics, thereby allowing an otherwise unstable product to be isolated.

In general, low-coordinate (unsaturated) compounds of the heavier main group elements are thermodynamically and kinetically unstable with respect to their saturated alternatives (i.e. $R_nE{=}ER'_n$ verses $R_{n+1}E{-}ER'_{n+1}$). One of the most common ways to provide both thermodynamic[111] and kinetic[112,113] stabilisation to a multiply bonded compound containing the heavier p-block elements, $R_nE{=}E'R'_n$, is through the use of large bulky substituents (such as those illustrated in Figure 5.1). The kinetic stabilisation is obvious, the size or bulk of the substituent inhibits the approach of reagents, thereby protecting the bond. The origins of the thermodynamic effects are less obvious.

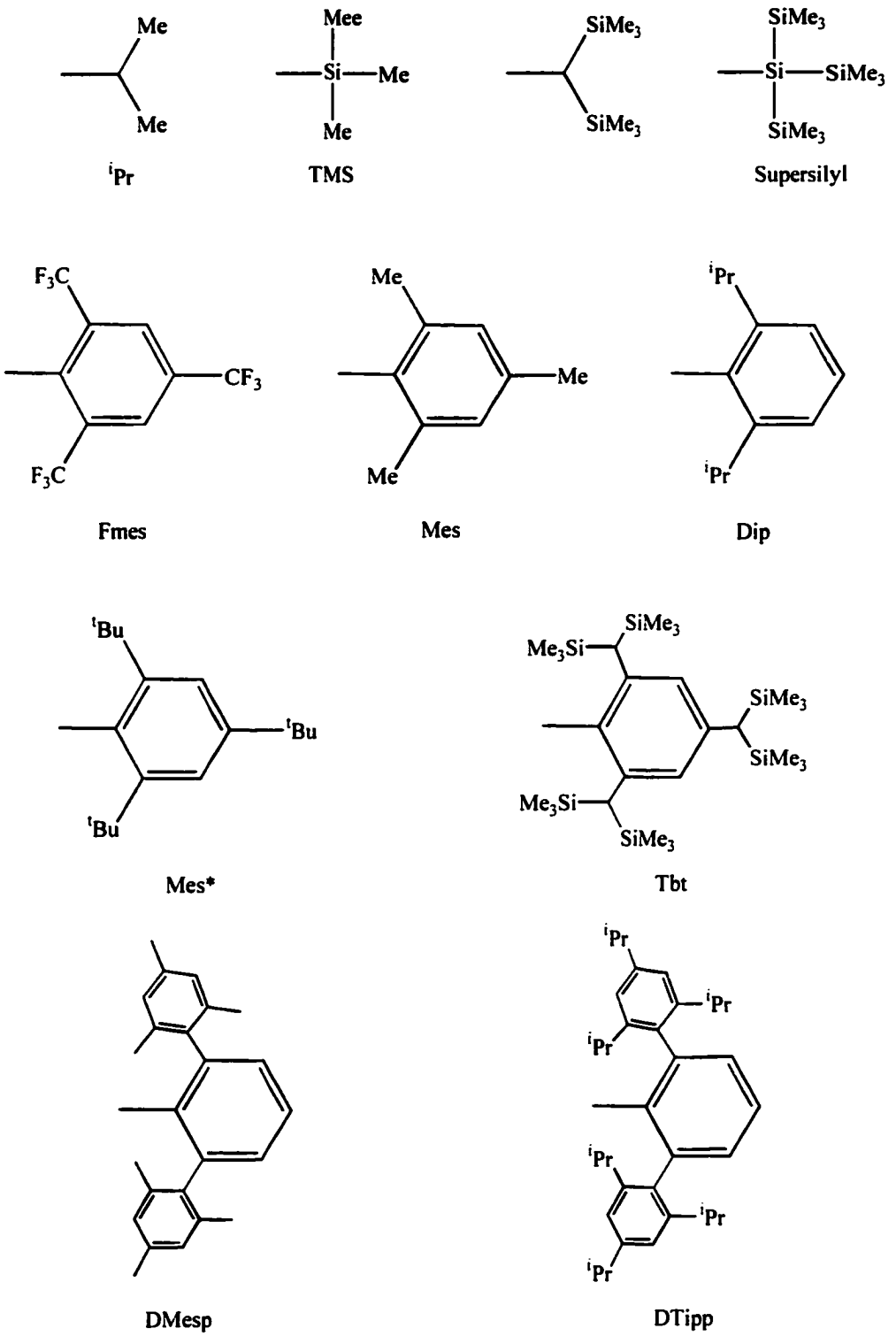

Figure 5.1 Examples of sterically demanding substituents.

Calculation of the enthalpies associated with the dimerisation reaction of *trans*-1,2-substituted ethenes to their corresponding cyclobutanes[111], provides a theoretical model of the thermodynamic consequences resulting when large substituents are used. When the substituent (R) is small, the reaction (shown in Figure 5.2) is exothermic, showing that the cyclobutane is thermodynamically stabilised with respect to the alkene. As the size of the substituent increases, the dimerisation reaction becomes increasingly more endothermic (see Table 5.1) with the alkene being thermodynamically preferred. Table 5.2 shows that the substituent steric strain increases for both the alkene and the cyclobutane as the bulk of the substituent increases. However for substituents larger than Ph, the magnitude of this increase is greater for the dimer. As a result the alkene (monomer) is thermodynamically stable with respect to the dimer when R is large.

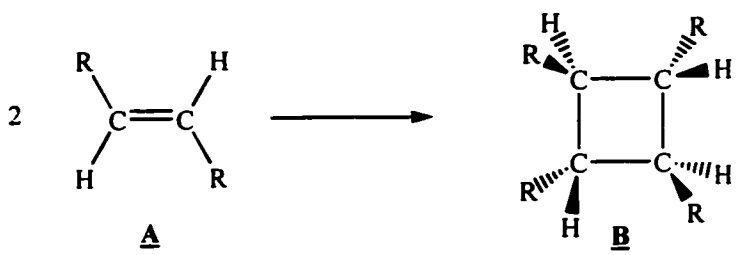

Figure 5.2 Dimerisation of 1,2-disubstituted alkenes to form 1,2,3,4-tetrasubstituted cyclobutanes.

Table 5.1 Calculated enthalpies[111] of the dimerisation reaction for 1,2-substituted (R) alkenes given in kJ/mol.

R	H	Me	^{t}Bu	Ph	Mes	Trip	Mes*
PCModel *(a)*	-87	-84	-10	-65	+21	+164	+429
MM3 *(a)*	-85	-83	-7	+19	+68	+282	+395
AM1 *(b)*	-142	-77	-23	-47	+46	+173	+475

(a) Heat of formation of cyclobutane - 2(heat of formation of alkene)

(b) Total energy of cyclobutane - 2(total energy of alkene).

Table 5.2 Calculated (PCModel) absolute strain energies[111] (kJ/mol) of 1,2-substituted alkenes and 1,2,3,4-substituted cyclobutanes.

	H	Me	^{t}Bu	Ph	Mes	Trip	Mes*
A (ethene)	0	0	50	100	150	220	330
B (cyclobutane)	110	100	190	290	360	740	1200

The effects of substituent steric strain can also be observed in compounds containing homoatomic (homonuclear) bonds for the non-metal elements[114]. The homoatomic σ and π bond energies for a number of p-block elements[114] are presented in Table 5.3. Examination of the group 15 elements shows that the π bond energy for nitrogen is considerably greater than its σ bond energy, indicating that N compounds thermodynamically prefer to form multiple bonds. For P and As, the relative energies are reversed, so that formation of two σ bonds is preferred over a σ + π bonding alternative. Considering the possible oligomers of the "PnR" subunit, (for Pn = P, As, Sb or Bi) the bond energies in Table 5.3 reveal that higher order oligomers are thermodynamically favoured over the (σ + π) double bond situation, **X** (see Figure 5.3). The difference

Table 5.3 Table of σ and π bond energies in kJ/mol for first and subsequent rows of the elements of groups 14-16 (taken from ref.[114]).

Bond Energies	C-C	N-N	O-O	Si-Si	P-P	S-S	Ge-Ge	As-As	Se-Se
σ (single bond)	335	160	145	195	200	270	165	175	210
π *(a)*	295	395	350	120	145	155	110	120	125

(a) The π bond energy is estimated by subtracting the single bond energy from the double bond energy. While this is not strictly accurate, the results support a qualitative argument for the trends associated with descending the various groups of the p-block elements[114].

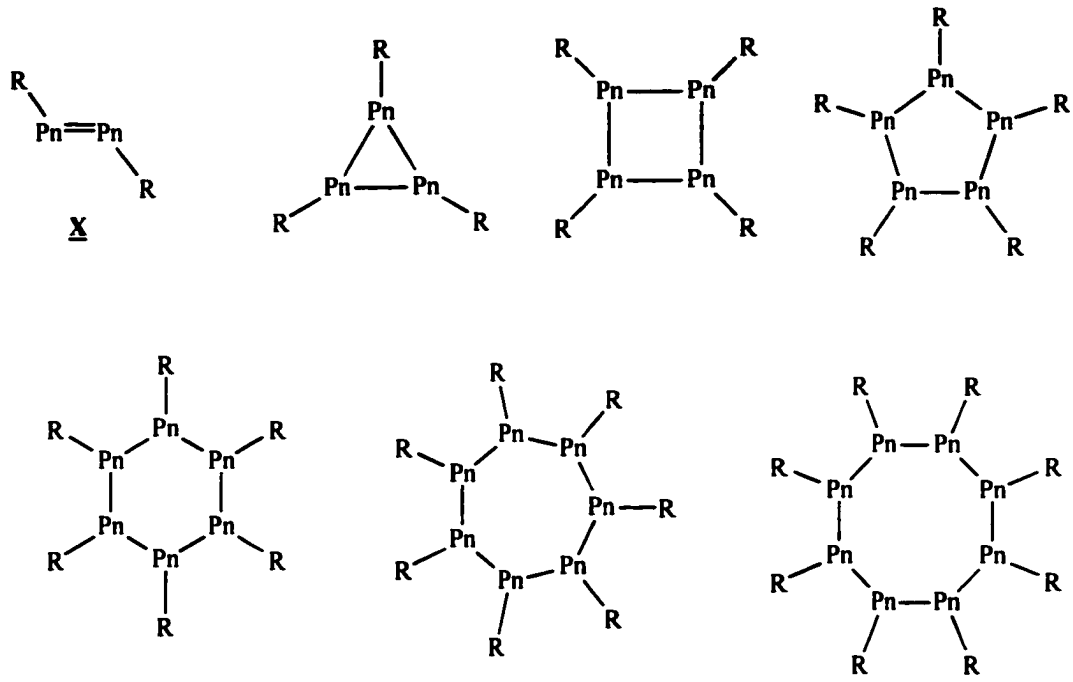

Figure 5.3 Pictorial representation for oligomers of the subunit "PnR".

between the π and σ bond energies (using the values from Table 5.3) for P and As is - 55 kJ/mol. Therefore, ΔH_{rxn} (see Figure 5.4) will be negative for all values of x (where x = number of "RPn" units). When Pn = N, the difference between the π and σ bond energies is +235 kJ/mol and ΔH_{rxn} will be positive for all values of x. As the size of the substituents increase, steric strain[115] is imposed on the system (as observed in the dimerisation reaction of alkenes to the corresponding cyclobutane). This strain[113] is less for smaller oligomers and is minimised in the double bonded dimer of "R-Pn" units. The trimer, $(RPn)_3$, would be expected to be inherently weak[113] based on the strain imposed by a 3-membered ring and on the configuration of the R substituents (i.e. one pair must be *cis*).

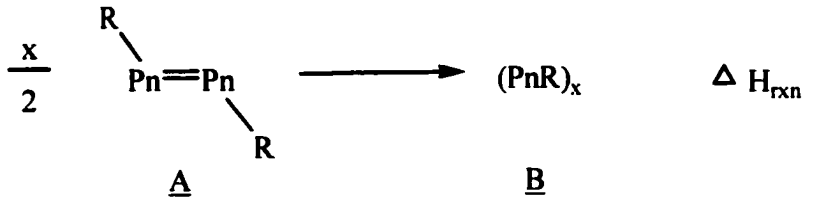

x = number of "RPn" units

$$\Delta H_{rxn} = \sum \text{bond energies of products} - \sum \text{bond energies of reactants}$$

Figure 5.4 ΔH_{rxn} showing the double bonded alternative (A) is thermodynamically less favourable compared with the oligomers, which involve a fully σ bonded situation (B), for the heavier pnictogen elements (P and As).

There is experimental evidence that supports this argument. Definite differences are observed between the substituents on the homoatomic four-membered, Pn_4 rings[116-125] and the dipnictenes, RPn=PnR. Some examples of homoatomic pnictetidines that have been characterised by X-ray analysis are shown in Figure 5.5. When larger, more sterically demanding groups (such as those shown in Figure 5.1) are used it is possible to isolate the dipnictenes, R-Pn=Pn-R. Examples for P (R = Mes*[126], $C(SiMe_3)_3$[127] or Fmes[62]), As (R = DMesp[128], DTipp[128] or $C(SiMe_3)_3$[129]), Sb (R = DMesp[128], DTipp[128] or Tbt[130]) and Bi (R = DMesp[128] or Tbt[131]) have been isolated and fully characterised.

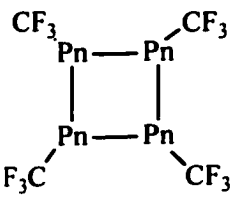

Pn = P, As

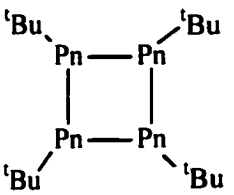

Pn = P, As, Sb

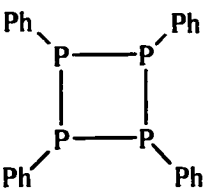

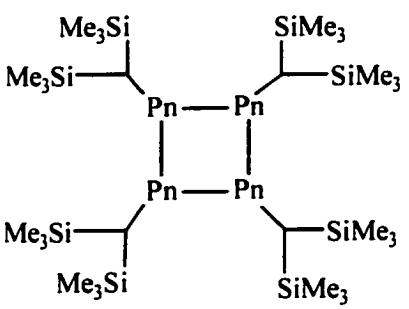

Pn = P, Sb, Bi

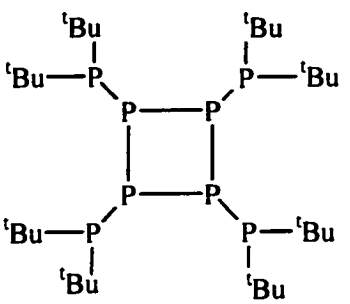

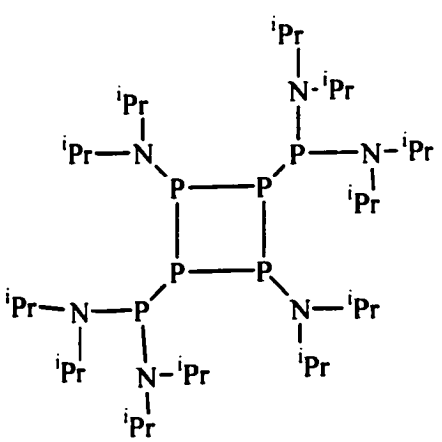

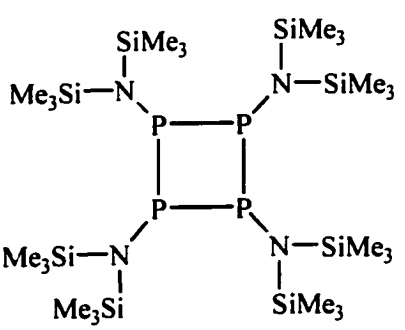

Figure 5.5 Examples of homoatomic pnictetidines (for P, As, Sb and Bi).

5.2 Systems involving N and the heavier pnictogens (P, As, Sb and Bi)

With respect to the bonds formed between N and the heavier pnictogens (P, As, Sb and Bi), the effects of substituent steric strain on the thermodynamics and the kinetics of the system should be similar to those observed for the homoatomic examples. Large sterically demanding substituents should thermodynamically and kinetically favour the formation of doubly bonded iminopnictines, RN=PnR' (where Pn = P, As, Sb or Bi), over the pnictetidines, $[RNPnR']_2$. Experimental evidence for this can be found by considering the reaction between $PnCl_3$ (where Pn = P, As, Sb or Bi) and three equivalents of the lithium amides, RN(H)Li, where R = Dip or Mes* (see Figure 5.6). For R = Dip the pnictetidines, $[DipNPnN(H)Dip]_2$, **28Pn** (where Pn = P, As, Sb or Bi), are formed, but the larger Mes* substituent produces the iminopnictines, Mes*N=PnN(H)Mes*, **52Pn** (for Pn = P, As). The Mes* substituent is sterically demanding enough to prevent dimerisation ($[Mes*NPnN(H)Mes*]_2$) from occurring for Pn = P or As. However, it does not provide sufficiently steric protection to stabilise the iminopnictines for the heavier pnictogens Sb and Bi. Instead they adopt an alternative, fully σ bonded arrangement, the trisaminopnictine, **71Pn**, (Mes*NH)Pn (where Pn = Sb or Bi).

The iminophosphine, Mes*NPCl (**50P**), is monomeric both in solution and in the solid state, as indicated by the similarities between the ^{31}P NMR chemical shift in solution and the ^{31}P NMR isotropic chemical shift in the solid state. Attempts to isolate the dimeric analogue, $[MesNPCl]_2$, by slow crystallisation, were unsuccessful. The

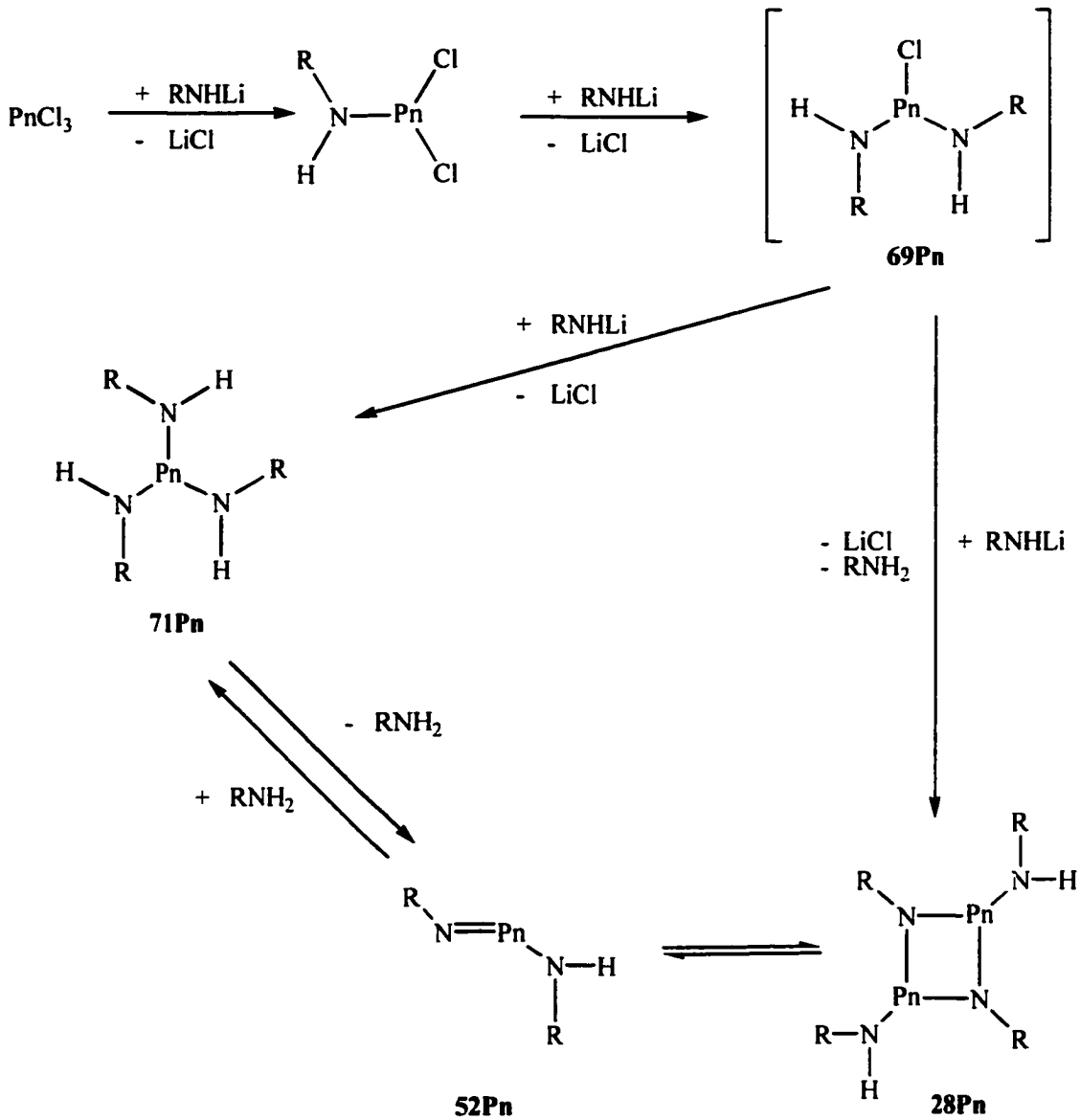

Figure 5.6 Possible products from the reaction of three equivalents of lithium amide, RNHLi, with $PnCl_3$ (Pn = P, As, Sb or Bi).

phosphetidine, $[DipNPCl]_2$ (**72P**), is dimeric both in solution and in the solid state (confirmed by ^{31}P NMR spectroscopy). The main difference between these two compounds is the bulk associated with the nitrogen substituent (i.e. Mes* versus Dip). The larger, more bulky Mes* group favours the iminophosphine, **50P**, with respect to the corresponding phosphetidine, $[Mes^*NPCl]_2$. In contrast, the smaller Dip group is not as sterically demanding and the iminophosphine, DipNPCl, is not observed.

5.2.1 Reaction of $[RNPCl]_n$ with $AgOSO_2CF_3$

Reaction of Mes*NPCl, **50P**[9], with $AgOSO_2CF_3$ gives $Mes^*NPOSO_2CF_3$, **60P**[132] (see Figure 5.7). However, depending on the crystallisation process, it is possible to isolate both the monomer (**60P**) and the dimer, $[Mes^*NPOSO_2CF_3]_2$ (**59P**), in the solid state. X-ray analysis, IR, Raman and solid state ^{31}P NMR spectroscopy has confirmed the existence of two distinct species, **60P** and **59P**. Interestingly, there is no evidence of the dimer in solution (as examined by ^{31}P NMR spectroscopy, in a variety of solvents). Preliminary observations[10] made by C. L. B. Macdonald, R. W. Schurko (solid state NMR spectroscopy) and T. S. Cameron (X-ray analysis) were inconsistent. Re-examination of the crystallisation process used to isolate **60P** revealed the presence of three crystalline materials in the solid. The major product, isolated from the recystallisation of a crude sample of $Mes^*NPOSO_2CF_3$, was the monomer, **60P** (large

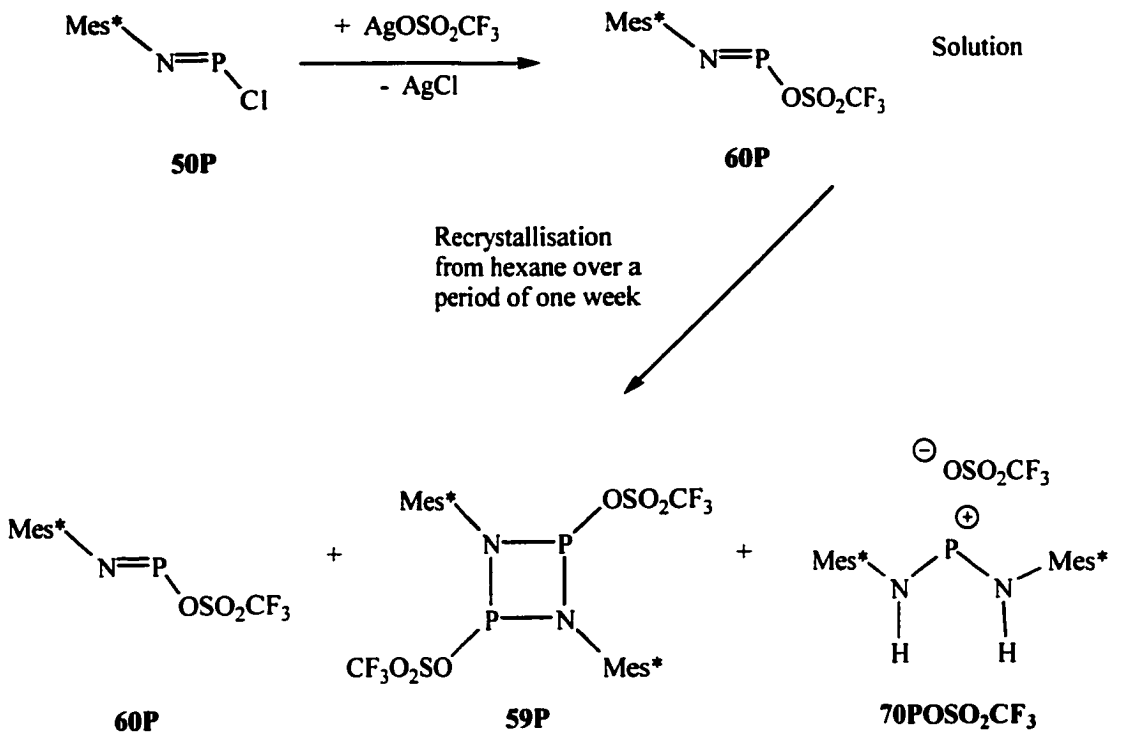

Figure 5.7 Reaction scheme for the formation of **60P** and **59P**.

orange crystals). This was confirmed by m.p., IR, and solid state ^{31}P NMR spectroscopy. Individual samples of the minor products were isolated and characterised as the dimer, **59P** (yellow crystals), and the phosphenium salt, **70POSO$_2$CF$_3$** (white crystals), by m.p. and X-ray crystallography. The presence of **70POSO$_2$CF$_3$**, while unexpected, arose from an impurity (**69P**) present in the starting material, **50P**. A sample of the entire mixture was used in the solid state ^{31}P NMR experiment (carried out by Mike Lumsden) and showed isotropic chemical shifts at 50.3 ppm (**60P**), 257.9 ppm (**59P**) and 282.7 ppm (**70POSO$_2$CF$_3$**).

In addition to the two distinct isotropic chemical shifts, the structural and spectroscopic (IR and Raman) features of **60P** and **59P** are also characteristic of two different compounds. Selected bond lengths and angles are given in Table 5.4 and Figures 5.8 and 5.9 show the molecular structures of **60P** and **59P**, respectively.

The P-N bond lengths (1.713(4) Å and 1.724(4) Å) in the dimeric structure, **59P**, are slightly shorter than the standard value for a P-N single bond (1.800(4) Å[110]). However, they are significantly longer than the P-N bond length (1.477(5) Å) found in the monomer, **60P**. The nitrogen atoms of **59P** are essentially planar (sum of the angles is 357.6°). The plane defined by the aromatic carbons of the Mes* substituent (for the dimer, **59P**) is twisted 112.7° from the NPNP plane. As a result the C_{ipso}-N bond length (1.462(6)Å) is significantly longer in the dimeric structure than it is in the monomer, **60P** (1.386(7) Å). The C_{ipso}-N-P bond angle in the monomer is almost linear (176.4(4)°) but **59P** has C_{ipso}-N-P bond angles (140.7(3)° and 119.7(3)°). The P-O bond length in the monomer (1.926(4) Å) is considerably longer than that of the dimer (1.787(3) Å) and both are longer than a typical P-O single bond (1.573(11) Å[103]).

The Raman spectrum of the dimer, **59P**, and the monomer, **60P**, are similar but not identical. There is an intense P-N stretch at 1464 cm^{-1} that is absent in the spectrum of **60P**. Differences are also found in the IR spectra and it is possible to distinguish the monomer from the dimer by a comparison of the two spectra. The m.p. of **60P** is

Table 5.4 Selected bond lengths (Å) and bond angles (°) for **60P** and **59P**.

	60P	**59P**
Pn(1)-N(1)	1.477(5)	1.713(4)
Pn(1)-N(1)'		1.724(4)
N(1)-C(ipso)	1.386(7)	1.462(6)
Pn(1)-O(1)	1.926(4)	1.787(3)
S(1)-O(1)	1.511(4)	1.550(3)
S(1)-O(2)	1.413(5)	1.411(4)
S(1)-O(3)	1.420(4)	1.429(4)
N(1)-Pn-N(1)'		82.8(2)
Pn(1)'-N(1)-Pn(1)		97.2(2)
Pn(1)-N(1)-C(ipso)	176.4(4)	140.7(3)
Pn(1)'-N(1)-C(ipso)		119.7(3)
N(1)-Pn(1)-O(1)	107.8(2)	102.2(2)
N(1)'-Pn(1)-O(1)		95.7(2)

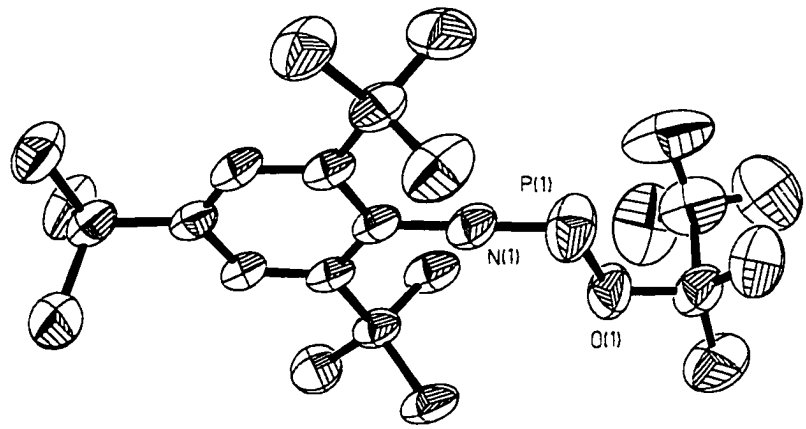

Figure 5.8 Diagram (ORTEP) of the molecular structure of **60P**.

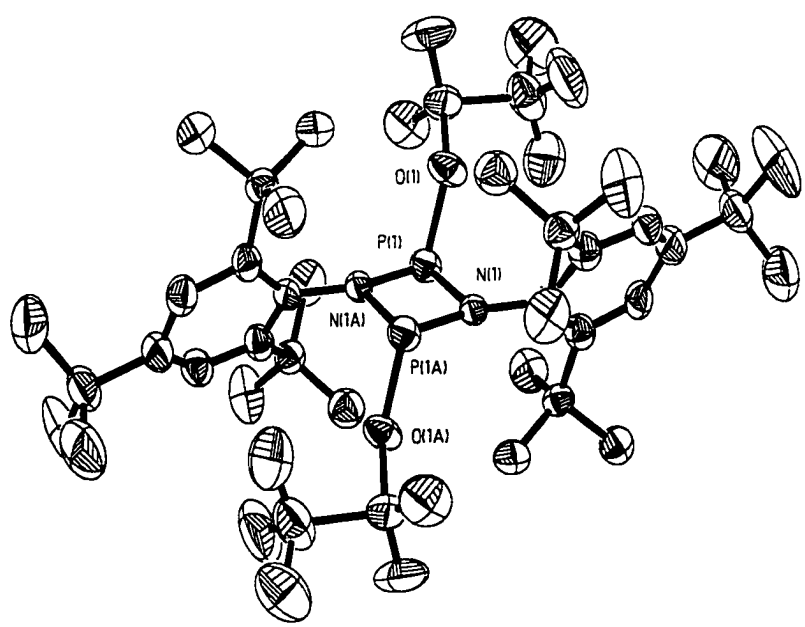

Figure 5.9 Diagram (ORTEP) of the molecular structure of **59P**.

124-126 °C. When the dimer was heated in a controlled manner a change in colour was observed (yellow to orange) at 113 °C before the compound melts at 124-126 °C. The heated sample was then examined by IR spectroscopy and was found to be characteristic of the monomer, **60P**[133]. This type of reactivity has been observed previously[54]; thermal dissociation of the phosphetidine (dimer), $[SiMe_3NPN(Me)N(SiMe_3)]_2$, results in the formation of the iminophosphine (monomer), $Me_3SiN{=}P\text{-}N(Me)N(SiMe_3)_2$.

The addition of $AgOSO_2CF_3$ to **72P** yields the dimer, $[DipNPOSO_2CF_3]_2$, suggesting that the Dip substituent does not provide sufficient steric strain to render the dimer less stable than the monomer. However the difference (thermodynamic and/or kinetic) between the monomer and dimer derivatives (**60P** and **59P**, respectively) are not significant. The strain induced by the larger Mes* group allows the monomer, **60P**, to be isolated but does not prevent the formation (under appropriate conditions) of the dimer.

5.3 Reaction of $[RNPCl]_n$ with $GaCl_3$

Reaction of **50P** with $GaCl_3$ produces the phosphoazonium cation, $[Mes^*NP]^+$, as either the gallate ($[GaCl_4]^-$) or digallate ($[Ga_2Cl_7]^-$) salt (depending upon stoichiometry)[134]. The phosphoazonium salts produced from reactions of Mes*NPCl with $GaCl_3$ can be considered ionic since discrete anions, $GaCl_4^-$ or $Ga_2Cl_7^-$, are observed in the presence of an arene solvent (which is π coordinated to the P atom). This results in

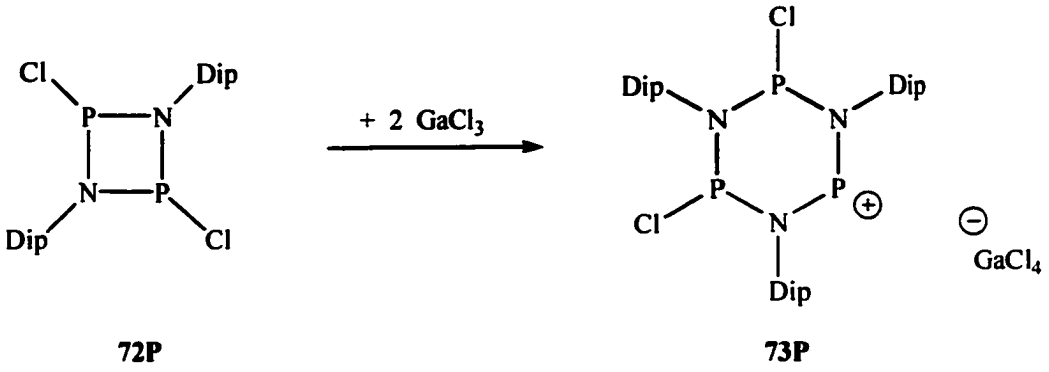

72P **73P**

Figure 5.10 Reaction scheme for the formation of **73P**.

an overall dependence of $[Mes^*NP]^+$ on the counter anion and the solvent used[134]. Reaction of **72P** with $GaCl_3$ produces the phosphazane, $[Dip_3N_3P_3Cl_2][GaCl_4]$ (**73P**) as shown in Figure 5.10 (This work was carried out in collaboration with B. Ellis and K. Conroy). This result can be understood, in that the dimer (**72P**) is disrupted by the presence of $GaCl_3$ and the monomer intermediate (either DipN=PCl or $[DipNP]^+$) reacts rapidly to form the cyclic species, **73P**.

The phosphazane, **73P**, has been characterised by m.p., IR, ^{31}P NMR (solid state and solution) and X-ray spectroscopy. The molecular structure of **73P** is shown in Figure 5.11. The unit cell contains a molecule of solvent (CH_2Cl_2), which has not been shown for clarity. The ^{31}P NMR spectrum of **73P** is complicated by the possibility of exchange between the P and Cl atoms (i.e. Cl atoms of the anion and/or the solvent molecule, CH_2Cl_2). Further examination (VT NMR) of the exchange process must be completed before a full understanding of the observed ^{31}P NMR spectrum can be reached.

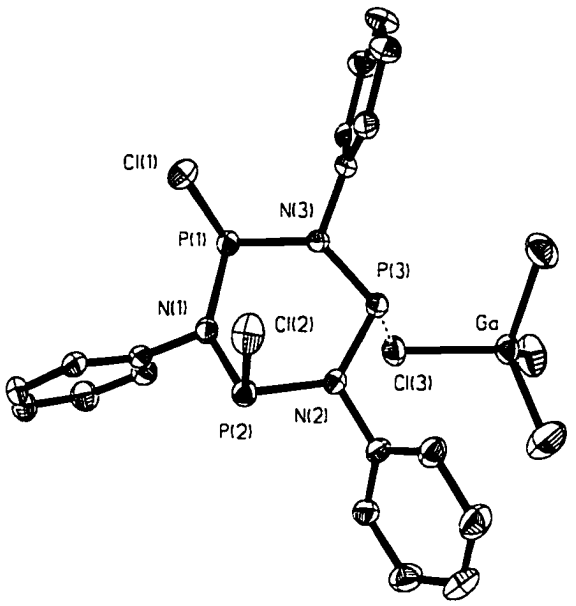

Figure 5.11 Diagram (ORTEP) of the molecular structure of **73P** (^{i}Pr groups removed from Dip substituent for clarity).

The N atoms of **73P** lie in a trigonal planar environment (sum of the angles are approximately 360°, see Table 5.5). However, the 6-membered ring is not planar, the P atoms are twisted out of the plane defined by the three N atoms. The P(1)-Cl(1) and P(2)-Cl(2) bond lengths (2.081(1) Å and 2.088(1) Å respectively) are longer than those found in PCl_3 (2.03 Å[135]). The closest non-bonded contact is between P(3)-Cl(3) (2.704 Å) and is considerably longer than a typical P-Cl bond length. The P-N bond lengths are shorter than a typical P-N single bond length (1.800(4) Å[110]) and are not equivalent (ranging from 1.650(1) - 1.753(1) Å).

Table 5.5 Selected Bond Lengths (Å) and Angles (°) for $[Dip_3N_3P_3Cl_2][GaCl_4]$ **73P**.

Bond Lengths		Bond Angles	
P(1)-N(1)	1.697(2)	N(1)-P(1)-N(3)	99.4(9)
P(1)-N(3)	1.753(2)	N(1)-P(2)-N(2)	100.8(1)
P(2)-N(1)	1.703(2)	N(2)-P(3)-N(3)	105.1(1)
P(2)-N(2)	1.736(2)	P(1)-N(1)-P(2)	131.8(1)
P(3)-N(2)	1.656(2)	P(1)-N(1)-C(11)	113.2(2)
P(3)-N(3)	1.650(2)	P(2)-N(1)-C(11)	114.7(2)
P(1)-Cl(1)	2.081(1)	P(2)-N(2)-C(31)	113.4(2)
P(2)-Cl(2)	2.088(1)	P(3)-N(2)-C(31)	116.2(2)
P(3)-Cl(3)	2.704(1)	P(2)-N(2)-P(3)	129.5(2)
		P(1)-N(3)-P(3)	134.5(1)
		P(1)-N(3)-C(51)	110.5(1)
		P(3)-N(3)-C(51)	113.9(1)

5.4 Summary

The differences in the steric strain imposed by the Dip and Mes* substituents on the "RNPCl" framework (when $AgOSO_2CF_3$ or $GaCl_3$ is added) have resulted in the isolation of both cyclic and monomeric species. The use of the Mes* substituent provides sufficient steric strain to stabilise the iminophosphine, $Mes^*NPOSO_2CF_3$, and the phosphoazonium salt, $[Mes^*NP][GaCl_4]$. However, the thermodynamic and kinetic influences of the Mes* substituent on this system are such that the dimer, $[Mes^*NPOSO_2CF_3]_2$, can also be isolated. In contrast, the use of the Dip substituent results in the isolation of cyclic species, $[DipNPOSO_2CF_3]_2$ (dimer) and $[Dip_3N_3P_3Cl_2][GaCl_4]$ (trimer). The isolation of **73P** suggests that in the latter case a monomeric intermediate species is formed. It is insufficiently stabilised and therefore reacts further to form the trimer.

Chapter 6 – Conclusions and Future Work

Deprotonation reactions involving the monoaminopnictines, **56As** and **56Sb·MesNH$_2$**, produced the pnictetidines, **58As** and **59Sb**, instead of the desired iminopnictines, Mes*N=AsCl and Mes*N=SbOSO$_2$CF$_3$. These results suggests that the steric strain imposed by the Mes* substituent is insufficient to stabilise the multiply bonded "N=Pn" environment for Pn = As, Sb. One way to prevent this from happening is to increase the steric protection on the Pn centre. Iminoarsines have been prepared using the Mes* substituent (i.e. Mes*N=AsN(H)Mes*, **52As**, and Mes*N=AsN(R)SiMe$_3$, **53As**) with bulky substituents on both N and As. Exchanging the chlorine atom on any of the dichloromonoaminopnictines (**55As**, **55Sb**, **56As**, **56Sb·MesNH$_2$**) by reaction with MR' (where M = metal such as Li and R' is an bulky substituent) would produce compounds of the type Mes*N(R)PnCl(R').

Some preliminary experiments using **55As** and **56Sb·MesNH$_2$** as starting materials (see Figures 6.1 and 6.2) accessed the intermediate, Mes*N(R)Pn-Cl(R') (where R = SiMe$_3$ or H and R' was a variety of substituents see below). Elimination of HCl (by the addition of NEt$_3$, as in previous reactions) or SiMe$_3$Cl (by the addition of SiMe$_3$OSO$_2$CF$_3$, as was shown to be successful for some monoaminophosphines[96]) was then attempted. However, the reactions outlined below produced a viscous oil from which a solid sample could not obtained. Discovery of the appropriate isolation or purification techniques could result in the isolation of solid samples.

Figure 6.1 shows the reaction of Mes*N($SiMe_3$)$AsCl_2$ with an equimolar amount of LiOR (where R = 2,6-tert-butyl-4-methylphenyl) followed by addition of an excess of $SiMe_3OSO_2CF_3$ to produce a dark purple mixture. This reaction was originally carried out by C.L.B Macdonald[10]. The principal product from this reaction was attributed to Mes*N=As-OR (*ca.* 65% total signal integration by ^1H NMR spectroscopy). Similar results were obtained when this reaction was repeated and additional attempts to isolate a solid material were unsuccessful. Addition of one equivalent of R'Li (where R = Mes* or DMesp) to **56Sb·Mes*NH$_2$** produces a dark purple reaction mixture. Removal of the solvent yields a purple coloured oil.

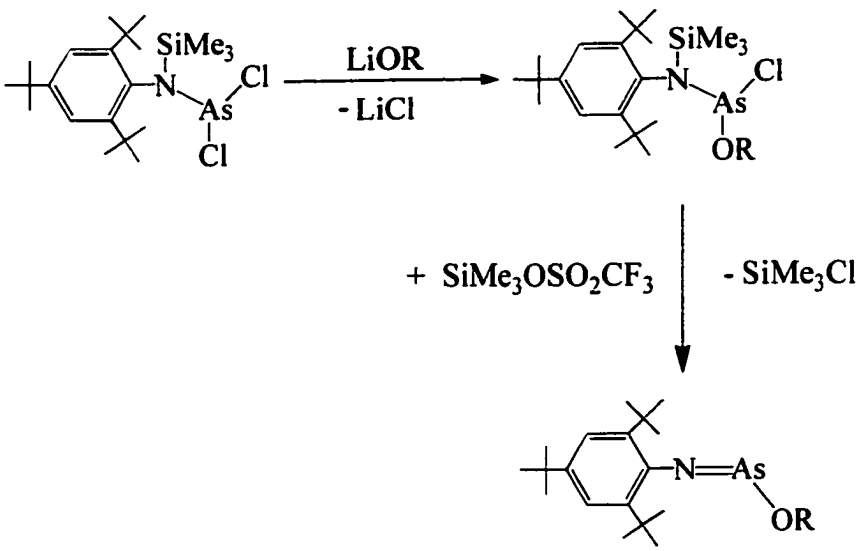

Figure 6.1 Desilylation reaction of Mes*N($SiMe_3$)AsCl(OAr).

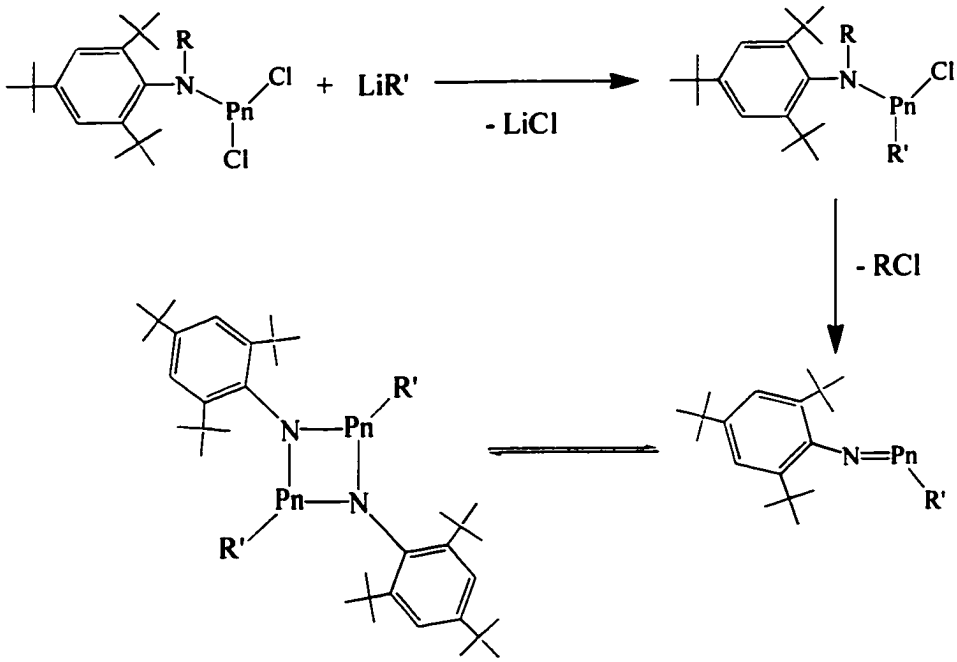

Figure 6.2 Potential synthesis of iminopnictines from **55As**, **55Sb**, **56As** and **56Sb·MesNH$_2$**.

In addition, reactions involving Mes*N(R)Li (where R = $SiMe_3$ or H) and R'$SbCl_2$ (where R' = Ph or $(SiMe_3)_2CH$) were carried out in an attempt to prepare Mes*N(R)Sb(R')Cl. The addition of NEt_3 (when R = H) or $SiMe_3OSO_2CF_3$ (when R = $SiMe_3$) resulted in the formation of an insoluble yellow solid that could not be characterised.

The *in situ* reaction of Mes*NHLi with $PnCl_3$, followed by addition of $AgOSO_2CF_3$, produced the pnictenium salts, **70PnOSO$_2$CF$_3$** (when Pn = P or As), and the stibetidine, **59Sb** (when Pn = Sb). The fundamental properties of the elements (such as electronegativity, ionisation energy or atomic radii) can account for differences in reactivity when considering reactions involving a series of analogous compounds, for a specific group within the Periodic Table. However, the isolation of the stibetidine, **59Sb**, instead of a bisaminostibenium salt (**70PnOSO$_2$CF$_3$**) suggest that the four-membered NSbNSb ring is kinetically or thermodynamically favoured over the $[N\text{-}Sb\text{-}N]^+$ fragment. All of the phosphenium and arsenium salts prepared have short Pn-N bond lengths and planar N environments, suggesting donation of lone pair of electrons on the N atom into the empty p-orbital of the pnictogen. A similar interaction for the Sb derivative would also be expected, but may not be favoured under these reaction conditions. However, under the more vigorous reaction conditions (i.e. the addition of $Sb(NMes^*H)_3$ and $HOSO_2CF_3$) the stibetidine, **70SbOSO$_2$CF$_3$**, can be obtained.

The isolation of the pnictenium salts, **70PnOSO$_2$CF$_3$** for Pn = As or Sb, are the first examples of acyclic pnictenium cations for these heavier elements. As mentioned in Chapter 1, few low-coordinate compounds exist for species containing both N and the heavier pnictogens (As and Sb). This series of pnictenium salts allows a comparative study of their reactivity to be undertaken. Reactions with donors or oxidising agents would allow fundamental properties (Lewis acidity and oxidation potential) of P, As and Sb in similar environments to be investigated.

The isolation and characterisation of **59P** and **60P** (*i.e.* $[Mes^*NPOSO_2CF_3]_n$ where n = 1 or 2) suggests that the energetics between these two species is not significant enough to prevent the isolation (in the solid state) of both the monomer and dimer forms of this compound. The change in colour observed when the iminoarsine, **58As**, is in solution (red or purple) and the solid state (yellow) suggest that there is a similar change in the nature of this species between the two states (i.e. solution and solid). In addition when **58As** is heated a colour change is also observed (yellow to red). When the phosphetidine, **60P**, is heated the iminophosphine, **59P**, is formed. It is therefore proposed that the monomeric from of **58As** may also be accessible.

The reaction of $[DipNPCl]_2$ (**72P**) with $GaCl_3$ also suggests that the monomeric form of **72P** can be accessed. Interestingly, when **72P** is heated very slowly a change in colour from clear to orange was also observed. The ability to use pnictetidines as precursors to iminopnictines would represent a significant development in the field of N-Pn (where Pn ≠ N) chemistry. Pnictetidines are generally stable and as discussed in the Introduction, a number of derivatives are known for P, As and Sb. The synthesis of $[DipNPnCl]_2$ and $[Mes^*NPnOSO_2CF_3]_2$ (for Pn = As, Sb or Bi) would allow these reactions (heating, slow crystallisation and addition of $GaCl_3$) to be examined for the heavier group 15 elements.

Chapter 7 – Experimental Procedures

7.1 General Procedures

All compounds were handled using methods developed for the absence of air and moisture[136]. Reactions were performed in evacuated (~ 10^{-3} Torr) vessels, which were assembled and flame-dried prior to use. Diethyl ether was obtained from ACP Chemicals Inc., hexane from Van Waters & Rogers and arsenic (III) chloride from Kodak Chemicals. All other chemicals and reagents were obtained from Aldrich Chemical Company. All solvents were degassed and stored in evacuated bulbs. Sample handling and reactions were performed under oxygen and moisture free conditions. $BiCl_3$, n-butyllithium (1.6 M in hexanes), triflic acid ($HOSO_2CF_3$), trifluoromethanesulfonate ($AgOSO_2CF_3$) and 2,6-diisopropylaniline ($DipNH_2$), N-(trimethylsilyl)-2,4,6-tri-tert-butylaniline ($Mes^*N(SiMe_3)NH_2$) and 2,4,6-tri-tert-butylaniline (Mes^*NH_2) were used as supplied. Dichloromethane was dried at reflux over CaH_2 and P_4O_{10}, hexane and toluene were dried over potassium, and diethyl ether and THF were dried over sodium/benzophenone. Deuterated solvents and triethylamine (NEt_3) were dried over CaH_2 and distilled prior to use. PCl_3 and $AsCl_3$ were distilled and $SbCl_3$ and $GaCl_3$ were sublimed *in vacuo* prior to use. $Mes^*N(H)As{=}NMes^*$[12], Mes^*NPCl[9], $Mes^*NPOSO_2CF_3$[132] and $(Mes^*NH)_3Sb$[13] were prepared as described in the literature. Lithium amides were prepared under an atmosphere of nitrogen *in situ* by adding an equimolar quantity of ^{n}BuLi *via* a septum to a stirred (RT) solution (diethyl ether or toluene) of the amine, followed by stirring for at least eight hours. The resultant mixture was then added to the pnictogen trichloride solution, over a period of 10-15 minutes.

Infrared spectra were recorded as Nujol mulls on CsI plates using a Nicolet 510 FT-IR spectrometer. FT-Raman spectra were recorded on powdered samples sealed under nitrogen in melting point tubes using a Bruker RFS 100 spectrometer. Vibrational spectra are presented as wavenumber (cm^{-1}) with ranked intensities for each absorption given in parentheses and the most intense peak is given a ranking of 1. Melting point samples were placed in 1.0-mm (OD) Pyres capillaries, sealed under nitrogen and measured using an Electrothermal® Melting Point Apparatus. Beller Laboratories, Göttingen, Germany, performed chemical analyses. UV-visible spectra were obtained on a Varian Cary 100Bio UV-visible spectrometer at room temperature. Solution NMR samples were flame-sealed in 5 mm Pyrex tubes and recorded on a Bruker AC-250 NMR spectrometer. NMR spectra were referenced to the solvent and chemical shifts are reported in ppm relative to an external standard (TMS for ^{1}H and ^{13}C, 85% H_3PO_4 for ^{31}P, CCl_3F for ^{19}F). Solid-state ^{31}P NMR spectra were obtained using a Bruker double-air-bearing MAS probes on a Bruker AMX-400 (9.4 T) spectrometer by Mike Lumsden. Powdered crystalline samples were carefully packed in 4 mm (AMX-400) zirconium oxide rotors under an inert atmosphere. The ^{31}P NMR chemical shifts were referenced with respect to 85% $H_3PO_{4\,(aq)}$ by setting the ^{31}P chemical shift of phosphorus in solid ammonium dihydrogen phosphate ($NH_4H_2PO_4$) to 0.81 ppm. Typical rotor speeds for the MAS experiments ranged from 7 to 12 kHz. Solid-state ^{31}P CP/MAS NMR spectra were acquired with proton-phosphorus cross-polarisation under conditions of Hartman-Hahn matching. The proton 90° pulse width was set to 6 μs, with a contact time and recycle delay of 8 ms and 3 s, respectively.

7.2 Crystallisation Methods

Unless otherwise indicated, crystallisation was performed directly from the reaction mixtures. All reactions were carried out in either a two or three chambered reaction vessel, which was placed under vacuum. This allowed solvent and other volatiles to be distilled into an adjacent empty chamber (or bulb), through cooling. The rate of distillation depends not only on the vapour pressure of the volatile components but also on the manner in which the chamber was cooled. In almost all cases the empty chamber was first cooled by slowly dripping cold water onto the empty bulb. The rate at which the water was dripped onto the bulb, could be altered in order to promote the formation of a crystalline sample. If this did not show evidence of a solid material being formed within 1-2 days the empty chamber was then cooled by placing it into a dewar of liquid nitrogen. At first the bulb is positioned just above the liquid nitrogen level. However, it was often necessary to place the bulb directly into the liquid nitrogen in order to promote the formation of a solid material through a more rapid removal of volatiles. For most reactions, this method of cooling produced a crystalline material suitable for X-ray analysis. However in some cases an oil was produced by the slow removal of volatiles and required further work in order to obtain a solid sample. Generally the oil was first placed under a dynamic vacuum, which either produced a solid sample or a viscous oil. At this point the oil was cooled (5-10 °C) for several days. If no solid sample was obtained, 5-15 mL of hexane was added. In some cases this resulted in the immediate formation of a solid material. Alternatively the above methods could be repeated in an attempt to promote crystallisation through the slow removal of hexane and any other volatiles still present in the reaction mixture. If crystallisation directly from the

reaction mixture produced a solid which was not suitable for X-ray analysis, the solid was isolated and recyrstallised from alternative solvents. When a sufficient sample of crystals were obtained the remaining oil or solution was decanted away and the crystals were washed by cold-spot back distillation, before they were isolated. Crystals were selected and mounted in thin wall glass capillaries in the dry box and sealed under nitrogen. Structure determination was performed by Dr. T. S. Cameron, Dr. K. Robertson and Dr. R. McDonald.

7.3 Lithiation Procedures

A typical reaction involves both a one neck and a two-neck bridge or reaction vessel. Each reaction vessel has one chamber (or bulb) equipped with a septum. The septum bulb on the two-neck bridge is also equipped with a frit. The vessels were evacuated and flame dried. The amine, RNHX, (where R = Mes* and X = H or $SiMe_3$ or R = Dip and X = H) was added to the one-neck bridge in the dry bag. $AsCl_3$ was distilled into the septum bulb of the second reaction vessel and $SbCl_3$ was introduced in the dry box. Solvent (diethyl ether or toluene) was distilled into both chambers and the vessels were placed under nitrogen (by allowing a rapid stream of N_2 gas to pass into the temporarily opened tap of the bridge). An equimolar volume of ^{n}BuLi was introduced, via the septum, into the amine solution while stirring. The mixture was allowed to stir for a minimum of 8 hours before it was added to the pnictogen trichloride solution (see specific procedures for the temperature), over a period of 15 minutes via a cannula, resulting in a coloured solution (see specific procedures) and a white precipitate. The

reaction mixture was stirred for several hours and then filtered. The resultant clear solution was frozen and the vessel was evacuated in order to allow volatiles to be removed by the methods discussed in section 7.2. Alternatively this mixture was reacted *in situ*, as indicated in the specific procedures of **59Sb**, **67AsOSO$_2$CF$_3$**, **70POSO$_2$CF$_3$** and **70AsOSO$_2$CF$_3$**.

7.4 Specific Procedures

Preparation of Mes*N(SiMe$_3$)AsCl$_2$, 55As

Mes*N(SiMe$_3$)H (0.73g, 2.2 mmol) in diethyl ether (20 mL), ^{n}BuLi (2.2 mmol), AsCl$_3$ (1 mL $^+$, > 12 mmol) in diethyl ether (20 mL) were combined as outlined above and left to stir at RT for 8 hours. The solution was filtered and removal of solvent *in vacuo* left a crystalline material surrounded by a viscous oil, which was recrystallised from hexane by slow evaporation (1 day) to give yellow crystals (isolated in 4 batches) characterised as Mes*N(SiMe$_3$)AsCl$_2$; (second batch) yield 0.19 g, 19%; m.p. 109-111 °C;

Anal. Calcd.: C, 52.72; H, 8.01; N, 2.93%;

Found: C, 53.03; H, 8.02; N, 2.96%;

IR (cm^{-1}): ~3685br.*(18)*, 3280*(28)*, 3231*(33)*, 3087*(34)*, 3065*(35)*, 1601*(30)*, 1403sh.*(16)*, 1391*(8)*, 1389*(11)*, 1256*(7)*, 1254*(9)*, 1213*(14)*, 1168*(13)*, 1196*(23)*, 1134*(32)*, 1089*(22)*, 1092*(3)*, 1019*(24)*, 908*(26)*, 883*(5)*, 855br.*(1)*, 841br.*(2)*, 773*(15)*, 762*(12)*, 751*(10)*, 742*(8)*, 695*(20)*, 676*(21)*, 636*(19)*, 546*(25)*, 477*(19)*, 458*(30)*, 428*(31)*, 379*(21)*, 364*(4)*, 347*(27)*, 321*(6)*;

Raman (cm^{-1}) 166 mW: 95*(17)*, 120*(5)*, 136*(19)*, 155(*6*), 189(*18*), 255(*20*), 322(*4*), 362(*2*), 429(*33*), 478(*34*), 547(*31*), 571(*11*), 635(*10*), 676(*29*), 696(*35*), 743(*23*), 818(*13*), 866(*16*), 922(*21*), 1027(*32*), 1094(*9*), 1134(*8*), 1179(*14*), 1197(*15*), 1239(*25*), 1285(*30*), 1362(*26*), 1392(*28*), 1444(*12*), 1601(*7*), 2709(*24*), 2905(*1*), 2965(*3*), 3073(*27*), 3089(*22*);

^{1}H NMR (ppm, CD_2Cl_2): 0.25 (s, 9H, $SiMe_3$), 1.22 (s, 9H, p-^{t}Bu), 1.48 (s, 18H, o-^{t}Bu), 7.42 (s, 2H, Ar-H);

^{1}H NMR (ppm, THF-d8): 0.34 (s, 9H, $SiMe_3$), 1.31 (s, 9H, p-^{t}Bu), 1.56 (s, 18H, o-^{t}Bu), 7.53 (s, 2H, Ar-H);

^{13}C NMR (ppm, CD_2Cl_2): 4.5, 31.2, 33.7, 35.4, 38.6, 122.4, 126.2, 148.5, 150.7;

Crystal data: Orthorhombic, space group: Pbca(#61), a = 19.771(2) Å, b = 19.607(2) Å, c = 12.940(2) Å; V = 5016.3(7) Å^3, D_{calc} = 1.267 g/cm^3, R_1 = 0.042.

Preparation of Mes*N(SiMe$_3$)SbCl$_2$, 55Sb

Mes*N($SiMe_3$)H (1.20 g, 3.58 mmol) and ^{n}BuLi (3.6 mmol) were added together as described in the lithiation procedures and then added to a solution of $SbCl_3$ (0.82 g, 3.6 mmol) in diethyl ether (20 mL) at 0 °C. The mixture was left to stir for 8 hours before it was filtered. Removal of solvent *in vacuo* left a yellow solid; yield 1.30 g, 69%, m.p. 110-112°C;

IR (cm^{-1}): 3079*(19)*, 1617*(15)*, 1601*(12)*, 1554*(21)*, 1392*(4)*, 1378*(7)*, 1269*(8)*, 1251*(2)*, 1235*(5)*, 1214*(10)*, 1198*(13)*, 1171*(6)*, 1136*(16)*, 1100*(3)*, 1023br.*(24)*, 910*(18)*, 863*(1)*, 812*(11)*, 769*(22)*, 753*(14)*, 690*(23)*, 671*(25)*, 643*(20)*, 575br.*(28)*, 540*(27)*, 511br.*(30)*, 471*(26)*, 438br.*(29)*, 406br.*(32)*, 376*(31)*, 337*(9)*, 313*(17)*;

Raman (cm^{-1}) 166mW: 91*(7)*, 132*(5)*, 147*(6)*, 212*(29)*, 259*(16)*, 313*(4)*, 338*(2)*, 394*(41)*, 430*(37)*, 459*(39)*, 473*(40)*, 542*(36)*, 571*(12)*, 631*(20)*, 672*(30)*, 691*(28)*, 713*(27)*, 746*(35)*, 770*(42)*, 823*(10)*, 853*(22)*, 921*(14)*, 933*(19)*, 1026*(33)*,1100*(18)*, 1173*(15)*, 1199*(17)*, 1237*(32)*, 1267*(38)*, 1275*(34)*, 1284*(31)*, 1326*(23)*, 1392*(23)*, 1405*(21)*, 1447*(9)*, 1465*(13)*, 1602*(8)*, 2710*(24)*, 2779*(25)*, 2904*(1)*, 2963*(3)*, 3082*(26)*; ^{1}H NMR (ppm, CD_2Cl_2): 0.31 (s, 9H, $SiMe_3$), 1.30 (s, 9H, p-^{t}Bu), 1.57 (s, 18H, o-^{t}Bu), 7.48 (s, 2H, Ar-H).

A small sample was recrystallised from diethyl ether to yield small yellow crystals which were characterised as Mes*N($SiMe_3$)$SbCl_2$ and shown to be spectroscopically identical to the bulk solid originally obtained;

Crystal data: Monoclinic, space group: $P2_1/n$ (#41), a = 12.836(2) Å, b = 13.066(5) Å, c = 15.306(2) Å, β = 92.59(1)°; V = 2564.6(8) Å^3, D_{calc} = 1.360 g/cm^3, R_1 = 0.058.

On one occasion a solid sample was isolated and shown to contain **55Sb** and Mes*NH_2·$SbCl_3$, yield 0.74 g, 1.4 mmol, 89%, m.p. 96-110 °C;

^{1}H NMR (ppm, CD_2Cl_2): 0.31s, 1.29s, 1.31s, 1.39s, 1.56s, 3.9br., 7.12s, 7.48s.

The remaining sample was recrystallised from diethyl ether and characterised as Mes*NH_2·$SbCl_3$, yield 0.52g, 1.0 mmol, 63%, m.p. 105-107 °C;

Anal. Calcd.: C, 44.16; H, 6.38; N, 2.86%;

Found: C, 44.81; H, 6.59; N, 2.80%;

IR (cm^{-1}): 3516*(22)*, 3443*(23)*, 2725*(11)*, 1598*(7)*, 1367*(1)*, 1296*(6)*, 1270*(12)*, 1241*(2)*, 1211*(13)*, 1170*(16)*, 1099*(5)*, 1020*(15)*, 914*(19)*, 876*(3)*, 862*(4)*, 769*(20)*, 653*(21)*, 643*(25)*, 610*(24)*, 572*(26)*, 377*(10)*, 324*(9)*, 318*(8)*, 302*(17)*, 298*(18)*;

Crystal data: Monoclinic, space group: $P2_1/n$ (#41), a = 9.042(2) Å, b = 14.854(4) Å, c = 17.292(2) Å, β = 90.74(2)°; V = 2322.3(7) $Å^3$, D_{calc} = 1.400 g/cm^3, R_1 = 0.035.

Attempted preparation of Mes*N(SiMe$_3$)BiCl$_2$ 55Bi

Mes*N(SiMe$_3$)H (0.55 g, 1.6 mmol) and ^{n}BuLi (1.6 mmol) were combined as described in the lithiation procedures and then added to a suspension of $BiCl_3$ (0.52 g, 1.6 mmol) in diethyl ether (30 mL) at -78 °C. The mixture was left to stir for 3 hours before it was filtered. Removal of solvent *in vacuo* left a mixture of orange and yellow solid materials; yield 0.76 g, orange material starts to decompose around 79 °C, yellow product m.p. 111-115 °C;

IR(cm^{-1}): 3517*(36)*, 3427*(16)*, 3394*(8)*, 3362*(21)*, 3322*(15)*, 3101*(30)*, 3002*(6)*, 2668*(28)*, 1768*(39)*, 1703*(40)*, 1619*(29)*, 1600*(20)*, 1577*(11)*, 1432*(1)*, 1391*(7)*, 1370*(5)*, 1360*(2)*, 1309*(18)*, 1290*(19)*, 1264*(14)*, 1252*(9)*, 1231*(3)*, 1201*(17)*, 1119*(23)*, 1100*(32)*, 1025*(33)*, 956*(22)*, 944*(24)*, 933*(25)*, 916*(26)*, 879*(4)*, 837*(13)*, 799*(10)*, 765*(34)*, 754*(38)*, 714*(27)*, 645*(37)*, 304*(35)*, 278*(31)*, 242*(12)*;

^{1}H NMR (ppm, CD_2Cl_2): 0.17s, 0.45s, 1.29s, 1.30s, 1.47s, 1.54s, 4.17s, 7.29s, 7.32s.

Preparation of Mes*N(H)AsCl$_2$, 56As

Mes*NH$_2$ (3.93 g, 15.0 mmol), ^{n}BuLi (15 mmol), AsCl$_3$ (>1.5 mL, > 17 mmol) in diethyl ether (15 mL) were combined at RT (as outlined in the lithiation procedures) producing a purple solution and a white precipitate. After three days, the now pink solution was filtered and removal of solvent *in vacuo* left a peach crystalline material characterised as Mes*(H)NAsCl$_2$, yield: 5.8 g, 95%, m.p. 60-65 °C;

IR (cm^{-1}): 3520*(33)*, 3453*(30)*, 3406sh.*(21)*, 3386*(11)*, 3095*(25)*, 3032*(16)*, 2744*(29)*, 1768*(28)*, 1620*(23)*, 1598*(13)*, 1558*(26)*, 1434sh.*(8)*, 1420*(4)*, 1393, 1361*(1)*, 1286*(14)*, 1265*(15)*, 1240*(6)*, 1216*(3)*, 1201sh.*(10)*, 1190sh.*(12)*, 1022*(32)*, 928*(31)*, 913*(34)*, 880*(5)*, 843*(9)*, 816*(19)*, 792*(22)*, 769*(27)*, 757*(18)*, 723*(35)*, 642*(20)*, 547*(36)*, 466*(24)*, 361*(2)*, 332sh.*(7)*, 281*(17)*;

Raman (cm^{-1}) 166 mW: 128*(5)*, 155*(4)*, 189*(6)*, 267*(9)*, 370*(3)*, 570*(14)*, 637*(17)*, 820*(7)*, 844*(19)*, 930*(16)*, 1116*(20)*, 1146*(12)*, 1192*(11)*, 1218sh.*(15)*, 1241*(18)*, 1393*(22)*, 1444*(13)*, 1468*(10)*, 1599*(8)*, 2706*(23)*, 2782*(25)*, 2911*(2)*, 2967*(1)*, 3034*(21)*, 3099*(24)*, 3385*(23)*;

^{1}H NMR (ppm, CD_2Cl_2): 1.30 (s, 9H, p-^{t}Bu), 1.51 (s, 18H, o-^{t}Bu), 5.48 (broad s, 1H, N-H), 7.38 (s, 2H, Ar-H);

Crystal data: Orthorhombic, space group: Pbca(#61), a = 16.412(3) Å, b = 25.188(2) Å, c = 10.088(3) Å; V = 4170(1) Å^3, D_{calc} = 1.294 g/cm^3, R_1 = 0.046.

Preparation of Mes*N(H)$SbCl_2$·Mes*NH_2, 56Sb·Mes*NH_2

Mes*NH_2 (1.87 g, 7.16 mmol) in toluene (20 mL) and ^nBuLi (4.5 mL, 7.2 mmol) were combined as outlined in the lithiation procedures. The lithium amide mixture was added to a solution of $SbCl_3$ (0.82 g, 3.6 mmol) in toluene (20 mL) over a period of 10 minutes at -78 °C. The mixture was filtered and the resultant clear solution was frozen and the vessel was placed under vacuum. Upon removal of volatiles the reaction mixture rapidly decomposed (turned a dark black colour), however a few yellow cube shaped crystals were isolated and crystallographically characterised as **56Sb**;

Crystal data: Triclinic, space group: P-1, a = 10.011(2) Å, b = 23.279(4) Å, c = 9.427(3) Å, α = 96.51(2), β = 117.06(2), γ = 92.38(2), V = 1933(1) $Å^3$, D_{calc} = 1.228 g/cm^3, R_1 = 0.2664.

Crystallisation of Mes*NPCl, 50P

Mes*NPCl was prepared as described in the literature[9] and a sample (2.65g, 8.13 mmol) was recrystallised from hexane (60 mL) over a period of one week by slow cooling of an adjacent empty chamber by a stream of water to produced a red coloured oil. When the empty chamber was placed under a stream of liquid nitrogen, immediate precipitation occurred. A small amount of hexane was added and the mixture was gently heated with warm water until the entire solid precipitated had redissolved. The solution was kept cold (approximately 10 °C) for a period of 3 days to yield small red coloured crystals, yield 2.27g, 86%, which were confirmed to be the monomer, Mes*NPCl by m.p., IR and solid state NMR spectroscopy.

Preparation of Mes*NAsCl derivatives, 57As and 58As

Et_3N (10 mL) in Et_2O (15 mL) was added to Mes*(H)$NAsCl_2$ (1.36g, 3.34 mmol) in Et_2O (15 mL), producing a dark purple solution and a white precipitate. The mixture was filtered and the volatiles were removed *in vacuo* from the filtrate to leave a yellow solid. The compound was extracted with hexane, filtered (to remove any remaining NEt_3HCl) and the solvent was removed by distillation. The resulting solid was recrystallised from Et_2O over a period of one week, during which the solution temperature was maintained below 10°C; yellow crystals of $[Mes^*NAsCl]_2$, yield 0.250g, 20%; m.p. 159-164 °C (colour change to red at 105°);

Anal. Calcd.: C, 58.46; H, 7.90; N, 3.79%;

Found: C, 59.04; H, 8.08; N, 3.75%;

IR (cm^{-1}): 2624*(29)*, 2606*(28)*, 2533*(43)*, 2499*(38)*, 1597*(24)*, 1409*(9)*, 1398*(7)*, 1392*(10)*, 1363*(3)*, 1291*(22)*, 1262*(16)*, 1241*(14)*, 1201*(6)*, 1188*(12)*, 1175*(5)*, 1141*(31)*, 1104*(1)*, 1037*(33)*, 1027*(34)*, 947*(44)*, 933*(37)*, 912*(18)*, 879*(11)*, 847*(2)*, 819*(27)*, 801*(4)*, 756*(17)*, 751*(20)*, 731*(8)*, 650*(39)*, 635*(19)*, 591*(32)*, 548*(23)*, 539*(36)*, 482*(21)*, 458*(42)*, 412*(35)*, 370*(15)*, 321*(13)*, 303*(40)*, 293*(26)*, 291*(25)*;

^1H NMR (ppm, CD_2Cl_2): 1.31 (s, 9H, p-^{t}Bu), 1.62 (s, 18H, o-^{t}Bu), 7.37 (s, 2H, Ar-H);

Crystal data: Monoclinic, space group: $P2_1/n$, a = 10.397(7) Å, b = 17.611(6) Å, c = 11.442(7) Å, β = 113.66(4) °; V = 1919(2) $Å^3$, D_{calc} = 1.280 g/cm^3, R_1 = 0.061.

When the reaction mixture was kept above 10°C a crystalline material was isolated and structurally characterised as the cyclodecomposition product, **57As**;

^{1}H NMR (ppm, CD_2Cl_2): 1.32 (s, 9H , p-^{t}Bu), 1.46 and 1.47 (two overlapping s, 15H total, 4-^{t}Bu and 2-CMe_2), 2.47 (very broad m, 2H, CH_2-As), 5.95 (broad s, 1H, N-H), 7.28 (d, $^4J_{H-H}$ 2.14 Hz, Ar-H)), 7.32 (d, $^4J_{H-H}$ 2.14 Hz, Ar-H);

Crystal data: Monoclinic, space group: $P2_1/n$, a = 12.088(2) Å, b = 9.614(6) Å, c = 16.7819(7) Å, β = 107.343(6) °; V = 1861.6(3) Å^3, D_{calc} = 1.319 g/cm^3, R_1 = 0.0399.

Crystallisation of $[Mes^*NPOSO_2CF_3]_n$, 59P and 60P

$Mes^*NPOSO_2CF_3$ was prepared as described in the literature[132] and samples (0.871g, and 1.780g) were slowly recystallised (empty chamber was cooled by a stream of cold water) from hexane over a period of one week. This produced crystalline samples (orange, yellow and white) which were isolated and characterised by m.p., X-ray analysis and IR and solid state NMR spectroscopy. Solution NMR and Raman data were performed previously by C.L.B. Macdonald and are included for reference to discussion in Chapter 5.

Solution NMR data of crystals redissolved in solvent:

^{1}H (ppm, CD_2Cl_2): 1.32 (s, 9H, p-^{t}Bu), 1.49 (s, 18H, o-^{t}Bu), 7.42 (s, 2H, Ar-H);

^{13}C (ppm, CD_2Cl_2): 29.9, 31.1, 33.9, 36.2, 98.9, 123.1, 135.7, 140.0, 150.7;

^{19}F (ppm, CD_2Cl_2): -78.3;

^{31}P (ppm, CD_2Cl_2): 50.1;

^{31}P (ppm, Et_2O): 51.4;

^{31}P (ppm, CH_2Cl_2): 50.0 (additional low intensity signal at 137 assigned to Mes*NPCl);

^{31}P (ppm, toluene): 51.7;

^{31}P (ppm, reaction mixture, hexane): 55.9;

Note: all ^{31}P spectra show an additional low intensity signal at 279 assigned to **70POSO$_2$CF$_3$**.

Orange crystals; assigned as Mes*NPOSO$_2$CF$_3$ on the basis of X-ray crystallographic analysis; m.p. 124-126 °C;

IR (cm^{-1}): 1599(9), 1464(1), 1398(15), 1366(3), 1296(sh), 1266(14), 1235(7), 1196(6), 1184(5), 1150(4), 1134(11), 914(2), 886(10), 629(8), 585(12), 532(13);

Raman (cm^{-1}) 166 mW: 2971(2), 2911(3), 1598(4), 1475(1), 1368(12), 1292(13), 1266(14), 1203(8), 1134(5), 1070(6), 926(15), 823(7), 781(11), 764(10), 571(16), 103(9);

Crystal data: Monoclinic, space group: $P2_1/n$, a = 10.454(2) Å, b = 10.741(2) Å, c = 20.489(2) Å, β = 97.834(10) °; V = 2279.2(5) Å^3, D_{calc} = 1.281 g/cm^3, R_1 = 0.0580.

Yellow crystals; assigned as [Mes*NPOSO$_2$CF$_3$]$_2$ on the basis of X-ray crystallographic analysis; m.p. 124-126 °C (colour change from yellow to orange at 113 °C),

IR (cm^{-1}): 1598(14), 1462(2), 1408(3), 1363(6), 1241(7), 1208(1), 1142(5), 1101(8), 1027(15), 916(13), 884(9), 827(4), 755(11), 752m, 638(12), 602(10);

Raman (cm^{-1}) 166 mW: 3016(17), 2973(1), 2914(2), 1598(4), 1468(13), 1447(12), 1230(8), 1206(9), 1152(10), 1029(11), 925(16), 824(3), 767(15), 568(7), 139(5), 117(6), 83(14);

Crystal data: Monoclinic, space group: $P2_1/n$, a = 11.368(2) Å, b = 16.429(3) Å, c = 12.013(2) Å, β = 90.59(3) °; V = 2243.5(7) Å^3, D_{calc} = 1.301 g/cm^3, R_1 = 0.0468.

White crystals; assigned as [Mes*N(H)PN(H)Mes*][OSO_2CF_3] by the basis of X-ray analysis (see preparation of **70POSO$_2$CF$_3$** for characterisation data);

^{31}P (ppm, solid mixture): δ_{iso} = 50.3 (monomer) **59P**, δ_{iso} = 257.9 (dimer) **60P** and δ_{iso} = 282.7 **70POSO$_2$CF$_3$**

Preparation of [Mes*NSbOSO$_2$CF$_3$]$_2$, 59Sb

Mes*NH_2 (4.93 g, 18.9 mmol) in toluene (30 mL) and ^{n}BuLi (18.9 mmol) were combined as outlined in the lithiation procedures. The lithium amide mixture was added to a solution of $SbCl_3$ (2.19 g, 9.60 mmol) in toluene (20 mL) over a period of 10 minutes at -78 °C. After 3 hours, the yellow solution was warmed to RT, filtered and added to $AgOSO_2CF_3$ (2.50 g, 9.73 mmol) in toluene (20 mL). After 15 minutes, the orange solution was filtered from the white precipitate and left to stand in the dark for several days to give orange crystals, yield 1.53 g, 1.44 mmol, 15%; m.p. solid above 360 °C;

Anal. Calcd.: C, 43.04; H, 5.51; N, 2.64%;

Found: C, 42.92; H, 5.59; N, 2.73%;

IR (cm^{-1}): 1599*(22)*, 1588*(27)*, 1568*(37)*, 1515*(33)*, 1424*(13)*, 1398*(18)*, 1367*(12)*, 1363*(11)*, 1312*(10)*, 1295*(6)*, 1269*(4)*, 1245*(5)*, 1229*(1)*, 1186*(7)*, 1182*(8)*, 1157*(0)*, 1109*(14)*, 1078*(29)*, 1022*(2)*, 964*(26)*, 942*(25)*, 915*(30)*, 879*(20)*, 856*(17)*, 821*(35)*, 804*(34)*, 784*(36)*, 765*(21)*, 756*(23)*, 733*(19)*, 704*(28)*, 694*(31)*, 670*(32)*, 646*(16)*, 635*(3)*, 576*(24)*, 519*(15)*, 470*(28)*, 353*(39)*;

^{1}H NMR (ppm, CD_2Cl_2): 1.30 (s, 9H, p-^{t}Bu); 1.65 (s, 18H, o-^{t}Bu); 7.41 (s, 2H, Ar-H).

^{19}F NMR (ppm, CD_2Cl_2): -78.1s;

Crystal data: Monoclinic, space group: $P2_1/n$, a = 11.4948(6) Å, b = 16.5251(9) Å, c = 12.0097(7) Å, β = 90.1491(10) °; V = 2281.27 Å^3, D_{calc} = 1.550 g/cm^3, R_1 = 0.0515.

Preparation of [Mes*N(H)AsN(H)Mes*][$GaCl_4$], 67As$GaCl_4$

Mes*NH_2 (1.28 g, 4.90 mmol) was dissolved in toluene (20 mL) and lithiated using ^{n}BuLi (3.1 mL, 5.0 mmol). The lithiated amine solution was slowly added to a mixture of $AsCl_3$ (0.21 mL, 2.5 mmol) in toluene (15 mL) at -78 °C and left to stir for seven hours. The resultant cloudy mixture was filtered producing a clear pale yellow solution. This reaction mixture was added to a $GaCl_3$ (0.43 g, 2.5 mmol)/toluene (15 mL) solution producing a dark red mixture which quickly faded to orange. This clear orange solution was left to stand over night to produce orange crystals, yield 1.46g, 1.81 mmol, 74%;

IR (cm^{-1}): 3231*(10)*, 1775*(32)*, 1599*(16)*, 1566*(21)*, 1542*(30)*, 1420*(3)*, 1395*(2)*, 1366*(1)*, 1360*(19)*, 1297*(14)*, 1269*(13)*, 1243*(8)*, 1214*(5)*, 1180*(9)*, 1151*(18)*, 1105*(4)*, 1011*(11)*, 938*(25)*, 926*(23)*, 912*(31)*, 882*(7)*, 851*(6)*, 820*(26)*, 797*(22)*, 762*(15)*, 695*(33)*, 649*(20)*, 634*(24)*, 627*(27)*, 583*(17)*, 544*(29)*, 464*(28)*, 414*(12)*;

^{1}H NMR (ppm, CD_2Cl_2): 1.29(s, 9H, p-^{t}Bu), 1.48(s, 18H, o-^{t}Bu), 7.51(s, 2H, Ar-H) and additional peaks indicating other products;

Crystal data: Monoclinic, space group: C2/c (#15) , a = 25.0948(8) Å, b = 10.184(1) Å, c = 16.426(2) Å, β = 93.545(5) °; V = 4189.7 Å^3, D_{calc} = 1.280 g/cm^3, R_1 = 0.045.

Preparation of [Mes*N(H)PN(H)Mes*][OSO_2CF_3], 70$POSO_2CF_3$

Mes*NH_2 (1.12 g, 4.27 mmol) was dissolved in toluene (30 mL) and lithiated using ^{n}BuLi (2.7 mL, 4.3 mmol). This lithiated amine solution was slowly added to a cooled (-78 °C) PCl_3 (2.2 mL, 4.3 mmol) solution (*i.e.* in 10 mL toluene). The mixture was allowed to stir for three hours before it was filtered producing a clear orange solution (at which point a small amount of the mixture was removed for reaction NMR spectroscopy). $AgOSO_2CF_3$ (0.55 g, 2.1 mmol) was placed in toluene (10 mL). The reaction mixture was slowly added to $AgOSO_2CF_3$ solution, after filtration a clear orange/yellow solution was obtained. The volatiles were removed and the mixture was dissolved in hexane. This produced an immediate white precipitate and orange/yellow coloured solution. The solution was decanted and the white crystalline material was isolated and characterised as **70$POSO_2CF_3$**, yield 0.20g, 0.3 mmol, 14%,

m.p. 125-130 °C;

IR (cm^{-1}): 3286*(34)*, 2710*(20)*, 1601*(17)*, 1569*(32)*, 1515*(30)*, 1488*(22)*, 1466*(7)*, 1424*(14)*, 1400*(16)*, 1364*(6)*, 1344*(19)*, 1313*(12)*, 1298*(4)*, 1272*(11)*, 1255*(9)*, 1246*(10)*, 1216br.*(2)*, 1183*(13)*, 1160*(5)*, 1107*(8)*, 1025*(1)*, 999*(15)*, 930*(27)*, 923*(25)*, 909*(29)*, 880*(18)*, 806br.*(24)*, 768*(31)*, 758*(28)*, 730*(33)*, 650*(23)*, 636*(3)*, 575*(26)*, 520*(21)*, 355*(33)*;

^{31}P NMR (ppm, reaction mixture): 270s, 152s, 150s, 148s, 147s, 131s;

^{31}P NMR (ppm), δ_{iso} = 282.7

^{31}P NMR (ppm, CD_2Cl_2): 279

^{31}P NMR spectroscopy was performed on the orange/yellow solution and showed peaks characteristic of with Mes*N=PN(H)Mes*[12] and Mes*N=$POSO_2CF_3$[132]; Crystal data: Monoclinic, space group: $P2_1/n$, a = 16.648(1) Å, b = 10.011(8) Å, c = 24.067(2) Å, β = 96.979(2) °; V = 3981.3 $Å^3$, D_{calc} = 1.169 g/cm^3, R_1 = 0.0581.

Preparation of [Mes*N(H)AsN(H)Mes*][OSO_2CF_3]

Method 1

A three chamber vessel was assembled, with 2 standard bulbs and an NMR tube. Mes*NAsN(H)Mes* (0.50 g, 0.85 mmol) was introduced into one bulb and $HOSO_2CF_3$ (0.24 mL, 2.7 mmol) to the second, both were dissolved in hexane, 50 mL and 20 mL respectively. Solutions were combined producing a bright yellow solution and precipitate. An aliquot of less than 5 mL was removed for ^1H, ^{13}C and ^{19}F reaction NMR, the remaining mixture was filtered and reduced in volume (by slow evaporation of volatiles), effecting additional precipitation. The mixture was recrystallised from toluene, resulting in the formation of a bright orange crystalline material, yield 0.25 g, 0.33 mmol, 40%, m.p. 168-170 °C.

Method 2

Mes*NH_2 (5.23 g, 19.2 mmol) was dissolved in toluene (20 mL) and lithiated using ^{n}BuLi (12.0 mL, 19.2 mmol). This lithiated amine solution was slowly added to a cooled (-78 °C) $AsCl_3$ (0.9 mL, 11 mmol) solution (*i.e.* in 20 mL toluene). The mixture was

allowed to stir for three hours before it was filtered producing a clear yellow solution. $AgOSO_2CF_3$ (2.60 g, 10.1 mmol) was placed in toluene (15 mL). The reaction mixture was slowly added to the partially dissolved $AgOSO_2CF_3$, after filtration a clear dark orange solution was obtained. The reaction mixture was left standing, protected from light for several days to produce bright orange crystals, yield 2.02g, 2.71 mmol, 28%, m.p. 168-170 °C;

Anal. Calcd: C, 59.66; H, 8.12; N, 3.76%;

Found: C, 59.49; H, 8.05; N, 3.76%;

IR (cm^{-1}): 3286*(21)*, 2667br.*(24)*, 2591br.*(25)*, 2361*(18)*, 2337*(23)*, 1652*(43)*, 1640*(39)*, 1635sh.*(42)*, 1617*(15)*, 1599*(12)*, 1576*(36)*, 1559*(41)*, 1554*(40)*, 1517*(6)*, 1496*(26)*, 1477*(8)*, 1435*(7)*, 1420sh.*(12)*, 1397*(16)*, 1378*(10)*, 1367*(11)*, 1294sh.*(13)*, 1223*(4)*, 1213*(9)*, 1182*(5)*, 1175*(2)*, 1123br.*(37)*, 1109*(27)*, 1087br.*(38)*, 1022*(1)*, 992*(20)*, 889*(29)*, 884*(28)*, 807br.*(14)*, 783br.*(33)*, 771br.*(35)*, 761*(34)*, 668*(30)*, 653*(31)*, 630*(3)*, 611*(22)*, 576*(32)*, 523*(19)*, 449br.*(46)*, 375*(54)*, 361br.*(47)*, 350*(45)*, 335*(53)*, 329*(52)*, 327*(50)*, 303*(49)*, 278*(51)*, 254*(48)*, 248*(55)*, 375*(54)*, 361br.*(47)*, 350*(45)*, 335*(53)*, 329*(52)*, 327*(50)*, 303*(49)*, 278*(51)*, 254*(48)*, 248*(55)*, 228*(44)*;

^1H NMR (ppm, CD_2Cl_2): 1.31 (18H, p-^{t}Bu), 1.55 (36H, o-^{t}Bu), 7.49 (4H, Ar-H), 8.55 (broad, 2H, N-H) performed on reaction mixture of method 1;

^{19}F NMR (ppm, CD_2Cl_2): -78.7 (s);

^{13}C NMR (ppm, CD_2Cl_2): 31.3, 31.8, 34.1, 35.4, 124.2, 143.9, 148.3, 152.3 (Note: quartet from CF_3 is not observed);

^1H NMR (ppm, CD_2Cl_2): 1.32 (18H, p-^{t}Bu), 1.58 (36H, o-^{t}Bu), 7.58 (4H, Ar-H), 11.95 (broad, 2H, N-H) performed on isolated crystals;

Crystal data: Monoclinic, space group: $P2_1/n$ (#14) , a = 16.713(2) Å, b = 10.259(2) Å, c = 24.024(2) Å, β = 93.41(1) °; V = 4112(1) Å^3, D_{calc} = 1.200 g/cm^3, R_1 = 0.063.

Preparation of [Mes*N(H)SbN(H)Mes*][OSO_2CF_3], 70SbOSO_2CF_3

$(Mes*NH)_3Sb$ (0.99g, 1.1 mmol) was added to one chamber of a two neck reaction vessel in the dry box. Triflic acid, $HOSO_2CF_3$ was carefully added to the second bulb in the glove bag. The reagents were frozen and the vessel was placed under vacuum. Hexane was distilled into both chambers (20 mL each) and the triflic acid solution was added to the trisaminostibine, producing a yellow coloured solution. The reaction was stirred for one hour and the volatiles were removed to yield a yellow solid. The solid was dissolved in hexane and the solution was decanted from the yellow solid. The solid was dissolved in toluene and the solvent was slowly removed *in vacuo* to yield a yellow micro crystalline sample, 0.22g, 0.28 mmol, 25%, m.p. 212-215 °C;

Anal. Calcd: C, 56.13; H, 7.64; N, 3.54%;

Found: C, 56.79; H, 7.52; N, 3.49%;

IR (cm^{-1}): 3285*(15)*, 2666*(24)*, 2588*(23)*, 1783*(40)*, 1598*(13)*, 1515*(7)*, 1479*(10)*, 1465*(8)*, 1435*(11)*, 1408*(25)*, 1397*(21)*, 1367*(12)*, 1336*(28)*, 1255*(1)*, 1222*(6)*, 1212*(9)*, 1182*(5)*, 1175*(3)*, 1109*(26)*, 1088*(27)*, 1048*(20)*, 1021*(2)*, 992*(14)*, 937*(32)*, 928*(34)*, 915*(31)*, 901*(39)*, 886*(15)*, 761*(29)*, 747*(36)*, 710*(33)*, 654*(22)*, 629*(4)*, 611*(17)*, 576*(16)*, 523*(11)*, 448*(38)*, 361*(30)*, 339*(37)*, 320*(35)*.

Preparation of [DipN(H)AsNDip]$_2$, 55As

Under an atmosphere of nitrogen, $AsCl_3$ (0.8 mL, 9.1 mmol) was added to a cooled (0 °C) solution of LiN(H)Dip (27 mmol) in Et_2O (50 mL) over a period of 10 minutes to give an orange solution and a white precipitate. After stirring at room temperature for 2 days, the solution was frozen and the vessel was evacuated. LiCl was filtered and volatiles were slowly removed under static vacuum to leave a red oil, which was dissolved in hexane and filtered. Slow removal of solvent under static vacuum gave a pale yellow crystalline solid with an oil, which was decanted, and the crystals were washed three times by cold spot back-distillation yield 0.67 g, 0.78 mmol, 17 %,

m.p. 166-169 °C;

Anal. Calcd.: C, 67.59; H, 8.27; N, 6.57%;

Found: C, 68.06; H, 8.01; N, 6.45%;

IR (cm^{-1}): 3398(19), 3055(20), 1432(1), 1383(7), 1327(12), 1313(5), 1254(21), 1242(4), 1234(6), 1186(3), 1104(24), 1098(13), 887(25), 856(11), 843(15), 820(17), 794(10), 785(2), 766(14), 696(23), 686(9), 518(22), 421(18), 368(15);

Raman (cm^{-1}) 166 mW: 3056(11), 3020(18), 2958(3), 2925(2), 2865(9), 1589(4), 1460(17), 1433(13), 1328(24), 1263(6), 1249(1), 1180(20), 1160(29), 1108(15), 1042(16), 954(28), 885(14), 843(26), 669(19), 605(25), 539(23), 507(30), 448(22), 364(12), 274(21), 223(27), 145(8), 102(10), 84(7), 71(5);

^{1}H NMR: 0.8 (d), 1.1 (d), 1.2 (d) 1.3 (d), 2.7 (sept), 3.0 (sept), 4.0 (sept), 4.2 (sept), 5.1 (s), 5.6 (s), 6.7-7.2 (m), additional minor signals;

UV-visible λ-max (nm) [ε determined using approximate concentrations], 230-250, 323 (1000).

Crystal data: Monoclinic, space group: $P2_1/c$(#14), a = 11.666(3) Å, b = 23.299(3) Å, c = 18.018(2) Å, β = 98.861(1)°; V = 4839(1) $Å^3$, D_{calc} = 1.171 g/cm^3, R_1 = 0.045.

Preparation of $[DipNPCl]_2$ 72P

Under an atmosphere of nitrogen, a solution of $DipNH_2$ (3.386g, 19.1 mmol) in 15 mL of toluene was added (*via* cannula) to a cooled (0 °C) solution of PCl_3 (0.83 mL, 9.5 mmol) in toluene (15mL) to give a pale orange solution. The reaction was stirred overnight and then filtered. The resultant clear yellow solution was frozen and the vessel was placed under vacuum. The volatile components were removed *in vacuo* (dynamic) leaving a yellow coloured oil. The oil was dissolved in hexane and an excess of triethylamine (5 mL) was distilled into the reaction mixture. The reaction was stirred for 3 hours and the then filtered to produce a clear yellow solution. The volatiles were removed to yield a clear crystalline solid yield 0.50 g, 1.2 mmol, 13%; m.p.; 197-202 °C;

^{31}P NMR (ppm, CD_2Cl_2): 211(s);

^{31}P NMR (ppm): δ_{iso} = 205

Characterisation data (m.p., IR, ^{31}P NMR and ^{1}H NMR) was consistent with $[DipNPCl]_2$ prepared by an alternative method[10].

Preparation of $[Dip_3N_3P_3Cl_2][GaCl_4]$ 73P

A solution of $GaCl_3$ (0.16g, 0.91 mmol) in toluene (15 mL) was slowly added to $[DipNPCl]_2$ **72P** (0.45g, 1.8 mmol) in toluene (10 mL) immediately forming an intensely coloured, orange solution. The reaction mixture was left to stir overnight before the solvent was removed to yield an orange coloured oil. The oil was dissolved in hexane producing a yellow precipitate. The resultant yellow solid was recrystallised CH_2Cl_2 producing yellow crystals, yield 0.083g, 0.092 mmol, 10%; m.p. 134-136 °C;

IR (cm^{-1}): 3061(29), 1436(6), 1384(8), 1364(9), 1349(24), 1316(25), 1264(28), 1180(26), 1152(10), 1095(7), 1056(23), 1041(14), 1006(13), 977(1), 970(3), 962(2), 932(19), 888(30), 856(18), 849(17), 803(4), 801(5), 712(21), 488(11), 472(16), 466(20), 427(15), 401(12), 363(27), 343(22);

^{31}P NMR is complicated both in solution and the solid state by rapid exchange between the chlorine atoms of anion ($GaCl_4$) and CH_2Cl_2 and ^{31}P VT-NMR work is being carried out by Korey Conroy.

Reference List

1) Brown, R.W. *Composition of Scientific Words*; Reese Press.: Baltimore, 1956, pp 620.

2) Arduengo(III), A.J.; Stewart, C.A.; Davidson, F.; Dixon, D.A.; Becker, J.Y.; Culley, S.A.; Mizen, M.B. *J. Am. Chem. Soc.* **1987**, *109*, 627-647.

3) Fraústo da Silva, J.J.R.; Williams, R.J.P. *The Biological Chemistry of the Elements*; Clarendon Press, Oxford, 1994, pp 545.

4) McMurry, J. *Organic Chemistry*; Brooks/Cole: Pacific Grove, 1999, pp 963.

5) Webster, M.; Keats, S. *J. Chem. Soc. A* **1971**, 836-838.

6) Lipka, A.; Wunderlich, H. *Z. Naturforsch.* **1980**, *35b*, 1548-1551.

7) Markovskii, L.N.; Romanenko, V.D.; Ruban, A.V. *Zh. Obshch. Khim.* **1979**, *49*, 1908-1909.

8) Scherer, O.J.; Kuhn, N. *J. Organomet. Chem.* **1974**, *82*, C3-C6

9) Niecke, E.; Nieger, M.; Reichert, F. *Angew. Chem. Int. Ed. Engl.* **1988**, *27*, 1715-1716.

10) Macdonald, C. L. B. *Steric and Electronic Control of Low-Coordinate Pnictogen Bonding*, Ph.D. Thesis, Dalhousie University, 1998.

11) Burford, N.; Cameron, T.S.; Lam, K.-C.; LeBlanc, D.J.; Macdonald, C.L.B.; Phillips, A.D.; Rheingold, A.L.; Stark, L.; Walsh, D. *Can. J. Chem.* **2001**, *79*, 342-348.

12) Hitchcock, P.B.; Lappert, M.F.; Rai, A.K.; Williams, H.D. *J. Chem. Soc., Chem. Commun.* **1986**, 1633-1634.

13) Burford, N.; Macdonald, C.L.B.; Robertson, K.N.; Cameron, T.S. *Inorg. Chem.* **1996**, *35*, 4013-4016.

14) Raston, C.L.; Skelton, B.W.; Tolhurst, V.-A.; White, A.H. *J. Chem. Soc., Dalton Trans.* **2000**, 1279-1285.

15) Carmalt, C.J.; Lomeli, V.; McBurnett, B.G.; Cowley, A.H. *Chem. Commun.* **1997**, 2095-2096.

16) Burford, N.; Parks, T.M.; Bakshi, P.K.; Cameron, T.S. *Angew. Chem. Int. Ed. Engl.* **1994**, *33*, 1267-1268.

17) Burford, N.; Macdonald, C.L.B.; Parks, T.M.; Wu, G.; Borecka, B.; Kwiatkowski, W.; Cameron, T.S. *Can. J. Chem.* **1996**, *74*, 2209-2216.

18) Veith, M.; Bertsch, B.; Huch, V. *Z. Anorg. Allg. Chem.* **1988**, *559*, 73-88.

19) Brusilovets, A.I.; Rusanov, E.B.; Chernega, A.N. *Zh. Obshch. Khim.* **1997**, *67*, 1070-1075.

20) Patt-Siebel, U.; Müller, U.; Ergezinger, C.; Borgsen, B.; Dehnicke, K.; Fenske, D.; Baum, G. *Z. Anorg. Allg. Chem.* **1990**, *582*, 30-36.

21) Raston, C.L.; Skelton, B.W.; Tolhurst, V.-A.; White, A.H. *Polyhedron* **1998**, *17*, 935-942.

22) Mitzel, N.W.; Smart, B.A.; Dreihäupl, K.-H.; Rankin, D.W.H.; Schmidbaur, H. *J. Am. Chem. Soc.* **1996**, *118*, 12673-12682.

23) Atwood, J.L.; Cowley, A.H.; Hunter, W.E.; Mehrotra, S.K. *Inorg. Chem.* **1982**, *21*, 1354-1356.

24) Frenzel, A.; Gluth, M.; Herbst-Irmer, R.; Klingebiel, U. *J. Organomet. Chem.* **1996**, *514*, 281-286.

25) Rømming, C.; Songstad, J. *Acta. Chem. Scand.* **1980**, *A 34*, 365-373.

26) Roesky, H.W.; Dhathathreyan, K.S.; Noltemeyer, M.; Sheldrick, G.M. *Z. Naturforsch.* **1985**, *40b*, 240-246

27) Edwards, A.J.; Paver, M.A.; Raithby, P.R.; Russell, C.A.; Wright, D.S. *J. Chem. Soc., Dalton Trans.* **1993**, 2257-2258.

28) Clegg, W.; Compton, N.A.; Errington, R.J.; Norman, N.C.; Wishart, N. *Polyhedron* **1989**, *8*, 1579-1580.

29) Clegg, W.; Compton, N.A.; Errington, R.J.; Fisher, G.A.; Green, M.E.; Hockless, D.C.R.; Norman, N.C. *Inorg. Chem.* **1991**, *30*, 4680-4682.

30) Markovskii, L.N.; Romanenko, V.D.; Ruban, A.V. *Zh. Obshch. Khim.* **1987**, *57*, 1433-1464.

31) Markovskii, L.N.; Romanenko, V.D.; Klebanskii, E.O.; Iksanova, S.V. *Zh. Obshch. Khim.* **1985**, *55*, 1867-1868.

32) Markovskii, L.N.; Romanenko, V.D.; Drapailo, A.B.; Ruban, A.V.; Chernega, A.N.; Antipin, M.Y.; Struchkov, Y.T. *Zh. Obshch. Khim.* **1986**, *56*, 2231-2242.

33) Scherer, O.J.; Conrad, H. *Z. Naturforsch.* **1981**, *36b*, 515-517.

34) Markovskii, L.N.; Romanenko, V.D.; Klebanskii, E.O.; Povolotskii, M.I.; Chernega, A.N.; Antipin, M.Y.; Struchkov, Y.T. *Zh. Obshch. Khim.* **1986**, *56*, 1721-1737.

35) Markovskii, L.N.; Romanenko, V.D.; Ruban, A.V.; Drapailo, A.B.; Chernega, A.N.; Antipin, M.Y.; Struchkov, Y.T. *Zh. Obshch. Khim.* **1988**, *58*, 291-295.

36) Markovsky, L.N.; Romanenko, V.D.; Ruban, A.V.; Drapailo, A.B.; Reitel, G.V.; Sarine, T.V. *Phosphor. Sulfur Silicon* **1990**, *49/50*, 329-332.

37) Brandl, A.; Nöth, H. *Chem. Ber.* **1988**, *121*, 1321-1327.

38) Jones, P.G.; Fischer, A.K.; Müller, C.; Pinchuk, V.A.; Schmutzler, R. *Acta Cryst.* **1996** , *C52*, 2750-2752.

39) Avtomonov, E.V.; Megges, K.; Li, X.; Lorberth, J.; Wocaldo, S.; Massa, W.; Harms, K.; Churakov, A.V.; Howard, J.A.K. *J. Organomet. Chem.* **1997**, *544*, 79-89.

40) Forster, G.E.; Begley, M.J.; Sowerby, D.B. *J. Chem. Soc., Dalton Trans.* **1995**, 377-382.

41) Gieren, A.; Betz, H.; Hübner, T.; Lamm, V.; Herberhold, M.; Guldner, K. *Z. Anorg. Allg. Chem.* **1984**, *513*, 160-174.

42) Weitze, A.; Lange, I.; Henschel, D.; Blaschette, A.; Jones, P.G. *Phosphorus Sulfur and Silicon, Relat. Elem.* **1997**, *122*, 107-120.

43) Weitze, A.; Blaschette, A.; Jones, P.G. *Phosphorus Sulfur and Silicon,Relat.Elem.* **1993**, *85*, 77-90.

44) Ang, H.G.; Kwik, W.L.; Lee, Y.W.; Rheingold, A.L. *J. Chem. Soc., Dalton Trans.* **1993**, 663-667.

45) Busch, T.; Schoeller, W.W.; Niecke, E.; Nieger, M.; Westermann, H. *Inorg. Chem.* **1989**, *28*, 4334-4340.

46) Westermann, H.; Nieger, M.; Niecke, E. *Chem. Ber.* **1991**, *124*, 13-16.

47) Menu, M.J.; Dartiguenave, M.; Dartiguenave, Y.; Bonnet, J.J.; Bertrand, G.; Baceiredo, A. *J. Organomet. Chem.* **1989**, *372*, 201-206.

48) Bender, H.R.G.; Niecke, E.; Nieger, M.; Westermann, H. *Z. Anorg. Allg. Chem.* **1994**, *620*, 1194-1202.

49) Gudat, D.; Haghverdi, A.; Hupfer, H.; Nieger, M. *Chem. Eur. J.* **2000**, *6*, 3414-3425.

50) Gudat, D.; Haghverdi, A.; Nieger, M. *Angew. Chem. Int. Ed.* **2000**, *39*, 3084-3086.

51) Bourissou, D.; Canac, Y.; Gornitzka, H.; Marsden, C.J.; Baceiredo, A.; Bertrand, G. *Eur. J. Inorg. Chem.* **1999**, 1479-1488.

52) Olmstead, M.M.; Power, P.P.; Sigel, G.A. *Inorg. Chem.* **1988**, *27*, 2045-2049.

53) Markovskii, L.N.; Romanenko, V.D.; Ruban, A.V.; Drapailo, A.B.; Reitel', G.V.; Chernega, A.N.; Povolotskii, M.I. *Zh. Obshch. Khim.* **1990**, *60*, 2453-2462.

54) Scherer, O.J.; Gläβel, W. *Chem. Ber.* **1977**, *110*, 3874-3888.

55) Scherer, O.J.; Kuhn, N. *Chem. Ber.* **1974**, *107*, 2123-2125.

56) Veith, M.; Bertsch, B. *Z. Anorg. Allg. Chem.* **1988**, *557*, 7-22.

57) Garbe, R.; Wocadlo, S.; Kang, H.C.; Massa, W.; Harms, K.; Dehnicke, K. *Chem. Ber.* **1996**, *129*, 109-113.

58) Plack, V.; Münchenberg, J.; Thönnessen, H.; Jones, P.G.; Schmutzler, R. *Eur. J. Inorg. Chem.* **1998**, 865-875.

59) Hitchcock, P.B.; Jasim, H.A.; Lappert, M.F.; Williams, H.D. *J. Chem. Soc., Chem. Commun.* **1986**, 1634-1636.

60) Ahlemann, J.-T.; Roesky, H.W.; Murugavel, R.; Parisini, E.; Noltemeyer, M.; Schmidt, H.-G.; Müller, O.; Herbst-Irmer, R.; Markovskii, L.N.; Shermolovich, Y.G. *Chem. Ber./Recueil* **1997**, *130*, 1113-1121.

61) Eichhorn, B.; Nöth, H.; Seifert, T. *Eur. J. Inorg. Chem.* **1999**, 2355-2368.

62) Lübben, T.; Roesky, H.W.; Gornitzka, H.; Steiner, A.; Stalke, D. *Eur. J. Solid State Inorg. Chem.* **1995**, *32*, 121-130.

63) Thompson, M.L.; Haltiwanger, R.C.; Norman, A.D. *J. C. S. Chem. Comm.* **1979**, 647-648.

64) Thompson, M.L.; Tarassoli, A.; Haltiwanger, R.C.; Norman, A.D. *Inorg. Chem.* **1987**, *26*, 684-689.

65) Keat, R.; Keith, A.N.; Macphee, A.; Muir, K.W.; Thompson, D.G. *J. C. S. Chem. Comm.* **1978**, 372-373.

66) Schick, G.; Loew, A.; Nieger, M.; Niecke, E. *Heteroat. Chem.* **1996**, *7*, 427-435.

67) Pohl, S. *Z. Naturforsch.* **1979**, *34b*, 256-261.

68) Niecke, E.; Flick, W.; Pohl, S. *Angew. Chem. Int. Ed. Engl.* **1976**, *15*, 309-310.

69) Hitchcock, P.B.; Lappert, M.F.; Layh, M. *J. Organomet. Chem.* **1997**, *529*, 243-255.

70) Thompson, M.L.; Tarassoli, A.; Haltiwanger, R.C.; Norman, A.D. *J. Am. Chem. Soc.* **1981**, *103*, 6770-6772.

71) Tarassoli, A.; Thompson, M.L.; Haltiwanger, R.C.; Hill, T.G.; Norman, A.D. *Inorg. Chem.* **1988**, *27*, 3382-3386.

72) Richter, V.H.; Fluck, E.; Riffel, H.; Hess, H. *Z. Anorg. Allg. Chem.* **1982**, *486*, 177-186.

73) Harvey, D.A.; Keat, R.; Keith, A.N.; Muir, K.W.; Rycroft, D.S. *Inorg. Chim. Acta* **1979**, *34*, L201-L202

74) Kumaravel, S.S.; Krishnamurthy, S.S.; Vincent, B.R.; Cameron, T.S. *Z. Naturforsch.* **1986**, *41b*, 1067-1070.

75) Kamil, W.A.; Bond, M.R.; Shreeve, J.M. *Inorg. Chem.* **1987**, *26*, 2015-2016.

76) Kamil, W.A.; Bond, M.R.; Willett, R.D.; Shreeve, J.M. *Inorg. Chem.* **1987**, *26*, 2829-2833.

77) Reddy, V.S.; Krishnamurthy, S.S.; Nethaji, M. *J. Chem. Soc., Dalton Trans.* **1994**, 2661-2667.

78) Chen, H.-J.; Haltiwanger, R.C.; Hill, T.G.; Thompson, M.L.; Coons, D.E.; Norman, A.D. *Inorg. Chem.* **1985**, *24*, 4725-4730.

79) David, G.; Niecke, E.; Nieger, M.; von der Gönna, V.; Schoeller, W.W. *Chem. Ber.* **1993**, *126*, 1513-1517.

80) Wirringa, U.; Voelker, H.; Roesky, H.W.; Shermolovich, Y.; Markovski, L.; Usón, I.; Noltemeyer, M.; Schmidt, H.-G. *J. Chem. Soc., Dalton Trans.* **1995**, 1951-1956.

81) Bohra, R.; Roesky, H.W.; Noltemeyer, M.; Sheldrick, G.M. *Acta Cryst.* **1984**, *C40*, 1150-1152.

82) Beswick, M.A.; Harmer, C.N.; Hopkins, A.D.; Paver, M.A.; Raithby, P.R.; Wright, D.S. *Polyhedron* **1998**, *17*, 745-748.

83) Edwards, A.J.; Paver, M.A.; Rennie, M.-A.; Raithby, P.R.; Russell, C.A.; Wright, D.S. *J. Chem. Soc., Dalton Trans.* **1994**, 2963-2966.

84) Beswick, M.A.; Elvidge, B.R.; Feeder, N.; Kidd, S.J.; Wright, D.S. *Chem. Commun.* **2001**, 379-380.

85) Haagenson, D.C.; Stahl, L.; Staples, R.J. *Inorg. Chem.* **2001**, *40*, 4491-4493.

86) Ross, B.; Belz, J.; Nieger, M. *Chem. Ber.* **1990**, *123*, 975-978.

87) Edwards, A.J.; Leadbeater, N.E.; Paver, M.A.; Raithby, P.R.; Russell, C.A.; Wright, D.S. *J. Chem. Soc., Dalton Trans.* **1994**, 1479-1482.

88) Garbe, R.; Pebler, J.; Dehnicke, K.; Fenske, D.; Goesmann, H.; Baum, G. *Z. Anorg. Allg. Chem.* **1994**, *620*, 592-598.

89) Wirringa, U.; Roesky, H.W.; Noltemeyer, M.; Schmidt, H.-G. *Inorg. Chem.* **1994**, *33*, 4607-4608.

90) Niecke, E.; Gudat, D. *Angew. Chem. Int. Ed. Engl.* **1991**, *30*, 217-237.

91) Niecke, E.; Rüger, R.; Schoeller, W.W. *Angew. Chem. Int. Ed. Engl.* **1981**, *20*, 1034-1036.

92) Zurmühlen, F.; Regitz, M. *Angew. Chem. Int. Ed. Engl.* **1987**, *26*, 83-84.

93) Markovski, L.N.; Romanenko, V.D.; Kirsanov, A.V. *Phosphorus and Sulfur* **1983**, *18*, 31-34.

94) Niecke, E.; Nieger, M.; Gärtner-Winkhaus, C.; Kramer, B. *Chem. Ber.* **1990**, *123*, 477-479.

95) Keat, R.; Rycroft, D.S.; Niecke, E.; Schäfer, H.-G.; Zorn, H. *Z. Naturforsch.* **1982**, *37b*, 1665-1666.

96) Romanenko, V.D.; Reitel, G.V.; Chernega, A.N.; Kirichenko, O.V.; Ruban, A.V. *Heteroat. Chem.* **1992**, *3*, 453-458.

97) Yoshifuji, M.; Shibayama, K.; Toyota, K.; Inamoto, N.; Nagase, S. *Chem. Lett.* **1985**, 237-240.

98) Scherer, O.J.; Klusmann, P. *Angew. Chem. Int. Ed. Engl.* **1969**, *8*, 752-753.

99) Lehousse, C.; Haddad, M.; Barrans, J. *Tetrahedron Lett.* **1982**, *23*, 4171-4174.

100) Kruppa, C.; Nieger, M.; Ross, B.; Väth, I. *Eur. J. Inorg. Chem.* **2000**, 165-168.

101) Ahlemann, J.-T.; Künzel, A.; Roesky, H.W.; Noltemeyer, M.; Markovskii, L.; Schmidt, H.-G. *Inorg. Chem.* **1996**, *35*, 6644-6645.

102) Nagase, S. *The chemistry of organic arsenic, antimony and bismuth compounds*; John Wiley and Sons: Toronto, 1994, pp 5.

103) Allen, F.H.; Kennard, O.; Watson, D.G.; Brammer, L.; Orpen, A.G.; Taylor, R. *J. Chem. Soc., Perkin. Trans. II* **1987**, S1-S19

104) Cowley, A.H.; Lasch, J.G.; Norman, N.C.; Pakulski, M. *J. Am. Chem. Soc.* **1983**, *105*, 5506-5507.

105) Denk, M.K.; Gupta, S.; Lough, A.J. *Eur. J. Inorg. Chem.* **1999**, 41-49.

106) Burford, N.; Losier, P.; Bakshi, P.K.; Cameron, T.S. *J. Chem. Soc., Dalton Trans.* **1993**, 201-202.

107) Nieger, M.; Niecke, E.; Detsch, R. *Z. Kristallogr.* **1995**, *210*, 971-972.

108) Burford, N.; Cameron, T.S.; Clyburne, J.A.C.; Eichele, K.; Robertson, K.N.; Sereda, S.; Wasylishen, R.E.; Whitla, W.A. *Inorg. Chem.* **1996**, *35*, 5460-5467.

109) Drapailo, A.B.; Chernega, A.N.; Romanenko, V.D.; Madhouni, R.; Sotiropoulos, J.-M.; Lamandé, L.; Sanchez, M. *J. Chem. Soc., Dalton Trans.* **1994**, 2925-2931.

110) Cameron, T.S.; Chan, C.; Chute, W.J. *Acta Cryst.* **1980**, *B36*, 2391-2393.

111) Burford, N.; Clyburne, J.A.C.; Chan, M.S.W. *Inorg. Chem.* **1997**, *36*, 3204-3206.

112) March, J.*Advanced Organic Chemistry: Reactions, Mechanisms and Structure*; John Wiley and Sons: New York, 1992.

113) Förster, H.; Vögtle, F. *Angew. Chem. Int. Ed. Engl.* **1977**, *16*, 429-441.

114) Norman, N.C. *Polyhedron* **1993**, *12*, 2431-2446.

115) Hein, J.; Gärtner-Winkhaus, C.; Nieger, M.; Niecke, E. *Heteroat. Chem.* **1991**, *2*, 409-415.

116) Palenik, G.J.; Donohue, J. *Acta Cryst.* **1962**, *15*, 564-569.

117) Mandel, N.; Donohue, J. *Acta Cryst.* **1971**, *27B*, 476-480.

118) Weigand, W.; Cordes, A.W.; Swepston, P.N. *Acta Cryst.* **1981**, *37B*, 1631-1634.

119) Mundt, O.V.; Becker, G.; Wessely, H.-J.; Breunig, H.J.; Kischkel, H. *Z. Anorg. Allg. Chem.* **1982**, *486*, 70-89.

120) Breen, T.L.; Stephan, D.W. *Organometallics* **1997**, *16*, 365-369.

121) Schmitz, M.; Leininger, S.; Bergstrasser, U. *Heteroat. Chem.* **1998**, *9*, 453-460.

122) Ates, M.; Breunig, H.J.; Ebert, K.; Gulec, S.; Kaller, R.; Drager, M. *Organometallics* **1992**, *11*, 145-150.

123) Breunig, H.J.; Rösler, R.; Lork, E. *Angew. Chem. Int. Ed.* **1998**, *37*, 3175-3177.

124) Fritz, G.; Mayer, B.; Matern, E.; Goesmann, H. *Z. Anorg. Allg. Chem.* **1991**, *602*, 73-78.

125) Appel, R.; Gudat, D.; Niecke, E.; Nieger, M.; Porz, C.; Westermann, H. *Z. Naturforsch., Teil B* **1991**, *46*, 865-883.

126) Yoshifuji, M.; Shima, I.; Inamoto, N.; Hirotsu, K.; Higuchi, T. *J. Am. Chem. Soc.* **1981**, *103*, 4587-4589.

127) Cowley, A.H.; Kilduff, J.E.; Norman, N.C.; Pakulski, M.; Atwood, J.L.; Hunter, W.E. *J. Am. Chem. Soc.* **1983**, *105*, 4845-4846.

128) Twamley, B.; Sofield, C.D.; Olmstead, M.M.; Power, P.P. *J. Am. Chem. Soc.* **1999**, *121*, 3357-3367.

129) Cowley, A.H.; Norman, N.C.; Pakulski, M. *J. Chem. Soc., Dalton Trans.* **1985**, 383-386.

130) Tokitoh, N.; Arai, Y.; Sasamori, T.; Okazaki, R.; Nagase, S.; Uekusa, H.; Ohashi, Y. *J. Am. Chem. Soc.* **1998**, *120*, 443-434.

131) Tokitoh, N.; Arai, Y.; Okazaki, R.; Nagase, S. *Science* **1997**, *277*, 78-80.

132) Niecke, E.; Detsch, R.; Nieger, M.; Reichert, F.; Schoeller, W.W. *Bull. Soc. Chim. Fr.* **1993** , *130*, 25-31.

133) Burford, N.; Cameron, T.S.; Kwiatkowski, W.; Macdonald, C.L.B.; Phillips, A.D.; Schurko, R.W.; Walsh, D.; Wasylishen, R.E.; Whitla, W.A. *in preparation.*

134) Burford, N.; Clyburne, J.A.C.; Bakshi, P.K.; Cameron, T.S. *J. Am. Chem. Soc.* **1993**, *115*, 8829-8830.

135) Huheey, J.E.; Keiter, E.A.; Keiter, R.L. *Inorganic Chemistry*; HaperCollins College: New York, 1993; pp A-31

136) Burford, N.; Muller, J.; Parks, T.M. *J. Chem. Educ.* **1994**, *71*, 807-809.